UNIVERSITÀ POLITECNICA DELLE MARCHE

PhD Course in Life and Environmental Sciences

Curriculum "Biomolecular Sciences"

XXXII cycle

Identification of the paracrine signals involved in immunomodulation, regeneration and cancer progression

PhD Student:

Salvatore Vaiasicca

Tutor:

Prof. Francesca Biavasco

Co-tutor:

Prof. Bruna Corradetti.

ABSTRACT

Immunotherapy and regenerative medicine involves the use of living cells, or their derivatives, to modulate the function of endogenous cells whose function has been compromised. Understanding the molecular mechanisms at the basis of cell communication is crucial to develop innovative approaches for cell therapy. Cell communication, named as "cross-talk", involves numerous paracrine signals, exchanged between cells, which have been reported to modulate the behavior of specific cell lines. One example is the established cross-talk between cancer cells and immune cells or between mesenchymal stem cells and immune cells. In particular, Mesenchymal Stem Cells (MSC) derived from bone marrow, blood, liver and adnexal fetal (amniotic fluid, umbilical cord blood, amniotic membrane, and chorionic villi) are very promising candidates for cell-therapy due to their properties, i.e. high proliferation rate, differentiation capacity, low immunogenicity and good immuno-suppressive and modulatory properties. In this PhD project, Human Chorionic Villi (hCV) and Amniotic Fluid (hAF) derived MSCs, retrieved from women in good health, have been characterized in terms of proliferative and differentiation abilities, resulting as potential candidates for therapeutic and regenerative medicine. Among them hCV-MSCs exhibited the best features for a possible application in regenerative medicine.

The first aim of this work was to study the interaction and the cross-talk responses in two ovarian cancer cell lines (SKOV and OVCAR), exposed to the conditioned medium of characterized hCV-MSCs and hAF-MSCs, focusing the attention on the influence of the soluble factors contained in the conditioned medium on cancer cells viability. Thus, the cells were exposed both to the whole conditioned medium and to its exosome component, previously purified and characterized by Atomic force microscopy and nanoparticle tracking analysis. Although the hCV-MSCs were more proliferative in term of proliferative rate, the conditioned medium and the exosomes derived from AF-MSCs showed a major effect on both ovarian cancer cells in 2D models. However, these results were not replicated when using 3D cell cultures and will require future confirmatory studies.

As second aim, the interference of pathological backgrounds, i.e. Down Syndrome, on the hCV-MSCs abilities was investigated by comparing Down Syndrome-affected hCV-MSCs with their euploid counterpart. The major discrepancies derived from the pathology were a reduced proliferative rate and an increased production of inflammation markers and radical oxygen species; however, the stemness properties were not significantly affected.

Finally, the third aim was to evaluate the growth inhibitory activity of the combination of two natural compounds, *Wasabia japonica*

(Wasabi) and the Active hexose correlated compound (AHCC), which is called bioactive immunomodulatory compound (BAIC), on human breast adenocarcinoma cells (MCF-7 line) and human pancreas adenocarcinoma (PANC02) cells. The combination effects were evaluated in terms of reduction of the cancer proliferation, cell-specific toxicity and immunomodulatory action towards the immune system cells. Our study demonstrated that the combination of these two natural compounds had a great inhibitory and anti-inflammatory activity compared to the single compounds on cancer cells and immune-system cells respectively, suggesting it as novel adjuvant therapy to support chemotherapy. However, further investigations are required to highlight the role of BAIC in modulating the immune system in case of inflammation, in comparison to physiological conditions.

Taken together our results demonstrated the pivotal role played by the cross-talk in the regulation of cellular processes and its extremely variable effects, dependent on the considered cell line. On the basis of its modulatory influence on immune and cancer cells, studies on the cross-talk could allow to design novel approaches to counteract different pathological conditions and to enhance the immune-system abilities.

Contents

Chapter I. Characterization and effect of conditional media and exosomes from Amniotic fluids and Chorionic Villus Mesenchymal stem cells on Ovarian Cancer cells.

1. INTRODUCTION

1.1 Cell-to-cell communication

Eukaryotic cells are typically organized in communities/tissues and constantly exchange signalling molecules. Cell-to-cell communication involves multiple cell types with different input-to-output relationships and even the cellular response to the same input stimuli can change according to cell lines. In cell communication, four types of cellular signals have been found, which change according to their reaction time and the inter-cellular distance:

- **Paracrine:** The cells release chemical signals that diffuse locally modulating the behaviour of neighbouring cells;
- **Autocrine:** The cells send chemical signals but the receptors for the signal are on the same cell;
- **Endocrine:** The cells produce hormones that travel throughout the organism via the circulatory system remaining stable for a long distance;
- **Synaptic:** The chemical signals are released into the synaptic structure (Gap) and are immediately taken up by the partner cell receptors.

Such heterogeneity makes cell-to-cell communication a complex process (1). Understanding the molecular mechanisms at the basis of cell communication is crucial to develop innovative approaches for cell therapy. The communication networks involve numerous paracrine signals, which have been reported to modulate the behavior of specific cell lines. Cells release diverse types of factors into the extracellular environment, including different extracellular vesicles (EVs), which act as intercellular messenger (2). These signals can be either intra- or inter-cellular and this phenomenon is known as "*cross-talk*". The concept of the cross-talk has been widely studied and interpreted by many authors (1, 3)**;** and it is generally assumed as explanation for the biological response to different inputs or stimuli. Moreover, according to Grégory Vert and Joanne Chory (2011), it regulates different gene pathways, directly or indirectly linked, in response to single or combinatorial signals (4). Depending on the cell line, the cross-talk can exert positive or negative effects, leading to the release of either synergistic or antagonistic factors to other cells (5). In particular cell-to-cell communication is pivotal in the coordination of cell functions for the development and adaptation of organisms.

Several studies evidenced the involvement of soluble factors such as cytokines, chemokines, growth factors and neurotransmitters in the cross-talk, highlighting the major role of extracellular vesicles from

different sources (6, 7). The Growth factors are essential for the cell cycle because they are responsible for a variety of cellular processes, such as mitosis and quiescent state; furthermore, they are also known as intercellular signaling molecules which promote cell proliferation, migration, differentiation and maturation (8). The release of the Growth factors depends on the cell line that produces them; indeed, through their study, the cell conditions, either in physiological or pathological state, could be understood. There are different pathways which can be activated during the latter condition; for example, during the wound healing or skin regeneration, the Platelet Derived Growth Factor (PDGF), Epidermal Growth Factor (EGF), Fibroblast Growth Factor (FGF), Insulin-like Growth Factor (IGF) and Tumour Growth Factor (TGF-β) family are activated. However, the same Growth factors play different roles i.e. FGFs and their receptors modulate a wide range of biological function such as cellular proliferation, migration and differentiation in cancer cells (9). Nevertheless, their clinical application is limited because of their low stability and short life.

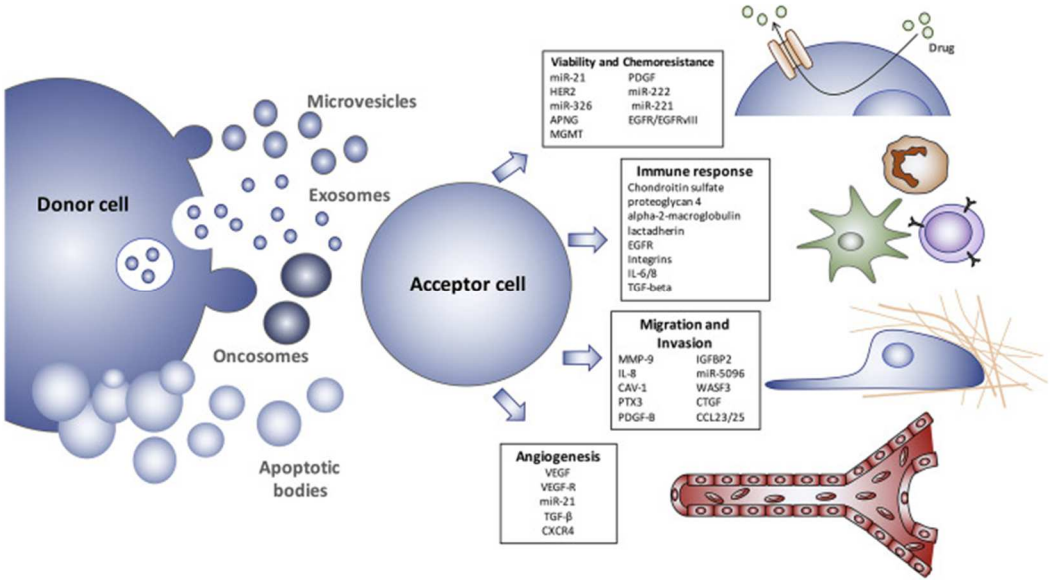

Figure 1 Donor cell of extracellular vesicles (EVs). The cells can secrete many components such as microvesicles (MVs), exosomes, oncosomes and or apoptotic bodies. These are received by an acceptor cell promoting several processes (chemoresistance, immune response, migration, invasion) (10).

The "extracellular vesicles" include different elements, i.e. microvesicles, ectosomes, shedding vesicles, and exosomes. These membrane systems are constantly exchanged between cells and contribute to the maintenance of the cell physiological conditions. Criteria for classification of EVs include the size, origin, function, shape, and the molecular content.

1.1.1 Microvesicles

The Microvesicles (MVs) are a heterogeneous group of membrane fragments from the cell surface. The size of MVs typically ranges from 100 nm up to 1 μm in diameter. In recent years, researchers have recognized the importance of MVs released in the microenvironment and important roles in altering both the extracellular environment and intercellular signaling have been attributed to them (2). Cells release vesicles through two distinct processes: i) extrusion from the endosomal membrane compartment through the cell surface after fusion with the plasma membrane of activated cells (11) and ii) direct budding from the cell plasma membrane (12). Their release can occur constitutively or consequently to cell activation by soluble factors, physical or chemical stress (13). The number of MVs released from the cells depend on the cell's physiological state and from its microenvironment.

1.1.2 Exosomes

Exosomes are membranous vesicles of endocytic origin that are released by various cell types into the extracellular space through exocytosis mechanism. Trams et al. (14) first describe exosomes in 1982 as microvesicles containing 5‘-nucleotidase activity, as proven few years later. They appear as globular shaped with a density between 1.13 and 1.19 g/ml and also have a size ranging from 30 to 200 nm (15). Exosomes can be identified by their lipid components which form a double lipid layer and are originated by reverse budding events (16). Hsu et al. found that the Rab25 protein, belonging to the GTPase protein family, regulates exosome binding, while Rab27b regulates exosome release (17). The latter plays a crucial role in the microenvironment-cell interaction because it can induce different signaling pathways, including activation, modulation and inhibition according to cells lines (18). Exosomes contain a high amount of transport proteins like tubulin, actin and actin-binding molecules; moreover, all exosomes carry MHC class I- molecules and heat shock proteins (HSP70 and HSP90) which are involved during diseases (19). In addition, exosomes carry high concentration of tetraspanins (CD9, CD63, CD81 and CD82), sphingolipids, cholesterol, glycerophospholipids, micro-RNA, mRNA and lnRNAs (long non-coding RNAs, >200 bp) that interfere with gene expression in various ways such as direct annealing with genomic DNA

or by modifying the histone complexes (20).

cytoskeletal proteins	e.g. actin, tubulin
signal transduction molecules	e.g. G-proteins
chaperones	e.g. HSP70, HSP 90
membrane transport/fusion	e.g. Rab 25, Rab 27b, annexins
antigen presentation	e.g. MHC-I, MHC-II
adhesion molecules	e.g. tetraspanins (CD9, CD63, CD81, CD82), integrins
ESCRT components	
other cytosolic proteins	e.g. histones, ribosomal proteins, proteasomes
other transmembrane proteins	e.g. LAMPs
lipids	e.g. sphingomyeline, ceramid, glycerophospholipids, cholesterol
nucleic acids	mi-RNA, lnRNA, DNA

Table 1 Exosome content.

Thanks to their content, exosomes can promote intercellular communication and modulate the immune-system; indeed the exosomes content can change according to the cell physiological state and origin (21). Exosomes from cancer cells expose specific characteristics; indeed, they can be used in diagnostics as biomarkers in cancer early state detection. For example, Glypican-1–carrying exosomes were detected in the serum of pancreatic cancer patients with 100% specificity and 100% sensitivity, suggesting their role as predictive biomarkers (22). Moreover, the transmembrane protein 256

was found in urine of patients with prostate cancer with 94% sensitivity and 100% specificity (23). On the other hand, the exosomes are used in therapy not only as cargo of transcription factors, nuclear proteins, microRNA, and mRNA, but also as chemotherapeutics transporter such as Doxorubicin and Paclitaxel. The latter compound used in combination with exosomes showed an increase of the chemotherapeutic toxicity (24). Although the exosomes showed unique properties, they have limitations, as their isolation is expensive and time consuming, thus these biomarkers are not used in the clinical routine (25).

1.2 Immunomodulation

1.2.1 The Immune System

The Immune System is composed by specialized cells and molecules against the microorganism infections such as bacteria, viruses, parasites and fungi, and it is active during the diseases, including cancer. Indeed, it is capable of distinguishing between cells known as “self-cells” and foreign cells called “non-self-cells”. All these cells are developed from pluripotent stem cells in the fetal liver and in bone marrow and then circulate through the extracellular fluid. There are two different types of response to infections which are the Acquired response and the Innate response. The Acquired response involves the proliferation of antigen-specific B and T cells. B cells and T cells work together, in particular T cells help B cells to produce antibodies and they activate the macrophages to eradicate the pathogens. The Innate Response, also called Natural Response, uses the phagocytic cells, such as neutrophils, monocytes, natural killer cells and macrophages. These cells release several molecular components, in particular acute-phase proteins and cytokines, enhancing the endurance to infection and promoting the repair of damaged tissues. A particular group is constituted by cytokines, also called soluble mediators. They act as messengers,

forming a complex network in the immune-system which regulates the immune-response (26).

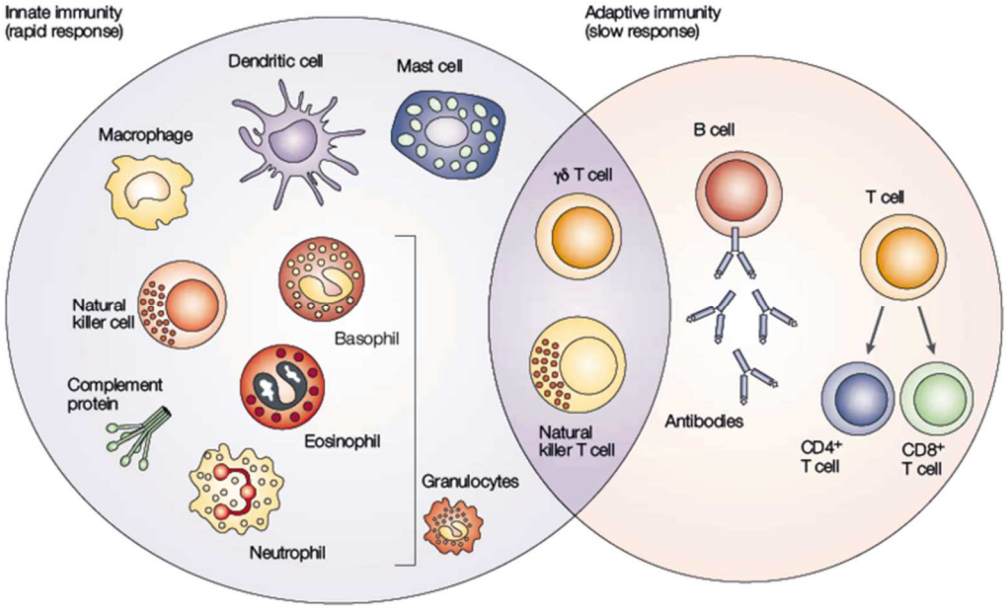

Figure 2. The immune system response. The immune system involves several cells which cooperatively together to respond to the infection.

1.2.2 Monocytes and Macrophages

Monocytes are a type of phagocytes originated in in the bone marrow, belonging to white blood cells. They derive from pluripotent stem cells, developing in monoblasts and then in promonocytes. The classical monocytes express the positivity for CD14 and CD16 markers (27). The production of monocytes in the bone marrow is governed by growth-stimulating cytokines such as interleukin 3 (IL-3), stem cell factor (SCF), granulocyte-macrophage colony-stimulating factor (GM-CSF), and macrophage colony-stimulating factor (M-CSF), and, during inflammation, also by the factor increasing monocytopoiesis (FIM). All these stimuli induce the monocytes differentiation, which take the name of Macrophages (28). Although these cells have common origin, they present different location: indeed, the monocytes are in the circulatory apparatus and their migration appears to be a random phenomenon in the absence of localized inflammation, while the macrophages are localized in inflamed tissues. The half-life of the monocyte is approximately three days, while the life span of individual macrophages in human tissues should be months but the precise data are not available. As cited above, during the inflammatory reaction, monocytes move to the specific tissue where they differentiate into macrophages under stimulation by the cytokine called M-CSF (29) and it has been observed that the specific macrophage differentiation status depends

not only on the local tissue environment but also on the type of stimuli they are exposed to. Thus, two phenotypes for the macrophages exist: the classically activated macrophages (M1) and the alternatively activated macrophages (M2), which exhibit different functions. In particular, the first exhibits the inflammatory functions while the second shows the anti-inflammatory functions (30).

1.2.3 Activation of Macrophages

The concept of activated macrophages was developed in the 1960s by Mackaness et al., who noted that macrophages had acquired resistance to infections and had increased microbicidal activity against several kinds of organisms (31). Several studies showed that there are two types of macrophages activation, the classical and the alternative activation. The classical activation occurs after the cell stimulation with two cytokines, the Lipopolysaccharide (LPS) or the interferon gamma (IFN-γ), which polarize the macrophages towards the M1 phenotype. The M1 phenotype is characterized by the secretion of large amounts of cytokines, such as interleukin-1- beta (IL-1β), tumor necrosis factor-alpha (TNF-α), interleukin-12 (IL-12), interleukin-18 (IL-18), interleukin-23 (IL-23) and interleukin-1 (IL-1). These cytokines are called pro-inflammatory cytokines and mediate resistance to infection by the production of reactive nitrogen and oxygen intermediates (NOS_2 or iNOS) (32). On the other hand, the alternative activation happens after the stimulation with interleukin-4 (IL- 4), interleukin-13 (IL-13), polarizing the macrophages towards the M2 phenotype. IL-4 and IL-13 upregulate the expression of the mannose receptor and Major Histocompatibility Complex MHC class II molecules, which stimulate endocytosis and antigen presentation and induce the expression of selective anti-inflammatory chemokines. These ones produce

interleukin-4 (IL- 4), interleukin-13 (IL-13), interleukin-10 (IL-10), transforming growth factor-beta (TGF-β), Prostaglandin E-receptor (Pge-2), cyclooxygenase 2 (Cox-2) and Arginase (ARG). M2 macrophages are involved in tissue remodeling, immune regulation and also tumor promotion (33).

The activation and the function of macrophages is flexible and continually changeable; indeed, the physiological state and thus the environment play a crucial role in that. The tumor microenvironment is a complex assembly of different cells (endothelial cells, cancer-associated fibroblasts, and different populations of immune cells including macrophages) that constitute the local environment affecting the macrophages function. Indeed, it has been observed a strong correlation between the density of macrophages and the cancer cells. In particular, macrophages displayed the ability to release the cytokines, such as IL-6, and growth factors, such as vascular-endothelial growth factor A (VEGF-A) and placental growth factor (PlGF), able to induce tumor angiogenesis (34). Another function where the macrophages are involved is the resistance to chemotherapy. Indeed, after the cytotoxic therapies, the expression of CSF-1 increased in tumor-associated macrophages, inducing their multiplication and favoring the tumor survival (35). Although, during the tumor, the macrophages display genes involved in M2 phenotype, this phenotype in is involved even in

tissue repair physiological conditions. In particular, during the regenerative processes, it was observed that the macrophages express various wound healing factors (arginase), and growth factors such as VEGF-A, platelet-derived growth factor (PDGF) and insulin-like growth factor (IGF) (36). Furthermore, they express IL-10 and TGFβ1, which are involved in several responses and IL-6 and IL-21 that have been found to enhance IL-4R (37, 38).

1.2.4 Mesenchymal stem cells (MSCs) and Immunomodulation

Mesenchymal stem cells (MSCs) were isolated by Haynesworth et al. and were first described in 1976 by Friedenstein et al. (39) as adherent fibroblast-like cells, characterized as undifferentiated cells, able to self-renew with a high proliferative capacity. Further, MSCs have the potential to differentiate into several types of cells, including at least those belonging to the mesodermic lineage, such as osteocytes, chondrocytes, and adipocytes. MSCs are characterized by the expression of specific surface markers (i.e. CD13, CD90, CD105, CD54, CD73, CD166, CD44 and STRO-1) and lack of the expression of the hematopoietic markers (i.e. CD11b, CD14, CD34, CD19, CD45 and HLA-DR) as reported by the International Society for Cell Therapy, in 2006 (40). MSCs are found in all tissues, such as bone, morrow, hair, follicles and scalp subcutaneous tissue. Furthermore, we can find them (41), in pre-natal tissues such as placenta (42), umbilical cord blood (43), and fetal bone marrow, blood, lung, liver and spleen (44).

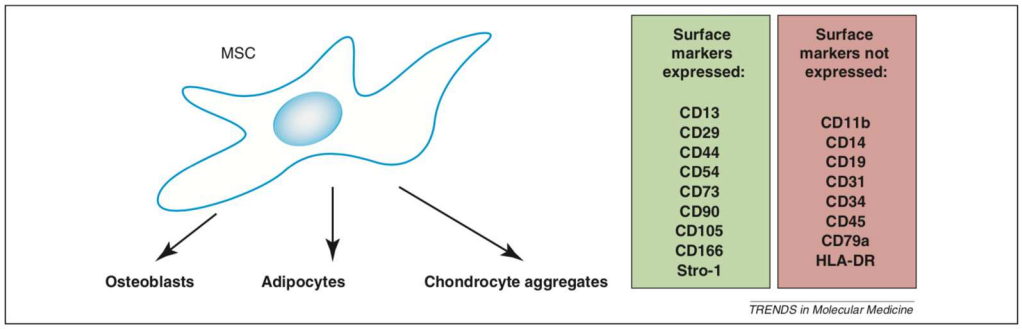

Figure 3 Main features of mesenchymal stem cells (MSCs). MSCs display specific markers and under specific culture condition can differentiate in osteoblasts, adipocytes and chondrocyte (40).

MSCs have many properties and they have been adopted in different fields, such as regenerative medicine or to regulate the immune response involved in tissue injury, transplantation, and autoimmunity (40). MSCs have been described to possess anti-inflammatory and immuno- modulatory properties, which represent the main contributing factors to tissue repair, through the reduction of immune-mediated damage and the lack of long term inflammation. They display their action through the release of numerous biologically active factors, such as growth factors, cytokines, chemokines, hormones, vesicles and exosomes, all of which exert paracrine effects (45). MSCs express a variety of chemokine receptors, such as CCR1, CCR4, CCR7, CXCR5 and CCR10, which might be involved in their migration into injured tissues (46). Some studies have shown that these cells, after the exposure to immune system cells, release active soluble factors, such as interleukin (IL)-6, the leukemia inhibitory factor (LIF), the stem cell

factor (SCF), Jagged 1 and specific immunosuppressive factors, such as IL-10, the transforming growth factor (TGF-β), the vascular endothelial growth factor (VEGF), human leukocyte antigen G soluble HLA-G (sHLA-G) and the hepatocyte growth factor (40). In particular, for the immunosuppressive action, the MSCs release specific factors such as IL-10, vascular endothelial growth factor (VEGF), tumor growth factor (TGF-β), Indoleamine-pyrrole 2,3-dioxygenase IDO, Nitric Oxide (NO) and PGE-2, creating an immunosuppressive environment (47). For example, MSCs are able to inhibit T cell proliferation by induction of CD3, CD25, CD28, CD38 and CD69. Furthermore, the soluble factors released by MSCs are able to modulate the immune-cells cycle. Indeed, in presence of MSCs, T cells arrested in G0/G1 phase which is involved in the proliferative process, and is governed by the downregulation of cyclin D2 (48). Thanks to their immunomodulatory properties, the MSCs are normally used in tissue repair, since they induce the anti-inflammatory macrophages; moreover, they are also used in the treatment of different autoimmune diseases, pulmonary fibrosis (inflammation reduction), acute renal nephropathy, and in preventing the development of diabetes (40). As cited above, the real actors for the cell-communication are represented by the soluble factors released by MSCs, which include the cytokines, growth factors and EVs. The last ones are the most important regulators

of immune cell activity, as they contain long non-coding RNA, mRNA, miRNAs and specific proteins, which represent modulatory elements. For example, the exosomes released from MSCs reduced the liver fibrosis through the inhibition of the TGF-β1 signaling pathway or the inhibition of the epithelial- to-mesenchymal transition of hepatocytes, mediated by miR-125b. Finally, MSC-derived exosomes can also inhibit the macrophage activation by suppressing TLR signalling.

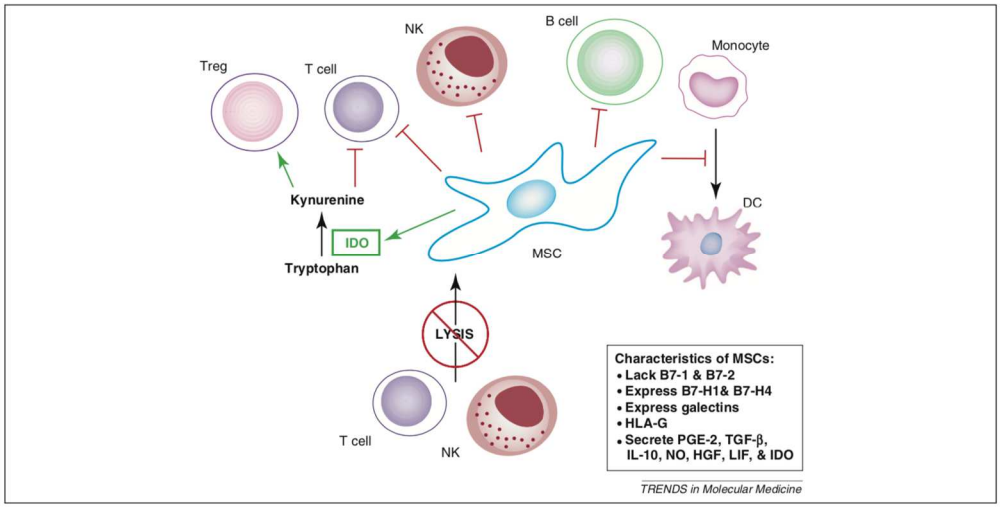

Figure 4. Immunosuppressive properties of mesenchymal stem cells (MSCs). MSCs can modulate through to release of soluble factors the immune-system component (T cell, NK, B cell, Monocytes) (40).

1.2.5 Natural compounds and immunomodulation

Natural compounds and their derivatives have been widely used in clinics for their ability to modulate cell function. They show a variety of biological activities, such as anticancer properties, stimulation of the immune system cell and antioxidant roles, which may be observed through the modification of cell metabolism. There are many classifications of natural compounds, according to their sources, chemistry structure and biological activities (49).

In addition to the traditional strategies adopted to counteract an inflammatory disease, many natural compounds are emerging as new therapeutic option. They are called nutraceuticals and have been shown to have some benefits in the infection treatment. They are derived from plants, spices, herbs, and essential oils, and many of these are still under investigation (50). Over the past two decades, the nutraceuticals have played an important role in the treatment of many human chronic diseases, and thus the main objective of researchers is to explore new drugs derived from medicinal plants (51). These compounds can be divided in different families according to their active principle; numerous compounds belong to the polyphenols family, such as resveratrol, green tea, curcumin, boswellia, fish oil, vitamin D, and probiotics (52).

In particular, these natural compounds have the ability to modulate the immune system and to disrupt the pro-inflammatory cascade, through several mechanisms that include oxidation reduction, cytokines production and alterations in cell signalling, such as the modification of the nuclear factor B pathway (NF-$_K$B) (53). For example, the natural polyphenol phytoalexin is present in a variety of plant species such as blueberries, mulberries, cranberries, peanuts and grapes. It has been described as having immunomodulatory properties, through by inhibition of the NADPH oxidase, the reduction of Reactive Oxygen Species (ROS) and, thus, the reduction of the inflammation in the environment. This ability suggests not only the increased expression of various antioxidant enzymes, but also a contribution to the immune-system action (54). Furthermore, natural compounds can modulate the extracellular vesicles content; indeed, they are able to stimulate the exosome secretion from immune cells through the modulation of microRNAs (55). They can even exert a beneficial effect on the immune-system, specifically by preventing the expression of various pro-inflammatory gene products such as nitric oxide synthase (iNOS), nuclear factor kappa B (NFK-B), several cytokines and chemokines.

1.2.5.1 Wasabi

Wasabi Japonica is a very pungent spice in Japan or Korea, where it is used to prepare traditional food such as sashimi and sushi. Among the internal components of Wasabi, the isothiocyanate family has been described as the major bio-active compounds, in particular the 6-(methylsulfinyl)-hexyl-isothiocyanate (6-MSITC). Wasabi shows important characteristics, such as anti-inflammatory, chemopreventive, antimicrobial, antigastric, antioxidant activities in different cells (56).

The anti-inflammatory effect of Wasabi generally consists in the gene modulation of the immune-system, as describe by many authors (57, 58). It was proved that the Wasabi affects around 200 inflammatory genes as, for example, the inhibition of the production of Nitric Oxide (NO), whose overexpression leads to oxidative stress. Also, wasabi plays a crucial role in the reduction of cyclooxygenase-2 (COX-2), IL-6, PGE-2, factors associated with inflammatory responses. Other studies on the modulation of the immune system by wasabi confirm its involvement in the mitogen-activated protein kinases, (MAPK pathways). The MAPK signalling pathways are divided into three major protein networks, involving the extracellular- regulated protein kinase (ERK), the p38 kinase, and c-Jun NH2- protein kinase (JNK). These are the most important pathways involved in the inflammatory response, as coordinate the induction of many inflammatory genes. In particular, the

exposition to 6-MSITC suppresses all the three MAPK pathways. Finally, it positively regulates the activator protein-1 (AP-1), that plays an important role in inflammatory response, since correlated with MAPK pathways and contributing to the inhibition of the iNOS (59).

1.2.5.2 Active hexose-correlated compound

Active hexose-correlated compound (AHCC) is used as a nutritional supplement in Japan. It derives from the culture of the basidiomycete mushroom *Lentinula edodes*. It consists in a mixture of polysaccharides, amino acids, lipids, and minerals; the oligosaccharides are the essential molecules (74% of the dry weight), in particular the α-1,4-glucans with a molecular weight of around 5.000 Daltons (60). They are also known to stimulate immune cells such as macrophages and dendritic cells. AHCC has showed several beneficial effects against obesity and hyperlipidemia; in addition, the anticancer effects against lung, liver, head, neck, ovarian and colorectal cancer were observed. Furthermore, AHCC showed the abilities to reduce adverse effects of chemotherapy (61) and to stimulate the immune system, modulating its response against pathogens (62). AHCC can enhance the immune response by multiple mechanism, including augmented macrophage and natural killer cell proliferation, high production of various cytokines by macrophages and T lymphocytes, such as interferon-c

(IFN-c), interleukin (IL)-2,-8 and -12, -1b, tumour necrosis factor (TNF-α) (63). Lee et al (64) reported that AHCC effect could modulate the monocytes gene expression, enhancing IL-17 and IFN-γ production; they were also proved to increase the production of IL-1β and IL-6 after the treatment. Regarding the anticancer activity, AHCC caused the inhibition of the expression of the signal transducer and activator of transcription (STAT) family which comprehends seven members, namely, STAT1, STAT2, STAT3, STAT4, STAT5a, STAT5b, and STAT6. In particular, STAT3 plays an important role in cell proliferation, through the cell cycle modulation, and also in the survival of various cancer, as stimulates the release of several cytokines, such as interleukin-6 (IL-6) and IL-11, involved in tumour proliferation. Choi et al. (65) proved that the treatment with AHCC on ovarian cancer inhibited the STAT3 and 2 genes involved in apoptotic mechanisms such as BCL-2 and Mcl-1. In addition, the AHCC could regulate the heat-shock protein 27 (HSP27) in pancreatic cancer cells, promoting the cytotoxic effect of chemotherapy.

Thus, the AHCC can be considered a possible candidate for combinatory therapies against cancer (60).

1.3 Anticancer activity

The tumor has been described as ‘a wound that never heals (66), and consists in a chronic state of inflammation. The research against cancer is active on numerous fields. For several years, researchers have been looking for new strategies to counteract cancer, as the last decades have revealed that the malignant properties and thus the tumor progression are not exclusively controlled by cancer cells themselves but involve several other cell lines such as fibroblasts, lymphocytes, inflammatory cells, endothelial cells, adipose tissue, and mesenchymal stem cells. All these form the tumor environment, making the complex heterogeneous interaction and contributing to the tumor destiny. Although in the early stages of tumor the microenvironment displays anti-tumor activities; the tumor development change it (67). The soluble factors involved are considered the most common mechanism of tumor-associated drug resistance and include genetic or epigenetic upregulation of pro-cancer signaling, inhibition of apoptotic pathways, drug inactivation, alteration of the drug targets, overexpression of multidrug resistance proteins (MDR) and increased drug efflux. In particular, it has been observed that the extracellular vesicles (EV) mediated the intercommunication between cancer cells, leading to the acquisition of drug resistance and tumor progression. This was specifically due to the EVs contents, i.e. miRNA, proteins and long non-coding RNA. For example, the

researchers found that miR-21 confers cisplatin resistance in gastric cancer cells (68). On the basis of this network stem cells and their derivatives, such as macrovesicles or exosomes, and natural compounds, which they are dealing in next chapter, can be considered as new approaches to modulate the cancer proliferation or to disrupt it.

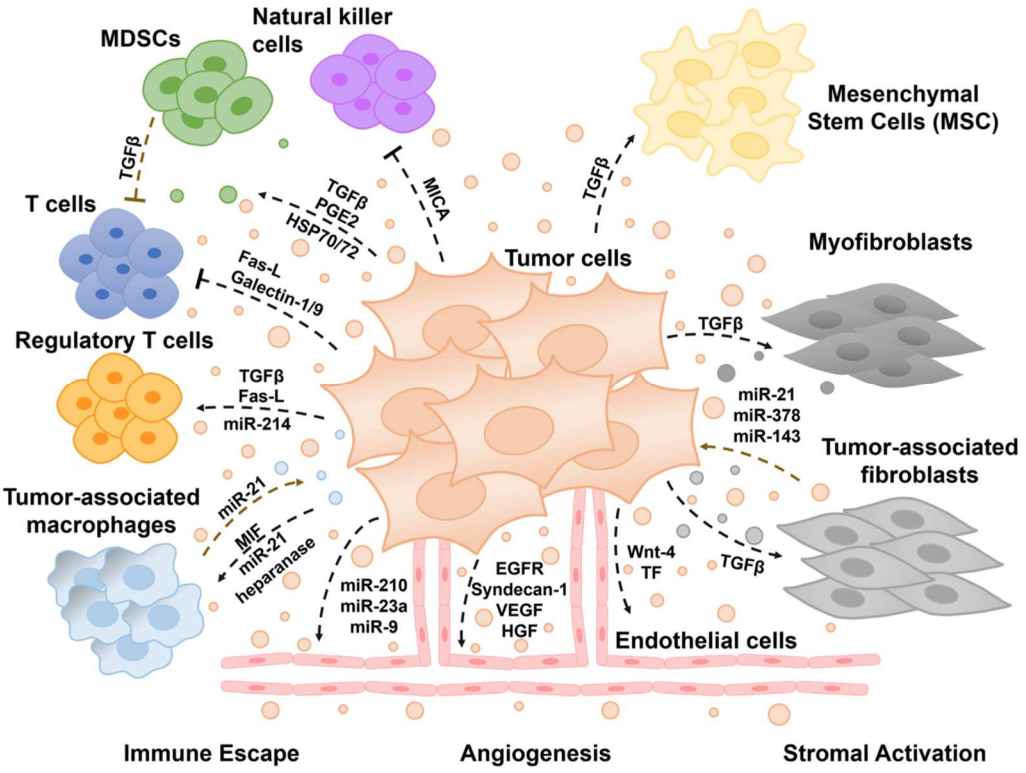

Figure. 5. Role of the extracellular vesicles-mediated intercommunication in tumor development and progression. Tumor environment is complex and heterogenic. The EVs can induce a tumor microenvironment favorable for tumor growth or chemotherapy resistance (68).

1.3.1 Mediated by stem cells

The role of MSCs in anticancer therapy has been suggested based on some of their capabilities. Indeed, many studies have described that MSCs have been involved in the promotion of tumor growth in numerous cancer types, such as follicular lymphoma (69) head and neck carcinoma (70), Glioma (71), Breast (72), Gastric (73), Colon (74), and prostate cancer (75). In particular, these findings indicate a role for MSCs in the promotion of metastasis from the tumour site, possibly through the induction of the epithelial-to-mesenchymal transition (EMT) in primary tumour cells. In contrast to these studies, there are evidences which prove that MSCs can also have an inhibitory effect on tumor growth; in particular, this has been noted in breast cancer (76) Kaposi's sarcoma (77) melanoma (78) and hepatoma (79) models. The last indicates that cancer suppression involves WTB/-catenin and/or AKT pathway inhibition by MSCs (78). These data suggest that the response to the tumor progression could be different according to the MSCs source (i.e. bone marrow, umbilical cord and adipose tissue).

In particular, research focused the attention on secretome of MSCs, as they can modulate the cancer cells in term of proliferative rate through paracrine signals (i.e. growth factors, cytokines and EV). Furthermore, the EVs derived from MSCs are normally safe and easy to obtain

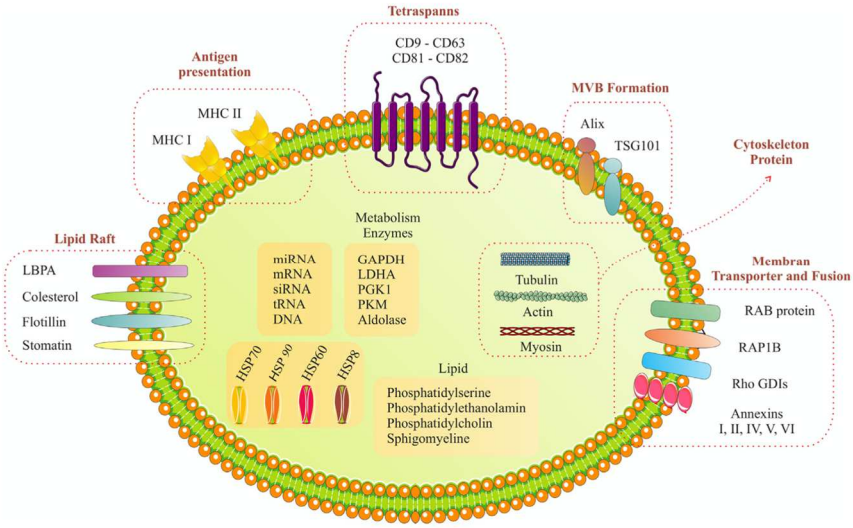

Figure 6. Exosome composition. Exosomes are spheroidal shaped and two-layer lipid particles containing various types of proteins, lipids, DNA, non-coding RNAs, miRNAs, and mRNAs which cause the exchange of the genetic information and the reprogramming of the recipient cells (80).

The MSC-EVs show the anticancer properties for the presences of miRNA, which affect the proliferative rate of the cancer cells.

As examples:

- miRNA 145 show an anti-tumor effects in various types of cancers, including pancreatic ductal adenocarcinoma cells (PDAC), hepatocellular carcinoma, colorectal, gastric, and breast cancers, as it inhibits cell proliferation, arrests the cell cycle and induces apoptosis by reducing Smad3 expression (81).
- miR-302a inhibits the proliferation of endometrial cancer cells by interferring with the Akt pathway and blocking the overexpression of cyclin D1, an important proto-oncogene that

promotes cell cycle progression from G1 to S phase and acts as transcriptional co-regulator.

- MiR-155-5p also interferes with the PI3k/Akt signaling pathway in activated B lymphocytes by reducing cell viability. In particular, this miRNA reduces the expression of PAN AKT pathway through the phosphorylation of ribosomal protein S6.
- miR-16-5p downregulates ITGA2 (integrin alpha-2) in colorectal cancer (CRC), stimulating apoptosis and blocking the proliferation, migration, and invasion of CRC cells.
- miR-126-3p interacts with malignant cells by inhibiting disintegrin and metalloproteinase domain-containing protein 9 (ADAM9) in pancreatic cancer (82).

Thus, the exosomes application as anticancer agents represents an interesting topic but warrants further elucidation.

1.3.2 Mediated by natural compounds

Many Natural Compounds have been reported to have several effects, such as the epigenetic modification of physiological processes, the DNA damage repairing, the response to inflammatory diseases and the inhibition of molecular mechanisms involved in tumor genesis. Anti-cancer natural compounds can be derived from various sources such as plants, fungi or marine organisms and over 60% derived from these (i.e. paclitaxel, camptothecin, topotecan). Other natural compounds, considered as promising anticancer agents, were purified from fruits and vegetables and include curcumin, catechins (green tea), eugenol (cloves), indole-3-carbinol (cruciferous vegetables), limonene (citrus fruits), (turmeric) and resveratrol (red grapes, peanuts and berries) (83, 84).

The de-regulated expression of transcription factors plays a critical role in various human cancers, and numerous naturals compounds have been reported to be able to induce genetic and epigenetic changes, (i.e.DNA hyper-methylation and histone deacetylation/acetylation), affecting the transcription factors production and resulting in tumor suppression. Many natural compounds such as, Curcumin (diferuloylmethane), have been shown to inhibit tumor cell growth, modulating various signaling pathways implicated in inflammation, proliferation, invasion, survival, and apoptosis (85). Specifically, the researchers described the inhibition

or the induction by curcumin of the crucial factors TP63 and MYC-a, which inhibited NFK-b and NOTCH1; moreover, curcumin modulates APAF1, an important component for the apoptotic mechanism (86, 87). Other naturals compounds can block the HIF1α, activate the capase-3/7, inhibit the expression of BCL-2 and XIAP proteins, reducing the proliferation and inducing the apoptosis of prostate cancer cells (88). Furthermore, some of these compounds can downregulate the expression of the miRNA miR-21, mirR-30a-5p, miR-19, miR-25, miR92a-2, involved in the survival and proliferation of cancer cells (89).

On the basis of these data, the natural compounds display different anti-cancer activities and this justifies both their use as supplements in common diets and their increasing application in anti-cancer therapies over the years.

2. Aims

According to these findings, the purpose of this work was to describe the cross-talk from different points of view as a first aim, two lines of ovarian cancer cells (SKOV and OVCAR) have been exposed to the conditioned medium of characterized MSCs derived from human Chorionic Villi (hCV-MSCs) and human Amniotic Cells (hAF-MSCs), to determine the contained soluble factors and monitor the cancer cells in terms of cells viability. As second aim, after the characterization of hCV-MSCs, we investigated whether pathological conditions, i.e. the trisomy 21, could interfere with the stemness properties and the immune-suppressive and immune-modulatory abilities of hCV-MSCs. Finally, we evaluated the possible synergistic effect between two natural compounds (Wasabi and AHCC) against two lines of cancer cells (PANC02 and MCF-7), monitoring the cancer cells response and excluding any cytotoxic effect on the immune-system.

Chapter I. Evaluation of the paracrine signals released by amniotic fluid- and chorionic villi-derived mesenchymal stem cells

1. Introduction

Ovarian cancer (OC) is the seventh most commonly diagnosed cancer in women worldwide (90). There are three major classifications of OC: epithelial, germ cell, and specialized stromal cell tumors. The majority ovarian cancer cases (60-80%) are represented by epithelial ovarian cancer (91, 92). Furthermore, the epithelial cancer can be divided in five histological subtypes: low-/high-grade serous, mucinous, clear cells, and endometriosis cancer, and the high-grade serous is the most common (93). Ovarian cancer is a heterogeneous disease and is mainly represented by epithelial tumors that develop from ovarian epithelial surface cells, giving rise to four main distinct histological subtypes. Because of its heterogeneity, the epithelial ovarian cancer is difficult to identify and, indeed, in most cases it is detected at late stages (94). Although the therapies against this cancer have improved over time, patients with advanced stage disease do not respond to treatment due to chemo-resistance. In particular, the researchers described in the *BRCA1* and *BRC2* genes DNA repair-associated reversion mutations, leading to chemo-resistance to platinum-based chemotherapy and PARP inhibitors (95). For these reasons, OC has become one of the greatest clinical challenges and requires alternative approaches (96). Many studies have focused the attention on the tumor microenvironment because it plays an important role in the cancer maintenance,

proliferation, invasion and response to therapy (97). In 1863, Rudolf Virchow first described the cross-talk between tumor cells and the microenvironment as a key factor for tumorigenesis (98). The tumor microenvironment consists of a combination of cancer and other different cell lines, including fibroblasts, stem cells, macrophages, regulatory T cells, endothelial cells and platelets, as well as molecules produced by the cells themselves (inflammatory cytokines, macrovesicles, anti-apoptotic body and exosomes) (99). Since many years the Stem Cells are considered as promising candidates for the use in cell-therapies, thanks to their capabilities showed in regenerative medicine (100) and immune-suppressive action (101). Mesenchymal stem cells (MSCs) have been reported to exert various actions, such as tissue homeostasis maintenance, immunomodulatory capacity and tissue reparative activities (102). In particular, MSCs derived from fetal adnexal such as chorionic villi (CV), amniotic fluid (AF) and amniotic membranes (AM), show functional characteristics comparable with those of adult MSCs. Furthermore, they even present safety and efficacy in therapies and the absence of tumorigenesis after *in vivo* transplantation (103, 104). The role of MSCs in tumor progression is controversial. According to Tong Gao et al., MSCs support tumor progression, promoting tumor metastasis and inhibiting apoptosis (99), On the contrary, Zhao JY et al. (105) and Bruno S et al. (106)

demonstrated that MSCs inhibit cancer cells proliferation, inducing apoptosis and then reducing the tumor size. MSCs exert their properties by releasing paracrine factors such as extracellular vesicles (microvesicles and exosomes), growth factors, lipid mediators, and cytokines. These signals are considered as the major players in the cross-talk between MSCs and target cells, thus mediating their biological effect (107). In particular, Abu Musa et al. (108) demonstrated that the biological molecules secreted by human adipose MSCs show anti-cancer activity on different ovarian cancer cells (SKOV3 and A2780), as demonstrated by the reduction in cell proliferation.

In this study, we hypothesize that the paracrine signals released by MSCs derived from fetal adnexa, such as cytokines, growth factors, and exosomes, might play an important role in the regulation of ovarian cancer. Specifically, we focused our attention on two sources of MSC: the Amniotic Fluid (hAF) and Chorionic Villi (hCV), to observe the respective tumor reaction, proposing them as a possible new therapy against ovarian cancer.

The MSCs (hCV- and AF-MSC) were firstly characterized in terms of proliferative rate and molecular phenotype. Secondly, we evaluated the effect of the conditioned medium derived from hCV- and AF-MSC on the proliferation of two epithelial Ovarian Cancer lines (OVCAR and

SKOV). In particular, we studied the possible conditioned medium (CM) effect in 2D and 3D culture, evaluating the cancer viability and different response in the two study models. Then we collected the exosomes present in the supernatant of each of these cell lines and characterized them through the Nanoparticle Tracking Analysis (NTA) and atomic force microscopy (AFM). Furthermore, we evaluated the exosomes uptake on SKOV and OVCAR by confocal microscopy. Finally, the potential therapeutic effect of exosomes derived from hCV- and AF-MSC was analyzed by evaluating the proliferation inhibition and the apoptosis in SKOV-3 and OVCAR cells.

2. *Materials and methods*

2.1 Cell culture

The cell lines used in this study include human Amniotic Fluid (hAF),- and Chorionic Villi (hCV)-derived MSCs and the ovarian cancer cell lines SKOV and OVCAR. MSCs were cultured in High Glucose-Dulbecco's Modified Eagle Medium (HG-DMEM) (Thermo fisher Scientific, Waltham, Massachusetts, United States) supplemented with 10% fetal bovine serum (FBS) (Sigma-Aldrich, St. Louis, Missouri, United States), 1% L-glutamine and 2% antimitotic/antibiotic. The OVCAR cells were cultured in RPMI-1640 media (Gibco, Thermo fisher Scientific, Waltham, Massachusetts, United States) supplemented with 20% fetal bovine serum (FBS) (Thermo fisher Scientific, Waltham, Massachusetts, United States), 1% L-glutamine and 1% Pen/Strep. The SKOV cells were cultured in MCCoy's 5A (Sigma-Aldrich, St. Louis, Missouri, United States) supplemented with 10% FBS (Thermo fisher Scientific, Waltham, Massachusetts, United States), 1% L-glutamine and 1% Pen/Strep. Cells were maintained at 37 °C in a humid atmosphere with 5% CO2.

2.2 Proliferation assays

2.2.1 Growth curves

Growth curves were set using hAF-MSCs and hCV-MSCs at passage 2 (P2) in 3 biological replicates. To this, hCV- and AF-MSCs were plated at density 10^4 cells/well into 12-well tissue culture polystyrene dishes (EuroClone S.p.A. Milano, Italia). Every 2 days, for 14-15 days, cells were trypsinized and counted by using trypan blue exclusion dye method.

2.2.2 Doubling time (DT) assay

Cells (density 1.5 x 10^4 cells/well) were seeded into 12-well tissue culture polystyrene dishes from P2 to P5. Cells were trypsinized every 3 days, counted and replated at the same density. The DT value was obtained for each passage according to the formula

$$DT=CT/CD$$

where CT represents the culture time and $CD = \ln(Nf/No)/\ln 2$ represents the number of cell generations (Nf represents the number of cells at confluence, No represents the number of seeded cells).

2.2.3 Colony-forming unit-fibroblastic (CFU-F) assay

Cells were seeded at P2 passage at different densities (1.5 x 10^3, 3 x 10^3, 4.5 x 10^3 cells/cm^2) in six-well plates and cultured in 5% CO_2 and 90% humidity at 37°C for 2 weeks in Standard Medium Culture. Then, colonies were fixed with 1% PFA, stained with Giemsa at room temperature, and washed twice. At the end of the 2 weeks culture period, the colonies were counted under an inverted research microscope (MEIJI TECHNO). The aggregation of 15-20 nucleated cells was considered as colony.

2.3 Evaluation of hCV and AF-MSC-associated markers by Flow Cytometry

MSCs isolated from the two tissues were analyzed at P2 for the presence of surface MSC-associated markers by flow cytometry. A total of 5 x 10^5 cells were trypsinized, fixed with 75% ethanol and incubated for 20 minutes with 0.5% bovine serum albumin (BSA) in Posphate Buffered Saline (PBS) to block all the non-specific sites. Aliquots containing 1 x 10^5 cells each were resuspended in PBS 1X and centrifuged at 500 x g for 5 minutes at 20 °C. The supernatant was then discarded and 5 µl of fluorescently labeled antibody were added to each aliquot. The following directly conjugated antibodies were used: phycoerythrin (PE)-conjugated ecto-5'-nucleotidase (PE-*CD73*;

Biolegend, Sandiego, California, United States), fluorescein isothiocyanate (FITC)-conjugated thymocyte differentiation antigen 1 (FITC-*CD90*; Biolegend, Sandiego, California, United States) and the glycoprotein *CD44* (FITC-CD44; Biolegend, Sandiego, California, United States), Allophycocyanin (APC)-conjugated for integrin b1 (APC-*CD29*; Biolegend, Sandiego, California, United States). Incubation was performed for 45 minutes at room temperature in the dark. Cells then were washed twice with filtered PBS to remove the excess of antibody and analyzed using Guava Easycite Millipore flow cytometer with GUAVASOFT 2.2.3 software.

2.4 Molecular analysis

Total RNA was extracted from hCV and AF-MSC cells at passages P2, to characterize cells from the two gestational tissues as presumptive mesenchymal stem cells. Total RNA was extracted from cells using TRI Reagent® (Sigma-Aldrich, St. Louis, Missouri, United States) according to the manufacturer's protocol. The cDNA was synthesized from total RNA (500 ng) using a PrimeScript RT-Reagent Kit (Takara, Kusatsu Japan) according to the manufacturer's protocol. The gene expression evaluation was performed using human specific sequences. Oligonucleotide primers were designed using open source Primer-BLAST, across an exon-exon junction, in order to avoid genomic DNA

amplification and make manual corrections to obtain a better amplification. Sequence conditions and the references used are shown in table 1. The Polymerase Chain Reaction (PCR) was performed in a 20 µl final volume with JumpStart™ Taq DNA Polymerase (Sigma-Aldrich, St. Louis, Missouri, United States) according to the manufacturer's protocol. After the amplification reaction, the resulting products were examined by electrophoresis in a 1,6 % agarose gel stained with ethidium bromide and photographed with a UV trans-illuminator (Kodak EDAS 2009).

Table 1. Transcripts and sequence of each primer used in real time RT-PCR to characterize Mesenchymal stem cell-associated properties.

GENE	Sequences (5'→3')	Tm (°C)	Product size (bp)
Mesenchymal markers			
CD44 molecule (Cd44)	S: GGAGCAGCACTTCAGGAGGTTAC	63	129
	A: GGAATGTGTCTTGGTCTCTGGTAGC	63	
5'-nucleotidase, ecto (Cd73)	S: GCTCTTCACCAAGGTTCAGC	59	203
	A: GTGGCTCGATCAGTCCTTCC	60	
Thy-1 cell surface antigen (Cd90)	S: CTTTGGCACTGTGGGGGTGC	64	211
	A: GATGCCCTCACACTTGACCAG	61	
Endoglin (Cd105)	S: CCTGGAGTTCCCAACGGGCC	65	186
	A: GGCTCTTGGAAGGTGACCAGG	62	
Hematopoietic marker			
CD34 molecule (Cd34)	S: GTGTCTACTGCTGGTCTTGG	57	200
	A: CAGTGATGCCCAAGACAGC	58	
CD45 molecule (Cd45)	S: GACAACAGTGGAGAAAGGACG	58	170
	A: GCTGTAGTCAATCCAGTGGGG	60	
Pluripotent markers			
Pou class 5 homeobox 1 (Oct-4)	S: CGATCAAGCAGCGACTATGC	59	200
	A: AGAGTGGTGACGGAGACAGG	60	
Nanog homeobox (Nanog)	S: GCAAGAACTCTCCAACATCC	56	178
	A: GGTCTGGTTGCTCCACAT	56	
Reference gene			
Glyceraldehyde-3-phosphatase dehydrogenase (Gapdh)	S: TCCACTGGCGTCTTCACC	68	78
	A: GGCAGAGATGATGACCCTTT	70	

S= sense primer, A= antisense primer Tm= melting temperature

2.5 Immunostaining

For the visualization of the MSCs from the two cell lines, through fluorescence microscopy (OLYMPUS BX51 with SPOT ADVANCED pc program), fluorescent probes such as ActinGreen (Life technologies, Carlsbad, California, United States) and Hoechst (Sigma-Aldrich, St. Louis, Missouri, United States) were used to highlight specifically the cytoskeleton and the nucleus, respectively. Cells were seeded at 1.4 x 10^4/well in chamber slide and let adhere. Cells were then washed in 200 µl/well of 1% PBS twice and immediately fixed with 200 µl/well of 4% PFA for 15 minutes. Subsequently, the cells were washed for another three times in 200 µl/well PBS. They were then permeabilized with 200 µl/well 0.1% Triton (in PBS) for 10-15 minutes and then washed for further three times in 200 µl/well PBS 1%. After the last washing, MSCs were blocked in 1% BSA in PBS for 30 minutes at room temperature. Subsequently the cells were incubated with 200 µl/well of ActinGreen for 20 minutes at room temperature in the dark and then washed in PBS. Cells were finally incubated with Hoechst for 5 minutes. Slides were kept in the dark until observation started.

2.6 Preparation of conditioned medium

To obtain conditioned medium (CM) generated from MSCs freshly isolated from early (CV and AF) fetal tissues, MSCs from each cell line were cultured for 3 days in T25 flask in Standard Culture Medium. At the end of the culture period, CM was collected, centrifuged at 500 x g, filtered through a 0.45 μm pore size and kept at -80 °C until use.

2.7 2D Cell Viability Assay

To evaluate on ovarian cancer (SKOV and OVCAR) viability in 2D culture the RealTime-Glo MT Cell Viability Assay (Promega, Madison, Wisconsin, United States) was performed. The OC cells were cultured in 96-well plates at $5x10^3$ cells per well for the OVCAR and at $1x10^3$ for SKOV. Then they were treated independently with both the two CM (hCV-CM; hAF-CM) for 96hrs. After each 24h the cells were analyzed following the manufacturer's indications.

2.8 3D Cell Viability Assay

The same experiment was performed in 3D culture using the CellTiter-Glo 3D Cell Viability Assay (Promega, Madison, Wisconsin, United States). The OC cells were cultured in Spheroid Microplate 96-well

plates (Corning Incorporated, New York, United States) at $5x10^3$ cells per well for 24h. Then they were treated by both different CM (hCV-CM; hAF-CM) for 72h. After each 24h the cells were analyzed following the manufacturer's indications.

2.9 Exosome isolation

Exosomes were isolated from MSCs using the ExcoQuick-TC® (SYSTEM BIOSCIENCES, Paolo Alto, California, United States) according to manufacturer instructions. Briefly, the MSCs conditioned medium was collected and centrifuged at 3,000xg for 15 minutes and the supernatant was recovered and used for the extraction. ExcoQuick-TC reagent was added to the CM and mixed by inverting the tubes several times. The mixture was incubated overnight at 4°C and centrifuged at 3,000xg at 4°C. The isolated exosomes were retained and purified in the kit column.

2.10 Atomic Force Microscopy (AFM)

A mica flake was freshly cleaved and 40 µl of exosome solution was deposited. The solution was left for 1 hour, rinsed with 1 mL PBS and analysed with AFM. Samples were scanned using Bruker ScanAsyst Fluid probes and a Bruker BioScope Catalyst (Bruker Instruments, Santa Barbara, California, USA). The probes were previously

calibrated to obtain deflection sensitivity (12 nm/V) and spring constant (0.6 N/m). Samples were scanned in PeakForce (PF), with a PeakForce Amplitude of 500 nm, a PeakForce Frequency of 0.5 KHz, a PeakForce Setpoint of 500 pN and a scan rate of 1 Hz.

2.11 Nanoparticle Tracking Analysis (NTA)

The exosomes solution was analyzed by NTA (ZetaView®) software, quantifying their concentration and size in scatter mode. Briefly, the exosomes solutions obtained by CV and AF-MSC were diluted 1/10 in PBS buffer. To perform the measurement the sensitivity (50) and the shutter (70) was set, detecting the exosomes in the recommended margin (50-200 particles). The setting used to collect data (size distribution and the concentration) was 30 frames/seconds for 11 positions.

2.12 Fluorescence-exosomes preparation and internalization by cancer cells

Fluorescent exosomes were prepared by staining with Vibrant Did Cell labeling solution (Thermo fisher Scientific, Waltham, Massachusetts, United States). Briefly 0.5 µl of dye (Thermo fisher Scientific, Waltham, Massachusetts, United States) were added to the 100 µl of

exosomes solution. Subsequently, the mixture was mixed by inversion and then incubated for 20 minutes at 37C°. The mixture was centrifuged through the spin column (Thermo fisher Scientific, Waltham, Massachusetts, United States) at 750g for 2 minutes at room temperature and the labelled-exosomes were delivered to cancer cells. Finally, the internalization was confirmed by confocal microscopy using a LSM-710 (Carl Zeiss, Oberkochen, Germany) microscope.

2.13 Evaluation of apoptosis

To analyze the possible apoptotic effect induced on SKOV3 and OVCAR cells by exosomes derived from hCV and AF-MSCs, the RealTime-Glo^{TM} Annexin V Apoptosis and Necrosis Assay (Promega, Madison, Wisconsin, United States) was used. Briefly, 1,000 cells for SKOV and 5,000 cells for OVCAR were seeded in 96 well/plate; after 24h, the cells were treated with 10^6 exosomes for 96h and incubated with Detection Reagents prepared following the manufacturer's indications. The cells apoptotic state was monitored each 24h by Spectrophotometer (SPECTROstar Omega). The percentage of early apoptotic and late apoptotic cells was established using MARS Data Analysis Software and comparing the treated cells to control groups (untreated cells).

2.14 Statistical analysis

Statistical analysis was performed using GraphPad Instat 3.00 for Windows (GraphPad Software). Three replicates for each experiment (doubling time, colony forming unit, quantitative PCR (qPCR) and cytometry analysis) were performed and the results are reported as average ± standard deviation (SD). One-way analysis of variance for multiple comparisons by the Student-Newman-Keuls multiple comparison test were used to assess differences between groups. Differences were considered statistically significant for p values < 0.05. For quantitative PCR data, non-parametric tests were used. Saphiro-Wilk normality test proved that the datasets were normally distributed ($p > 0.05$).

3. Results

3.1 Growth curve

To build the growth curve, three biological replicates of MSCs from the two cell lines at passage P2 were used. As shown in the chart (Figure 1), the lag phase (3 days) was similar for the two samples. After 3 days in culture, significant differences in proliferation activity were found ($p < 0.05$) and it was possible to notice that cells derived from different fetal adnexal had different exponential growth phases. The *in vitro* proliferative capacity of hCV-MSCs was generally greater with a more extensive log phase (3-13 days) than the one registered for hAF-MSCs (3-11 days).

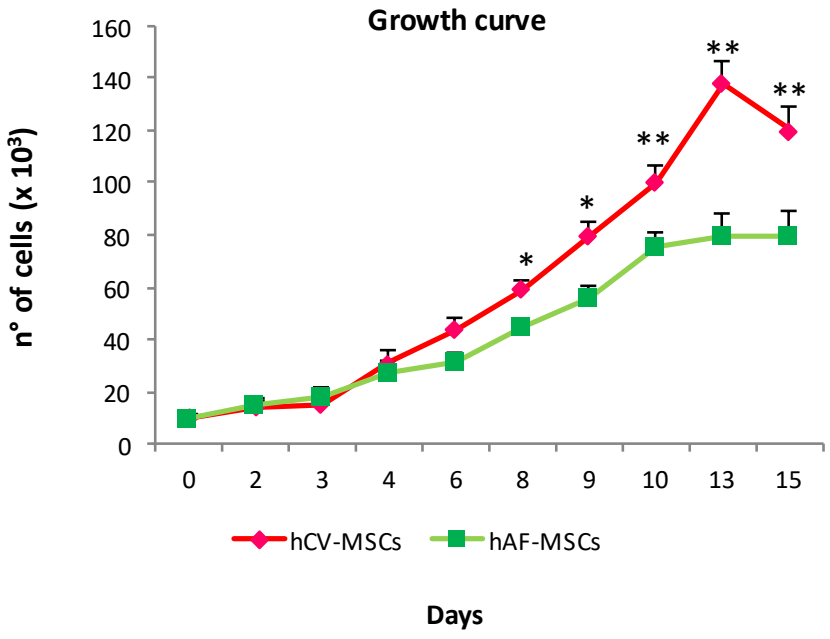

Figure1. Growth curves of hCV and hAF-MSCs. Cell cultures at P2 were monitored in terms of proliferative capacity for 15 days and cell counts were performed mostly every 48h. The results are reported as average of three biological replicates ± standard deviation. *p <0.05, and **p <0.01.

3.2 Doubling time (DT)

Doubling time (DT) confirmed the data provided above. In fact, it resulted constantly and significantly $p<0.0.1$ lower (5.5 ± 0.3) in hCV-MSCs compared with hAF-MSCs (8.5 ± 0.5) (Figure 2).

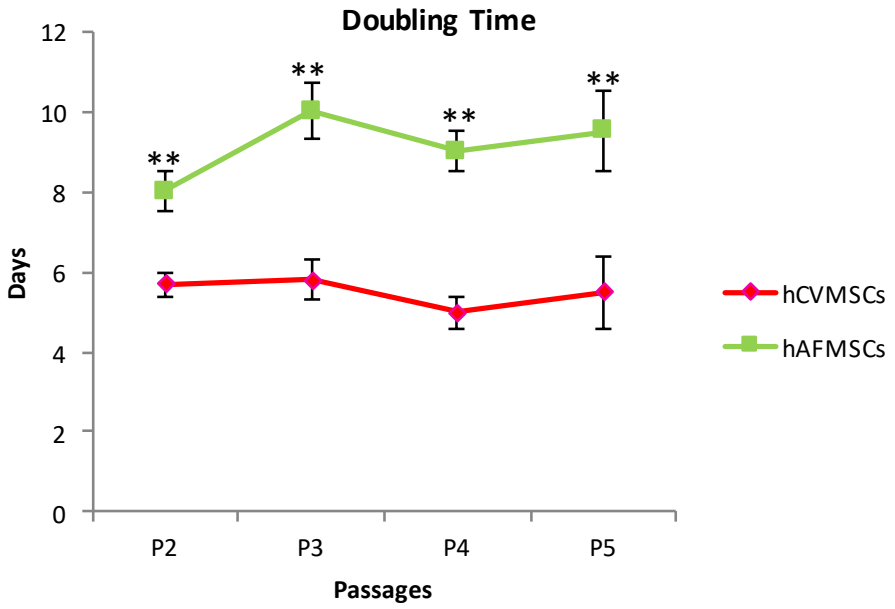

Figure 2. Doubling time (DT) of hCV-MSC and hAF-MSC. The doubling time of cell cultures was calculated from p2 to p5 by trypan blue exclusion the results are reported as average of three biological replicates ± standard deviation. *p <0.05, and **p <0.01.

3.3 Colony-forming unit (CFU) assay

CFU assay was performed on hCV-MSCs and AF-MSCs to analyze their clonogenic potential. After 15 days of culture, the number of colonies formed at P2, after seeding cells at different densities, was counted. The results obtained are shown in Table 2 and demonstrate an increase in CFU frequency directly proportional to cell seeding density. For each density of seeding, hCV-MSCs showed higher CFUs in comparison with hAF- MSC.

Table 2. CFU-F assay of hAF- and hCV-MSCs.

	density cells/cm^2	Total cells	CFU	1 CFU each
hAF MSCs	1500	14250	2.5 ± 0.7	7125
	3000	28500	4 ± 0.4	5700
	4500	42750	10.5 ± 0.7	4275

	density cells/cm^2	Total cells	CFU	1 CFU each
hCV MSCs	5000	47500	4 ± 1.4	15833
	10000	95000	8 ± 0.7	11875
	15000	142500	14 ± 0.7	10178

the results reported as average of three biological replicates ± standard deviation.

3.4 Flow Cytometry Analysis

Flow cytometry analysis showed a positivity for *CD44*$^{+}$, *CD29*$^{+}$, *CD73*$^{+}$ and *CD90*$^{+}$ in the cell populations from both the fetal tissues evaluated at P2. The Mean Fluorescence Intensity (MFI) values of mesenchymal markers were significantly higher ($p<0.01$) in hCV-MSCs (CD44 200± 40, CD29 1722± 120, CD73 1400± 200 and CD90 340± 40) than in AF-MSCs (CD44 105± 24, CD29 1040± 70, CD73 1020± 120 and CD90 80± 12) (Fig 3 A-B).

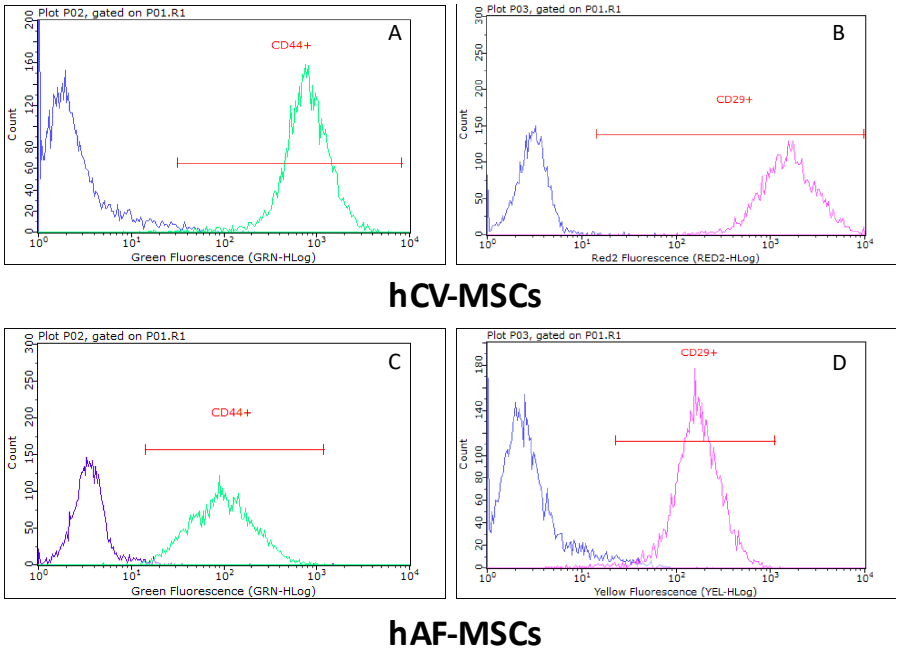

Figure3A. Flow cytometric analysis of in hCV-(a-b) AF- MSC(c-d). The results revealed CD44^{+} (green) and CD29^{+} (red) cells in comparison to unstained cells (blue).

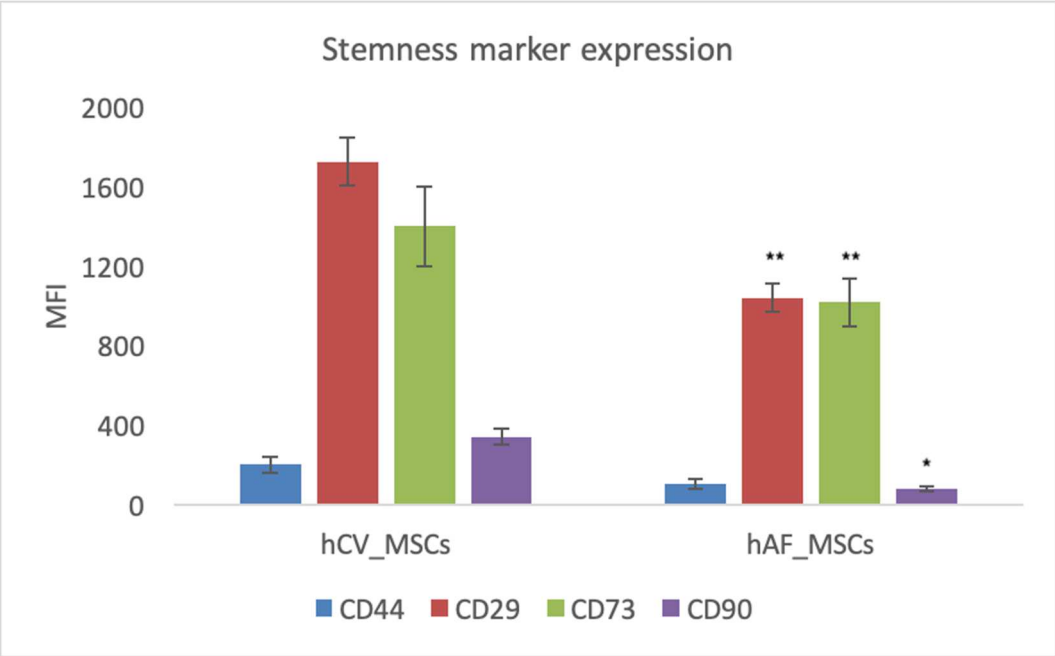

Figure 3B. ***MFI ratios variation of hCV-MSCs and hAF-MSCs.*** The MFI for each mesenchymal marker was calculated in each cell lines. *=p<0.05, ** = p<0.01

3.5 Molecular characterization

MSCs from the two different tissues at passage P2 were characterized from a molecular point of view and they have revealed to retain pluripotent features and typical mesenchymal phenotype (Figure 4). Indeed they resulted positive for Nanog and Oct-4 markers, indicating pluripotency and for CD73, CD90, CD44, CD105, markers of the mesenchymality. Moreover, all categories of MSCs did not express the hematopoietic markers CD34 and CD45.

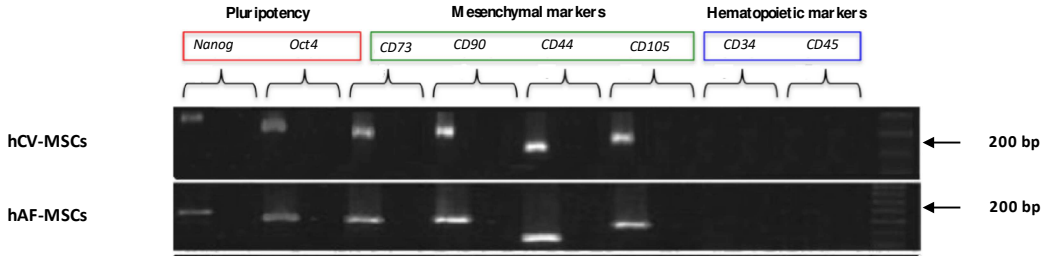

Figure 4. Molecular characterization of MSCs from each cell line. the presents/absence of pluripotency, mesenchymaly or hematopoietic markers respectively was investigated by PCR assays. The obtnained amplicons for each gene are showed for each cell line

3.6 Immunostaining.

The MSCs structure was visualized by fluoresce microscopy. The cytoskeleton was highlighted through the green staining that derives from the high affinity between a green probe, the ActinGreen (Life Technologies) and the F-actin structures. The nucleus was highlighted by Hoechst (Sigma-Aldrich, St. Louis, Missouri, United States). Differences in cell shape/morphology/arrangements were observed between the two cells lines with two predominant morphological cell types: I) cobblestone-like cells, resembling epithelioid cells (Figure 5A). II) small spindle-shaped cells (Figure 5B).

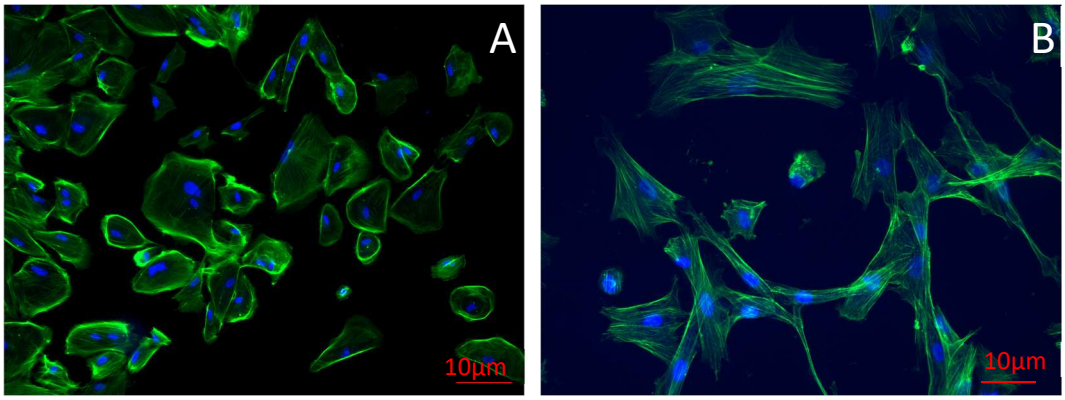

Figure 5. hAF(A)- hCV (B)-MSCs respectively. Cell culture at P2 where observed at fluoresces microscope at 10X magnification. Green fluoresces evidenced the: F-actin while Blue fluoresces: the nuclei.

3.7 Cytotoxic effect of tumor cells in 2D model

Treatment with CM derived from hCV and AF-MSCs altered the cell proliferation in SKOV and OVCAR cells lines reducing their viability. As shown in Figure 6, a significant decline of the viability of both cells lines was observed at 72h, with an 85.5 % ± 3 reduction for CM-CV and a 98% ± 1.5 for CM-AF in SKOV-3 cells, and a 88% ± 6.4 for CM-CV and 88% ± 1.7 for CM-AF in OVCAR cells compared to untreated cells (Control). Furthermore, reduction in cell viability was also observed after the treatment of cancer cells with standard medium for MSCs (C-MSC), showing a reduction of 57% ± 2 for SKOV-3 and 63% ± 1.8 for OVCAR.

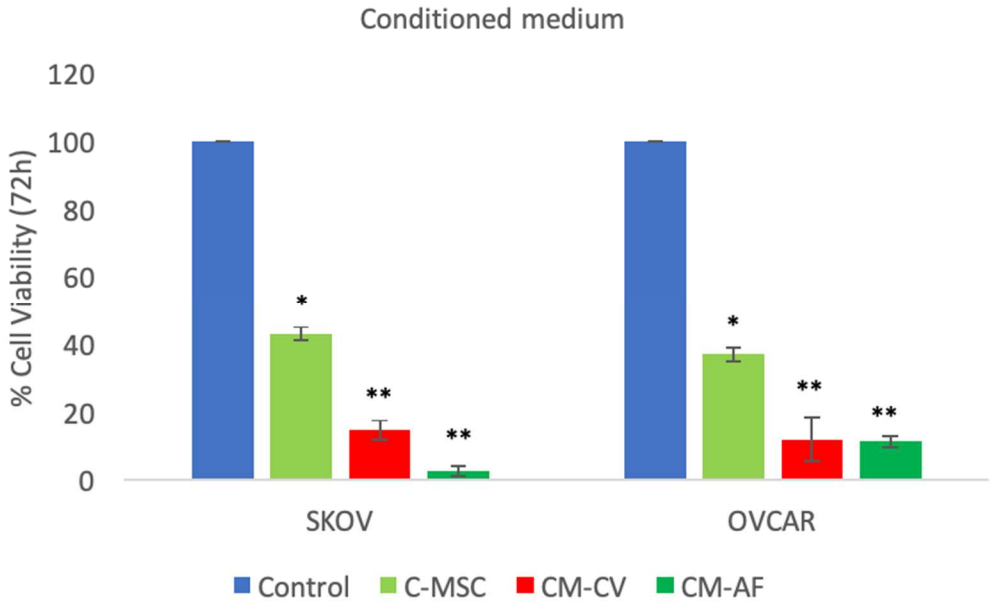

Figure 6. Effect of MSCs conditioned medium on OC cells in 2D models. The SKOV and OVCAR cultures were exposed for 72h to the CM derived from hCV-MSCs (CM-CV) or AF-MSCs (CM-AF) and to the normal medium adopted for MSCs (C-MSC). The cell viability is reported for each condition as average of three biological replicates, ± standard deviation, and it is expressed as percentage of the viable cells compared to untreated cultures (Control). *=p<0.05, **=p<0.01

3.8 Conditioned medium cytotoxic effect on tumor cells in 3D model

To analyze the CM effect on 3D models of SKOV and OVCAR cells lines, cell viability was measured on spheroids of the two cell lines exposed to the MSCs CM. Although the viability levels for C-MSC and CV-MSC (FIG 7) did not evidences significant differences in SKOV cells, we revealed a significant viability reduction ($P<0.1$) caused by the treatment with CM-AF, specifically 56% ± 8.2 compared to the Control. On the other hand, in OVCAR cells reductions of cell viability of 16% ± 13, 27% ± 3.7, and 42.4% ± 9 were observed for C-MSC, CM-CV and CM-AF respectively, in comparison to the CONTROL. Even in this cell line, CM-AF exerted a greater viability reduction compared to CM-CV.

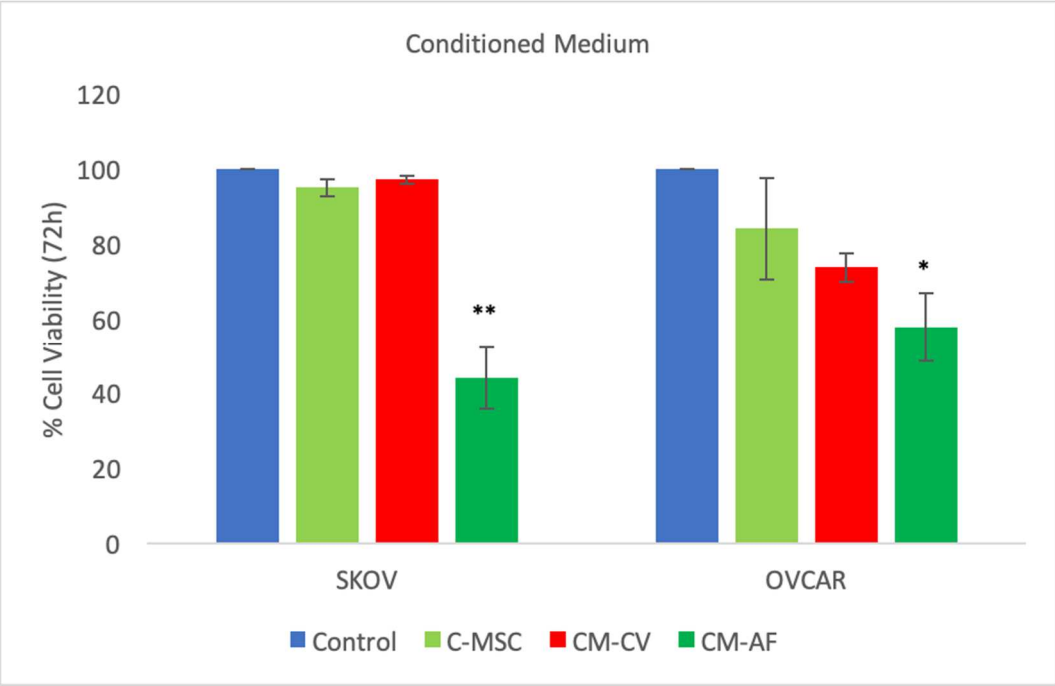

Figure 7. Effect of MSCs conditioned medium on OC cells in 3D models. The SKOV and OVCAR spheroidss were exposed for 72h to the CM derived from hCV-MSCs (CM-CV) or AF-MSCs (CM-AF) and to the normal medium adopted for MSCs (C-MSC). The cell viability is reported for each condition as average of three biological replicates, ± standard deviation, and it is expressed as percentage of the viable cells compare to untreated cultures (Control). *=$p<0.05$, **=$p<0.01$

3.9 Exosomes Characterization

The exosomes derived from hCV- (EXO CV-MSCs) and AF-MSCs (EXO AF-MSCs) were characterized by AFM and NTA analyses, evaluating their concentration and size. They appeared to have cup form (FIG 8) and with a diameter (nm) size of 168 ±31 and172 ±33 for EXO CV- and EXO AF-MSC, respectively.

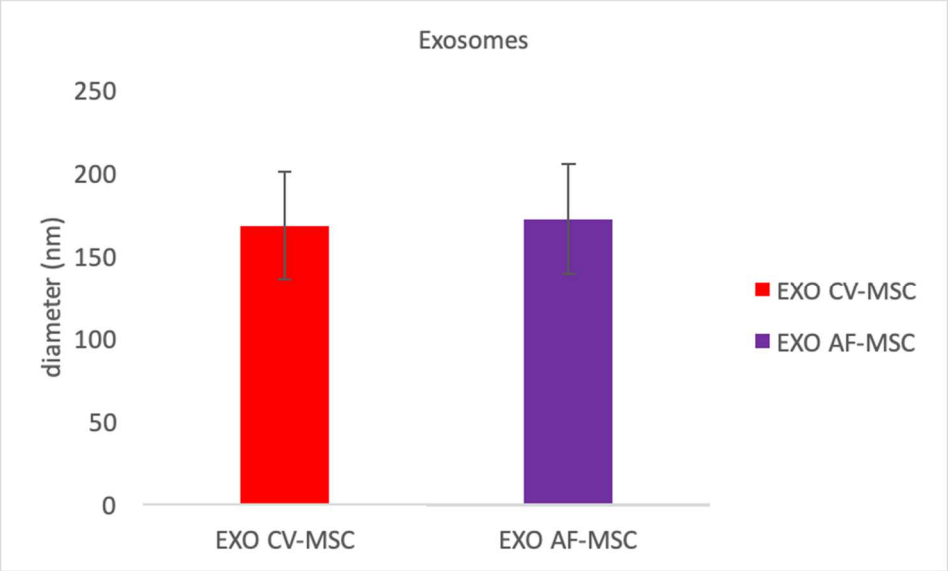

Figure 8. MSCs-derived exosomes characterization. Exosome derived from hCV- (EXO CV-MSC) and AF-MSCs (EXO AF-MSC) were characterized by AFM and NTA analyses. The main size is reported ± standard deviation.

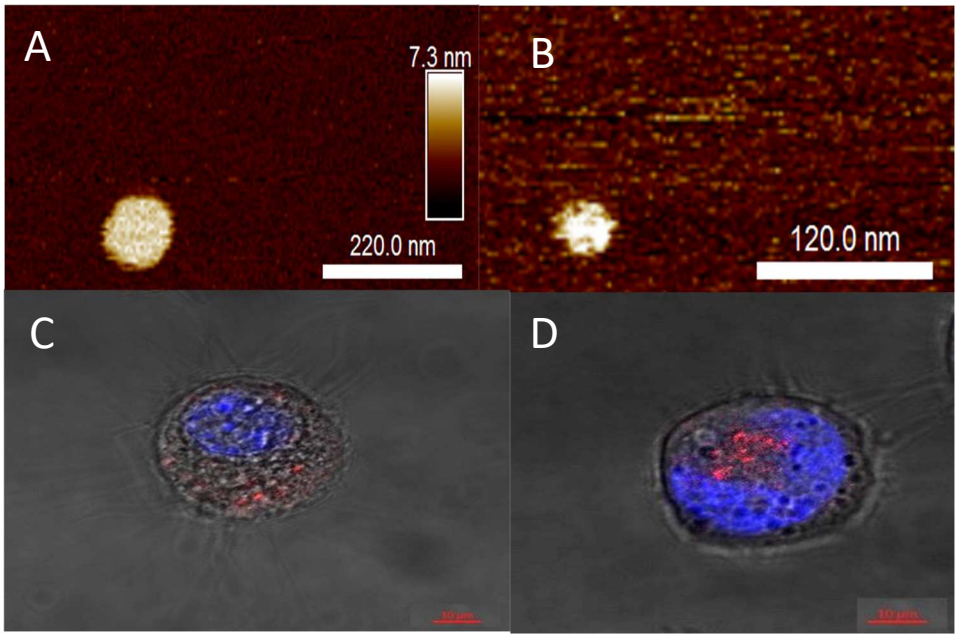

Figure 9. Examples of exosomes derived from EXO CV-MSC (A) and EXO AF-MSC (B) analyzed by AFM. Internalization of EXO AF-MSC in SKOV (C) and in OVCAR (D)

3.10 2D Cell Viability Assay

The viability assays were repeated testing the exosomes derived by hCV- and AF-MSCs on SKOV and OVCAR 2D cultures. As shown in FIG 8, we detected just a slight reduction at 72h in both cells lines (SKOV and OVCAR), of 10% ± 9.5 and 8% ± 12.3 respectively after the treatment with EXO CV-MSC. On the contrary, a greater reduction was induced in both cells lines by EXO hAF-MSC, with values around 27% ± 19.8 and 44.4% ± 1.6 (statistically significant) for SKOV-3 and OVCAR, respectively (FIG 10).

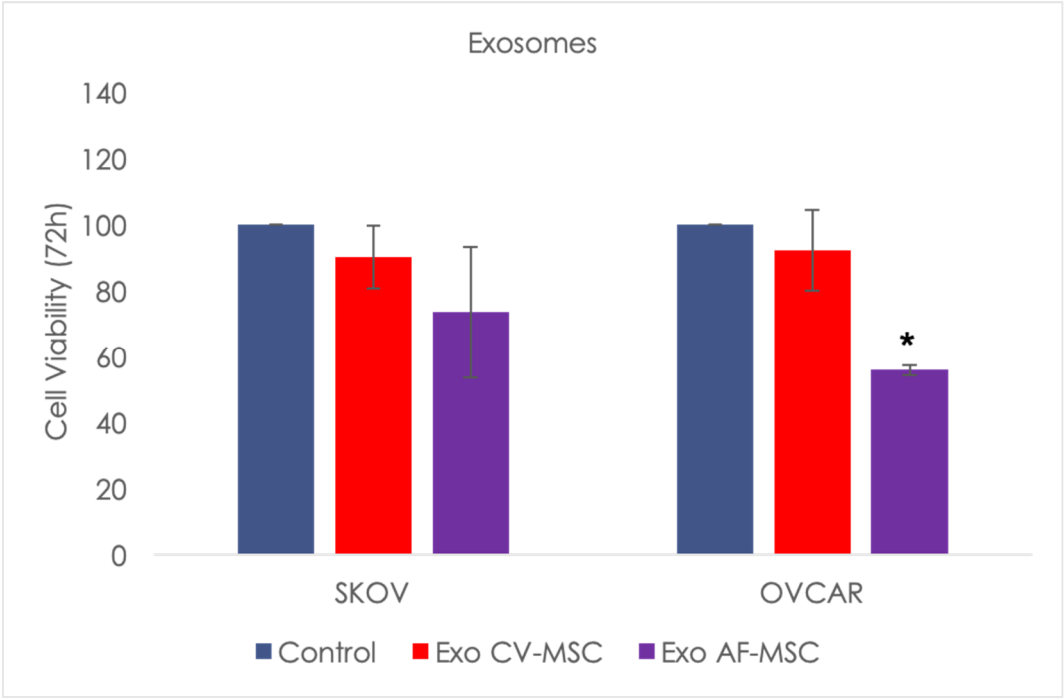

Figure 10. Effect of exosomes derived from MSCs on OC cells in 2D models. The SKOV and OVCAR cultures were exposed for 72h to the exosomes derived from hCV-MSCs (EXO CV-MSC) or AF-MSCs (EXO AF-MSC) The cell viability is reported for each condition as average of three biological replicates, ± standard deviation, and it is expressed as percentage of the viable cells compare to untreated cultures (Control). *=p<0.05, **=p<0.01

3.11 3D Cell Viability Assay

The same assay was performed in 3D cultures. As shown in the Figure 11, we observed a slight reduction of viability in SKOV-3 cells, specifically 20% ± 12 after exposure to EXO CV-MSC and 24% ± 5.6 after exposure to EXO AF-MSC, in comparison to untreated cells. However, OVCAR cells evidenced an opposite response, showing an increase in cell viability after exposure to both EXO CV-MSC (5% ± 14) and EXO AF-MSC (20% ± 8.7), compared to the Control (untreated cells).

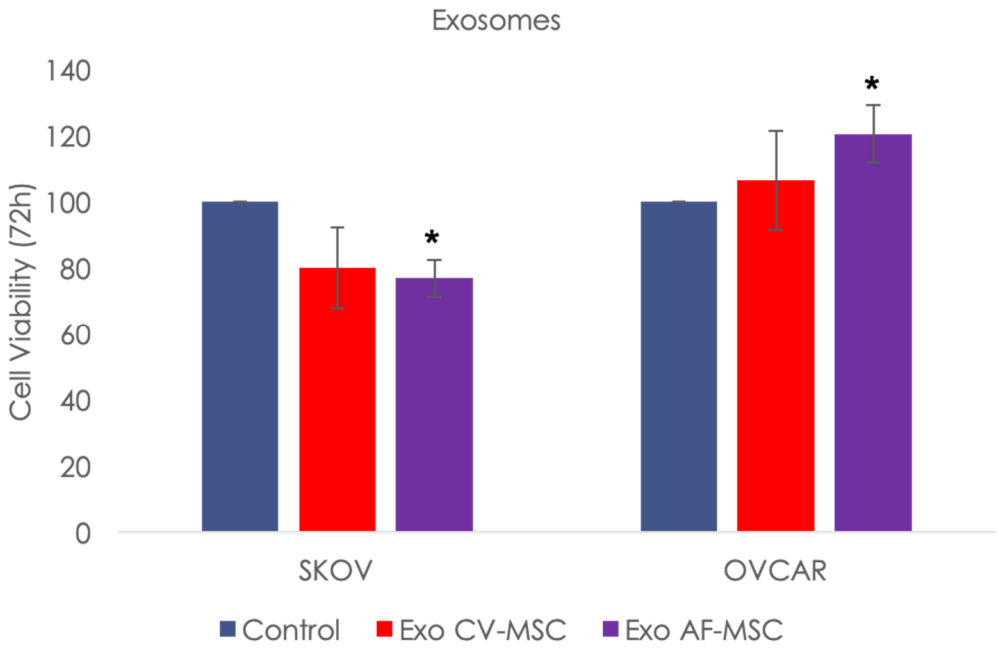

Figure 11. Effect of exosome derived from MSCs on OC cells in 3D models. The SKOV and OVCAR spheroids were exposed for 72h to exosomes derived from hCV-MSCs (EXO CV-MSC) or AF-MSCs (EXO AF-MSC) The cell viability is reported for each condition as average of three biological replicates, ± standard deviation, and it is expressed as percentage of the viable cells compare to untreated cultures (Control). *=$p<0.05$, **=$p<0.01$

3.12 Evaluation of apoptosis

The OC cells were evaluated for the apoptosis induction after the treatment with exosomes (EXO CV-MSC and EXO AF-MSC) for 72h, by the spectrophotometric detection of the light signal (i.e. early apoptosis) or fluorescent signal (i.e. late apoptosis). As shown in Figure 12, the majority of SKOV-3 cells were found in late apoptosis after the treatment with exosomes, with an increase of 53% ± 15.6 after treatment with EXO CV-MSC and 54% ± 11.8 with EXO AF-MSC, respectively, in comparison to untreated cells. However, a small part of SKOV-3 cells was revealed in early apoptosis induced by the treatment with EXO AF-MSC, with an increase of 44% ± 30 of the luminescence. Differently, OVCAR cells showed a different trend, reporting cells in early apoptosis and showing an increase of 22% ± 21 and 20% ± 4.5 in the luminescence after treatment with EXO CV-MSC and EXO AF-MSC respectively.

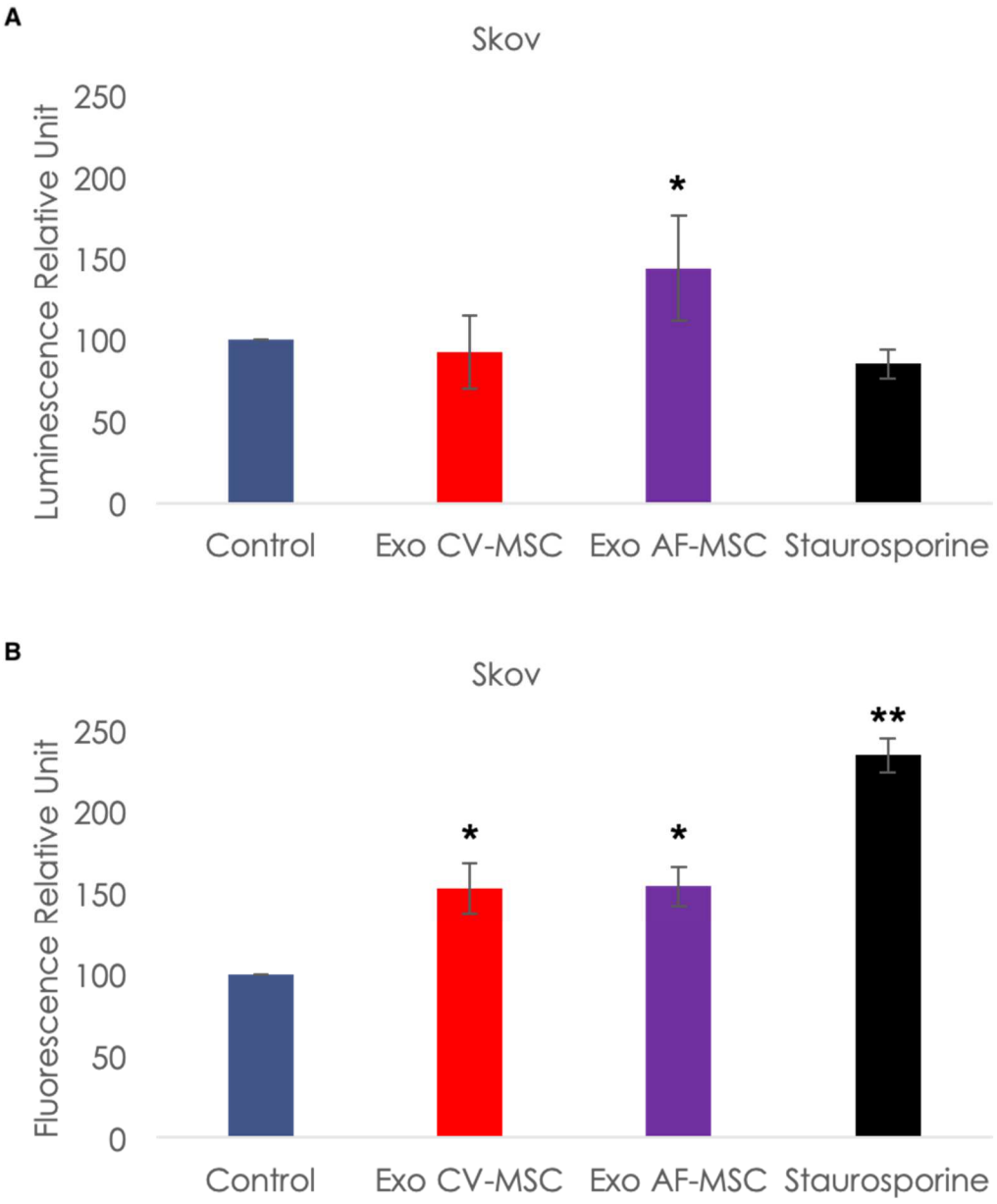

Figure 12. Apoptotic status evaluation in SKOV cells. The induction of apoptosis was evaluated in SKOV cells after 72h-treatment with exosomes derived from hCV-MSCs (EXO CV-MSC) and from AF-MSCs (EXO AF-MSC). The detection of early apoptosis (A), given by a luminescent signal, or late apoptosis (B) given by a fluorescent signal, was reported. The exosomes effect was compared to the behaviour of untreated cells (Control) and cells exposed to Staurosporine, considered as negative and positive controls, respectively. * = $p < 0.05$, ** = $p < 0.01$

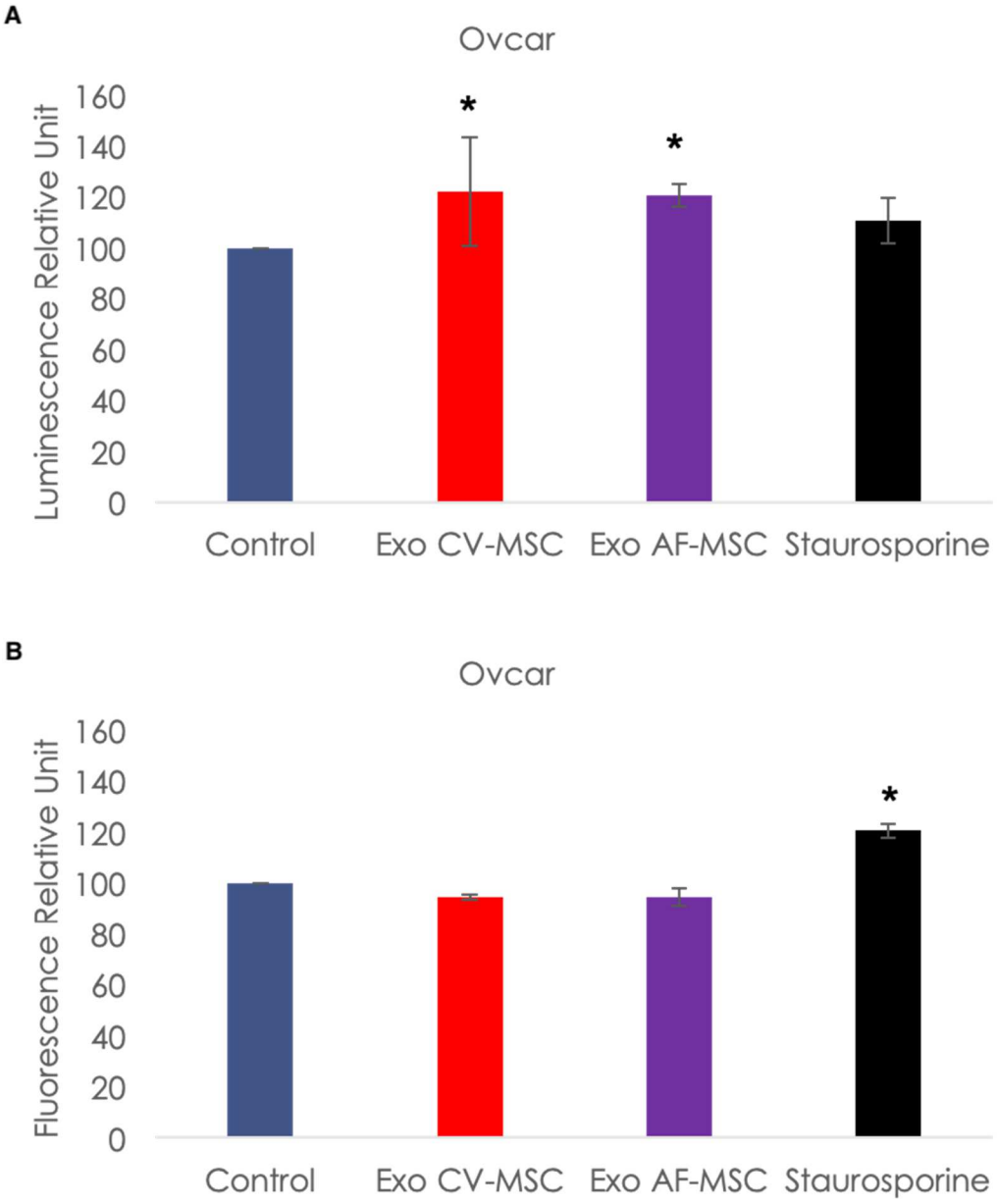

Figure 12. Apoptotic status evaluation in OVCAR cells. The induction of apoptosis was evaluated in OVCAR cells after 72h-treatment with exosomes derived from hCV-MSCs (EXO CV-MSC) and from AF-MSCs (EXO AF-MSC). The detection of early apoptosis (A), given by a luminescent signal, or late apoptosis (B) given by a fluorescent signal, was reported. The exosomes effect was compared to the behaviour of untreated cells (Control) and cells exposed to Staurosporine, considered as negative and positive controls, respectively. * = $p < 0.05$, ** = $p < 0.01$

4. Discussion

The tumor genesis is a complex process, involving different factors, directly related to the cell itself (i.e. genetic mutations) or present in the cell environment. For the latters, a major role is played by the cell- to-cell communication (109), which can differently influence the cellular destiny. In the specific case of ovarian cancer, the cells are exposed to stimuli from different cells lines (fibroblasts, stem cells, macrophages, regulatory T cells, endothelial cells and platelets) and various soluble factors, which affect them inducing different responses (99). The aim of this study was thus to determine the effect of exposure of ovarian cancer cells (SKOV and OVCAR) to MSCs derived from human Chorionic villi and Amniotic fluid. At first, the mesenchymal stem properties were tested, confirming that these cells have high proliferative rate (Fig.1-2 and Table 2) consistently with literature, and exhibit the specific mesenchymal markers ($CD44^+$, $CD73^+$, $CD90^+$, $CD105^+$, $CD29^+$ and lack $CD34^-$ $CD45^-$). Moreover, their pluripotency was determined by the detection of the specific NANOG and OCT-4 markers (101). Remarkably, MSCs derived from hCV showed higher proliferative activity and mesenchymal markers expression then those derived from hAF. Subsequently, the influence of these cells lines (hCV- and AF-MSC) was tested through the exposure of ovarian cancer cells (SKOV and OVCAR) to MSCs conditioned medium. This

approach was selected in order to efficiently assess the effect of the factors released by MSCs into the medium on ovarian cancer, avoiding the direct contact between the cell lines. All experiments were performed in two settings i.e. 2D and 3D cultures, to understand the possible effect derived by conditional medium derived from both MSCs. Although a great viability reduction (SKOV 57% ± 2; OVCAR 63 ± 1.8) was observed after the exposition of CM-MSC in both ovarian cancer cells, we didn't note the same behavior in 3D models, which represent a more realistic setting, especially regarding the stimuli the cells are exposed to (110, 111). On the other hand, it was observed the significant viability reduction after the exposure of CM-CV and CM-AF at 72h on SKOV and OVCAR 2D cultures. Subsequently, these data have been confirmed in 3D model (FIG 7) and are in agreement with the data obtained by Reza et al. (108). These results confirmed the effect of the paracrine signals released by mesenchymal stem cells (112), and thus we decided to focus the attention on the role of exosomes inside at the CM derived by hCV- and AF-MSCs. First, the extraction of exosomes was performed from both cells lines (hCV and AF-MSC) and the exosome shape and concentration were determined through the AFM and NTA analyses. Then, OC cells were treated with the recovered exosomes, testing their action in both 2D and 3D models. The experiments performed in SKOV revealed a great viability reduction

after the exposition to EXO CV-MSC and EXO AF-MSC, observed in both 2D and 3D cultures and reporting even the activation of an apoptotic mechanism. The same experiments performed on the OVCAR cell line produced a decrease of cell viability just in the 2D model (FIG 8), together with the detection of an apoptotic mechanism. The 3D cultures showed discordant data; however, this study model is affected by a great heterogeneity, as already reported in literature (113), so the results will be confirmed in future studies. Remarkably, both the CM and the EXO derived from AF-MSCs, induced the greater and most significant reduction in ovarian cancer cells in comparison to CV-MSC, suggesting their potential action against cancer cell and warranting further studies. Taken together, our preliminary data demonstrate that the soluble factors involved in the cross-talk play an important role in ovarian cancer genesis/modulation (114) and in particular the exosomes derived from AF- and CV-MSCs demonstrate to have an effect on SKOV and OVCAR cells. This work opens an applicative scenario, proposing the mesenchymal stem cells derived from fetal adnexa as promising candidates for the cell therapy; however further studies will be required to elucidate the target mechanisms involved in the cancer proliferation reduction. In particular, we suggest to investigate and focus the attention on the genes involved in the apoptotic cascades activation.

Chapter II Characterization and Evaluation of the potential of Human Chorionic Villi-Mesenchymal Stem Cells derived from fetuses diagnosed with Down Syndrome

1. Introduction

Regenerative medicine involves the use of living cells to repair, replace or restore normal functions in injured tissues and organs (100, 115). Mesenchymal Stem Cells (MSC) derived from fetal (bone marrow, blood and liver) and extraembryonic tissues (amniotic fluid, umbilical cord blood, amniotic membrane, and chorion) are very promising candidates for cell-therapy due to their properties, in particular the high proliferation rate, the differentiation capacity and the low immunogenicity. This last comprehends both good immuno-suppressive and modulatory properties. In previous study performed in Dr. Corradetti's laboratory at Polytechnic University of Marche, Human Chorionic Villi (hCV) and Amniotic Fluid (hAF) MSCs derived from women in good health have been characterized, resulting as optimal candidates for therapeutic and regenerative medicine. Among them, hCV-MSC showed the best features for a possible use in regenerative medicine, especially for clinical application that requires an immunomodulatory approach. hCV are normally isolated from fetuses at the first gestational trimester for diagnostic purposes. At this stage the villi are considered the basis for growth and differentiation of the villous trees. Moreover, the stem cells isolated from placenta, including the chorionic villi, are considered to be in an intermediate status between embryonic stem cells and adult MSC. Previous studies

performed on hCV-MSCs showed different functional characteristics, specifically high proliferative potential, non-teratogenic activity and the ability of differentiate in various tissue such as osteoblast (bone cells), chondrocytes (cartilage cells) and adipocytes (fat cells which give rise to marrow adipose tissue), mesoderm and ectoderm)(116).

Trisomy 21, trisomy 18 and trisomy 13 are the most common constitutional trisomies in humans (117). In particular Down Syndrome (DS), which is caused by the trisomy of chromosome 21 (HSA21), is the most common genetic developmental disorder, with an incidence of 1 in 800 live births (118). DS is a multisystem disorder caused, in most cases, by meiotic non-disjunction of the maternal Hsa21, resulting in a third copy of the entire Hsa21 in all cells (119, 120). This disorder causes craniofacial abnormalities, hypotonia and cognitive impairment. Furthermore, the individuals with DS are subjected to the development of additional pathological conditions such as thyroid disease, gastrointestinal defects, leukemia, cardiac defects and cancers. The aim of this study was to characterize hCV-MSCs from women carrying fetuses with diagnosed Down Syndrome in comparison to their euoploid counterparts in terms of proliferation, identification of specific MSC-associated markers, cell cycle, production of free radicals and immunosuppressive molecules, after exposure to pro-inflammatory cytokines. This allowed us to evaluate the possible interference of DS

in the hCV-MSCs stemness properties and their putative application in regenerative medicine.

2. *Materials and Methods*

2.1 Cell cultures

hCV-MSC were obtained from pregnant women undergoing prenatal diagnosis between the 10^{th} and the 13^{th} weeks of gestation. Cells were allowed to migrate out of the tissue and to adhere to the surface of the flask using an explant culture method. These primary cells, proliferating in clusters, were let to expand in High Glucose-DMEM (Corning) supplemented with 10% fetal bovine serum (FBS), 1% L-glutamine, 2% antimitotic-antibiotics (EuroClone S.p.A, Pero, Milano, Italy).

ThP1 cells (ATCC Manassas, Virginia, United States) were cultured in RPMI-1640 media (Gibco) supplemented with 10% fetal bovine serum (Corning), 1% L-glutamine, and 2% antimitotic/antibiotic. All cells were cultured under an atmosphere of 5% CO_2 at 37◦C

2.2 Proliferation assay

Growth curve analysis, Doubling time, Colony-forming unit-fibroblastic like (CFU-F) and immunostaining assays were performed as described above (chapter I, methods section, pages 49-50)

2.3 Cell cycle

To determine possible differences in the cell phases distribution (G0/G1, S and M), cell cycle was examined using flow cytometry

(Guava Millipore cytometer). Briefly, cells (1×10^6) at passage P2 were harvested and were fixed by overnight incubation with cold ethanol (70%). They were then resuspended with a staining solution containing Propidium Iodide (PI) (40 μg/ml), RNase (100 μg/ml) and PBS 1x. Flow cytometry data were acquired using a Guava Millipore cytometer. At least 20 000 cells/sample were run. The percentage of cells in sub G0, G1, S, and G2/M was established using GUAVASOFT 2.2.3. software.

2.4 Evaluation of MSC-associated markers

MSCs were characterized at P2 for surface MSC-associated markers by flow cytometry. A total of 5×10^5 cells were trypsinized, fixed with 75% ethanol and incubated for 20 minutes with 0.5% bovine serum albumin (BSA)/PBS to block non-specific sites. The sample was centrifuged at 500xg for 5 minutes at 20°C and additioned with 5μl of fluorescently labeled antibody. Directly conjugated antibodies were as follows: phycoerythrin (PE)-conjugated ecto-5'-nucleotidase (PE-CD73; BioLegend), fluorescein isothiocyanate (FITC)-conjugated thymocyte differentiation antigen 1 (FITC-CD90; BioLegend) and the glycoprotein CD44 (FITC-BioLegend), Allophycocyanin (APC)-conjugated for integrin b1 (APC-CD29; BioLegend). Cells were incubated for 45 min at room temperature in the dark, then washed

twice with filtered PBS, to remove the excess of antibody, and analyzed using Guava Easycyte Millipore flow cytometer with GUAVASOFT 2.2.3 software.

2.5 Molecular characterization

MSC-associated markers were evaluated even by quantitative reverse transcription polymerase chain reaction (qRT-PCR), as shown in Table 1; moreover, pro and anti-inflammatory genes expression was assessed as shown in Table 2. In all cases, total RNA was isolated using TRI-reagent (Invitrogen) and purified from genomic DNA through digestion with DNAse (Sigma). RNA concentration and purity were measured using a NanoDrop ND1000 spectrophotometer (NanoDrop Technologies). The cDNA was synthesized from 500 ng of total RNA using the PrimeScript RT Master Mix (TAKARA), and quantitative PCR was run in the StepOnePlus Real-time PCR termocycler (Applied Biosystems), using a commercially available master mix (PowerUp SYBER Green Master Mix; Applied Biosystems).

Table 1. Transcripts and sequence of each primer used in real time RT-PCR to characterize Mesenchymal stem cell-associated properties.

GENE	Sequences (5'→3')	Tm (°C)	Product size (bp)
Mesenchymal markers			
CD105	S: CCTGGAGTTCCCAACGGGCC A: GGCTCTTGGAAGGTGACCAGG	65 62	186
CD90	S: CTTTGGCACTGTGGGGGTGC A: GATGCCCTCACACTTGACCAG	64 61	211
CD73	S: GCTCTTCACCAAGGTTCAGC A: GTGGCTCGATCAGTCCTTCC	59 60	203
CD44	S: GGAGCAGCACTTCAGGAGGTTAC A: GGAATGTGTCTTGGTCTCTGGTAGC	63 63	129
CD29	S: GAGTGCCGTAACAACTGTGG A: AAGCTACCTAACTGTGACTATGG	59 57	116
Reference gene			
Glyceraldehyde-3-phosphatase dehydrogenase (*Gapdh*)	S: TCCACTGGCGTCTTCACC A: GGCAGAGATGATGACCCTTT	68 70	78

S= sense primer, A= antisense primer Tm= melting temperature

2.6 Differentiation potential

To evaluate MSC plasticity, hCV-MSC and DS-hCV-MSC were differentiated into the adipogenic and osteogenic lineages. MSCs were seeded at the density of 1.4 x 10^4 cells/cm^2 in 12-well plates and cultured until they reached about 80-90% confluence. For the induction of osteogenic and adipogenic differentiation, cells were cultured using StemProOsteogenic and Adipogenic Differentation Kit (Gibco), according to the manufacturer's instructions up to 21 days. To confirm mineral deposition and cytoplasmic inclusions of lipids, conventional Von Kossa and Oil Red O stainings were performed.

2.7 Reactive Oxygen Species (ROS) Detection

To evaluate cellular oxidative stress, the reactive 2',7'-dichlorodihydrofluorescein (H2-DCFDA Sigma-Aldrich) assay was performed. Cells were trypsinized, washed two times with cold PBS, suspended with prewarmed PBS containing the probe at a working concentration of 10 μM and incubated for 30 minutes at 37°. Then the cells were washed two times in PBS and labeled with 10μg/ml Propidium Iodure (PI) to remove false negative results. Fluorescent cells were analyzed using Guava Easycyte Millipore flow cytometer with GUAVASOFT 2.2.3software.

2.8 Immunosuppressive potential assessment

hCV- and DS-hCV-MSCs were seeded at the density of 2 x 10^4 in the 24-wells plate at passage P2 and cultured for 24h at 37°C before stimulation. The cells were washed with PBS and exposed to soluble recombinant rat *TNF-α* and *IFN-γ* (Prepotech) at the concentrations of 20 ng/mL each, for 24h and 48h. At each time point cells were collected and total RNA was extracted using TRI REAGENT according to manufacturer's instruction. The expression of immunosuppressive-associated markers (table n 2) in hCV-MSC and DS-hCV-MSCs was performed by qPCR.

Table 2. Sequence of each primer used in real time RT-PCR to evaluate pro and anti-inflammatory genes.

GENE	Sequences (5'→3')	Tm (°C)	Product size (bp)
Pro-inflammatory genes			
Interleukin 1 beta (*Il-1β*)	S: TGCTCTGGGATTCTCTTCAGC A: CTGGAAGGAGCACTTCATCTG	59 60	164
Tumor necrosis factor a (TNF-a)	S: TCTGGCCCAGGCAGTCAGATC A: TACAGGCCCTCTGATGGCACC	64 64	180
Interleukin 6 (IL-6)	S: AACTCCTTCTCCACAAGCGC A: ATGCCGTCGAGGATGTACCG	60 62	188
Anti-inflammatory genes			
Prostaglandin E-receptor (*Pge-2*)	S: GGAAGGAGAAAGCTCGCAAC A: TGAGCCAGTACTTATTGCCG	58 57	173
Transforming growth factor beta (*Tgf-β*)	S: TGGTCATGAGCTTCGTCAAC A: TCTCATTGTCGAAGCGTTCC	58 58	171
Cytochrome c oxidase subunit II (*Cox-2*)	S: TGAGTTATGTGTTGACATCCAG A: TCATTTGAATCAGGAAGCTGC	62 60	190

S= sense primer, A= antisense primer Tm= melting temperature

2.9 RNA-sequencing – Differential Expression Analysis

Total RNA was extracted and purified from hCV-MSCs and DS-CV-MSCs at passage P2 using Total RNA Purification Plus Kit (Norgen, Biotek Corp) and processed by an external core based in Verona University (Functional Genomic Center, University of Verona). RNA purity and quantity were measured using a NanoDrop Spectrophotometer, (NanoDrop® Spectrophotometer ND-1000, Nd-1000 V3.5.2 software). while RNA integrity was assessed using the RNA 6000 Nano Kit (Agilent Technologies). RNA-seq library preparation was performed using the TruSeq stranded mRNA kit (Illumina) from 1μg of RNA samples. Librarie size was assessed by capillary electrophoretic analysis with the Agilent 4200 Tape station.

RNA libraries were analyzed on an Illumina NextSeq 500 sequencer using 75nt single reads. For each sample, the sequencing generated an average of 34 million fragments per sample.

The quality of the reads was checked using software FastQC (http://www.bioinformatics.babraham.ac.uk/projects/fastqc/), discarding those reporting more than 50 bp with low scores. Subsequently, through the software Scythe (**https://github.com/vsbuffalo/scythe**) the adapters inside at the reads were took off, then the reads showing low quality were modified at their endings using the software Sickle (**https://github.com/vsbuffalo/sickle**).

Gene ontology (biological processes) was analyzed for discrepancy in gene expression between hCV-MSCs and DS-MSCs by using Enrichr (https://amp.pharm.mssm.edu/Enrichr/), followed by REVIGO (http://revigo. irb.hr) to visualize the top enriched GO terms (biological processes).

2.10 Preparation of conditioned medium

The conditioned medium (CM) produced by CV and DS-CV grown for 48 h in Standard Culture Medium with addition of FBS exosomes depleted at the density of $2.5x10^6$ in T25 flask. The CM was collected,

centrifuged at 500 x g, filtered through a 0.45 μm pore size and kept at -80 °C until use.

2.11 Immunomodulatory potential

The ability of Euploid and Down Syndrome MSCs to induce the phenotype changes in mononuclear cells (THP-1) was assessedThp-1 cells were plated at density $5x10^5$ in 24-wells plate and then treated with the conditioned medium obtained from Euploid and Down Syndrome for 24/48 hrs. At each time point, the cells were collected, washed with PBS and total RNA was extracted using TRI REAGENT according to manufacturer's instruction. Finally, the expression of immunosuppressive- associated markers (table n 2) was evaluated by qPCR in hCV-MSC and DS-hCV-MSC.

2.12 Statistical analysis

Statistical analysis was performed using GraphPad Instat 3.00 for Windows (GraphPad Software). Three replicates for each experiment (growth curve, doubling time, colony forming unit, qPCR and cytometry analysis test) were performed and the results are reported as mean ± standard deviation (SD). One-way analysis of variance for

multiple comparisons by the Student-Newman-Keuls multiple comparison test were used to assess differences between groups. Differences were considered statistically significant for p values were < 0.05. For quantitative PCR data, non- parametric tests were used.

3 Results

3.1 Proliferation assays

Preliminary data demonstrate that differences between hCV-MSCs and DS-hCV-MSCs derived from women carrying fetuses with or without diagnosed Down Syndrome exist. DT resulted similar both Euploid and DS cell lines for all passages (from P2 to P5) and it remained constant until P5 as shown in the fig n° 1

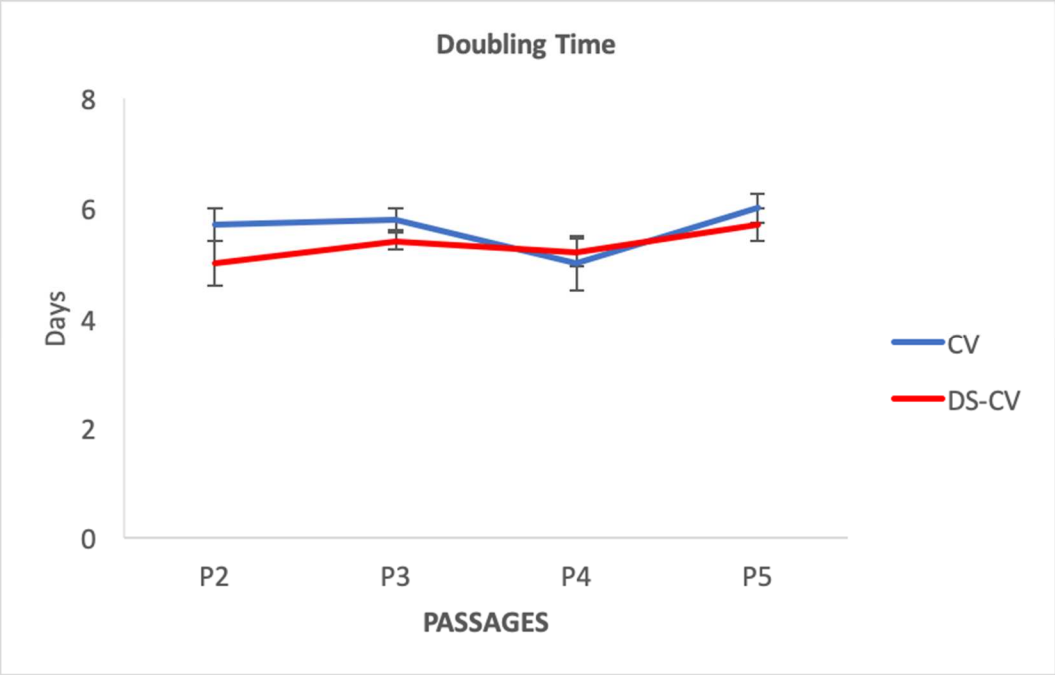

Figure 1 Proliferation studies, Doubling Time assays. Euploid (hCV-MSCs, blue line) and Down Syndrome MSCs (DS-hCV-MSCs, red line) were evaluated for their DT from P2 to P5. The results are reported as average of three biological replicates ± standard deviation.

However, As shown in the chart (Figure 2), after 3 days of culture, significant differences in proliferation parameters were found ($p < 0.05$), reporting a greater proliferative capacity of hCV- MSCs in comparison to DS-hCV-MSC.

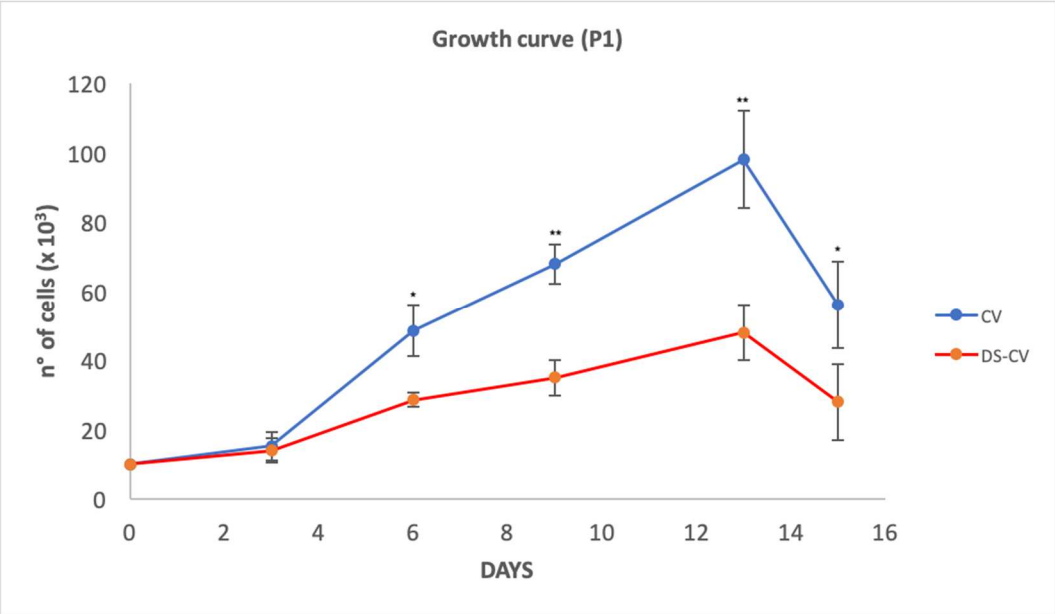

Figure 2 Proliferation studies, growth curve analysis. Euploid (hCV-MSCs, blue line) and Down Syndrome MSCs (DS-hCV-MSCs, red line) were cultured from P2 for 15 days and counted mostly every 2 days. The results are reported as average of three biological replicates ± standard deviation. *= p< 0.05, **= p< 0.01

On the contrary, the CFU-F assay proved that DS-hCV-MSCs display the same capability to form colonies as normal hCV-MSCs, as reported in Table n 3

Table 3 Colony-forming unit-fibroblast assay performed on hCV-MSCs and DS-hCV-MSCs. Determination of total collected cells and CFU for each tested cell density/ cm^2.

	density cells/cm ^{2}	Total cells	CFU
hCV-MSCs	350	3325	0
	1000	9500	2 ± 0.3
	3500	33250	10 ± 0.6

	density cells/cm ^{2}	Total cells	CFU
DS-hCV-MSCs	350	2175	0
	1000	7230	2 ± 0.2
	3500	3148	8 ± 0.6

The results are reported as average of three biological replicates ± standard deviation. .

3.2 Cell cycle

Cell cycle analysis was performed to determine the influence of chromosome 21 trisomy on the cell phases distribution (G1, S and G2/M). Consistently with growth curve analysis, our results indicated that the number of cells in G1 phase (78%) and S phase (6.21%) increased in the DS-CV, compared to control cells (CV) (Fig 3)

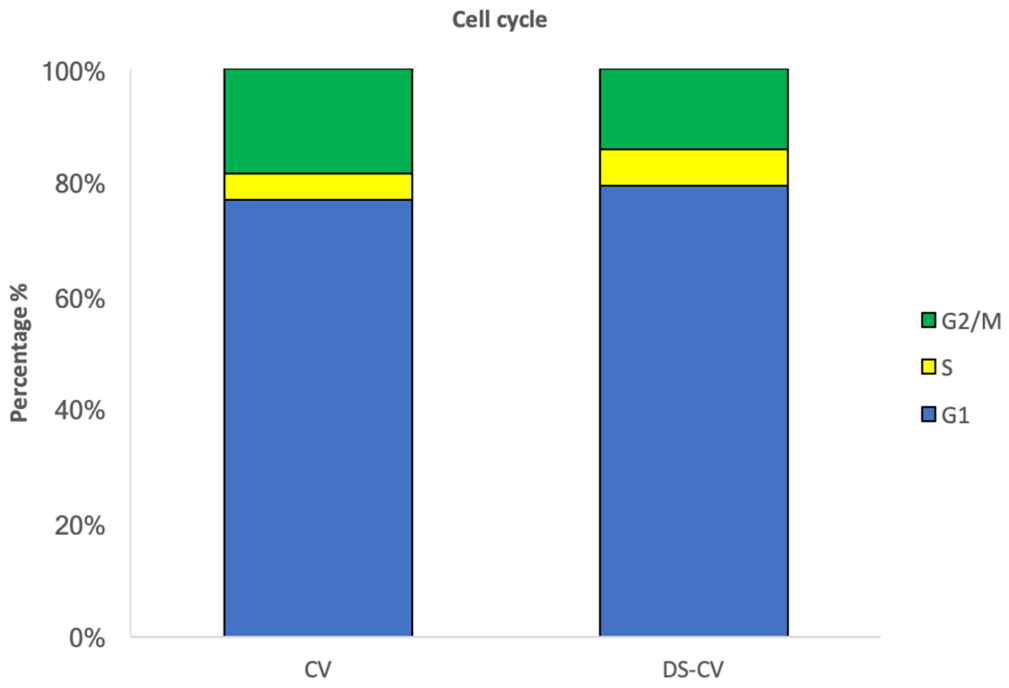

Figure 3. Cell cycle analysis performed on hCV-MSC (Euploid) and DS-CV-MSC (DS). Data are reported as average of the percentage of cells distributed in the subG0, G1, S, and G2/M phase ± SD (n = 3).

3.3 Immunostaining

Cell structures were visualized through immunostaining. As shown in Figure 4, the MSCs in culture were plastic adherent and showed a fibroblastic-like morphology, confirming the first criteria that define MSCs.

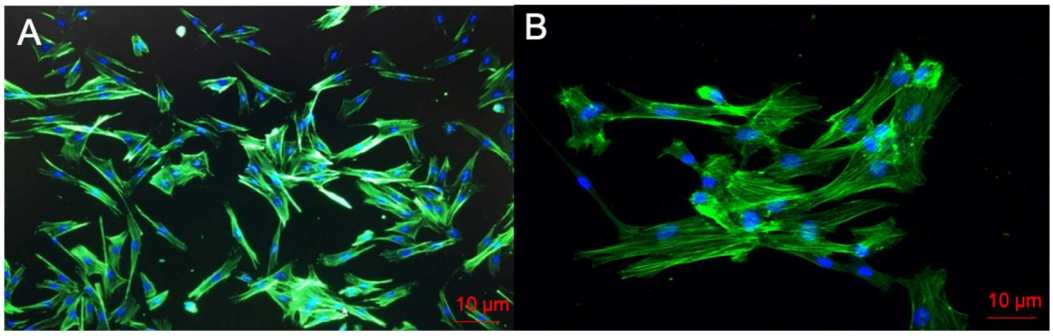

Figure 4. **hCV- (A) and DS-CV-MSCs (B), respectively.** Green: F-Actin, Blue: Nuclei. 10X magnification

3.4 Flow Cytometry Analysis

The main mesenchymal-associated markers (CD73, CD44, CD29 and CD90) were detected through flow cytometry even in DS-hCV-MSCs at passage 2, as in euploid hCV-MSCs. Remarkably, the CD73 expression resulted significantly higher in the cells affected by DS, as shown in Figure 5-6.

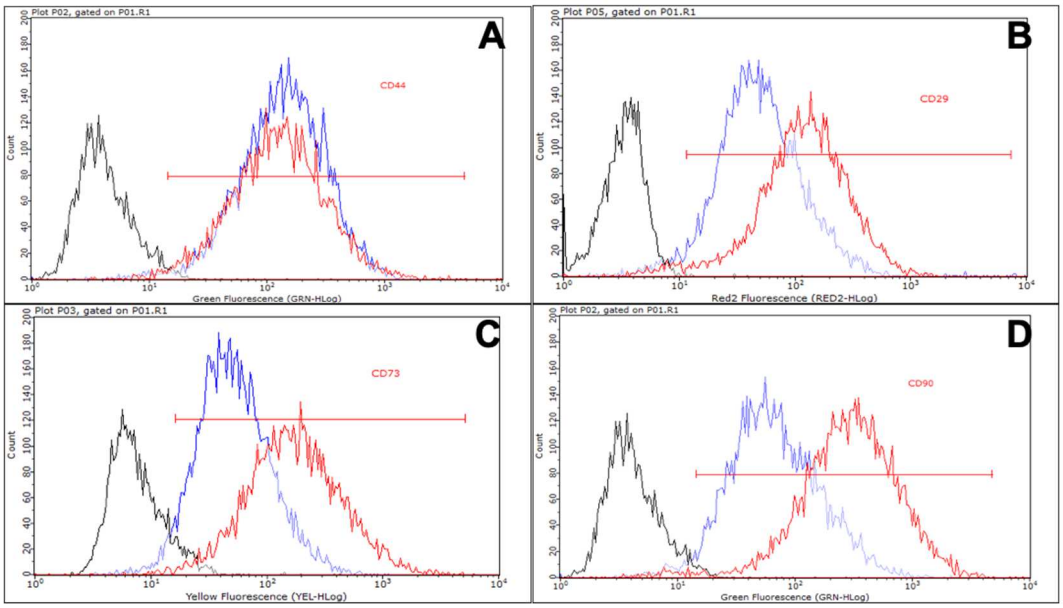

Figure 5. Determination of mesenchymal markers by flow cytometry; hCV-MSCs (blue) and DS-hCV-MSCs (red) were analysed for the expression of the mesenchymal markers CD44+ (A), CD29+ (B), CD73+ (C) and CD90 (D). The results are compared to unstained cells (black).

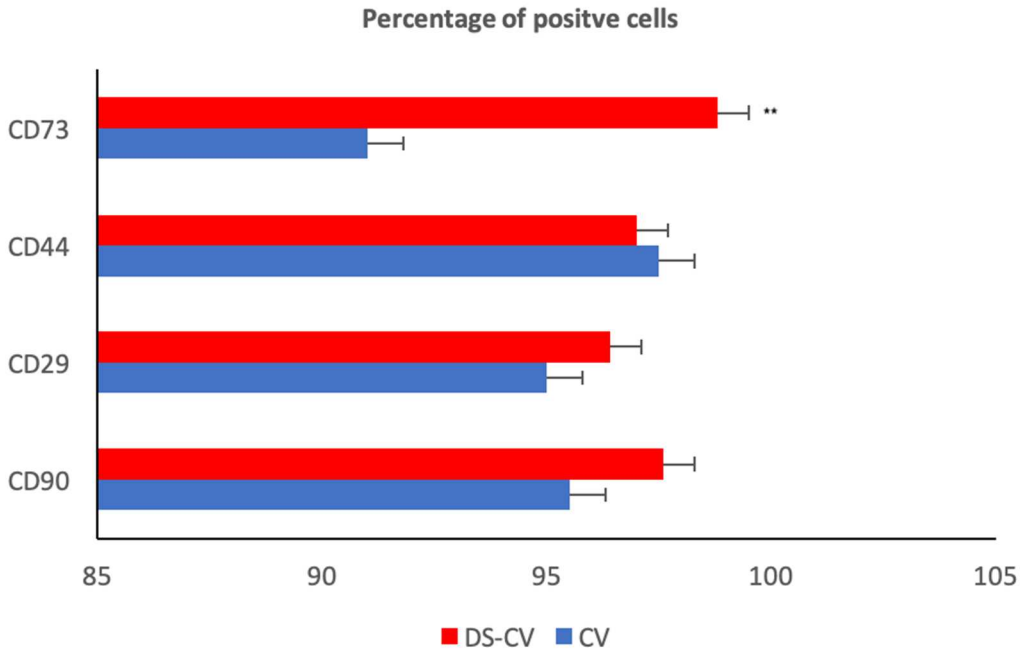

Figure 6. Determination of mesenchymal markers by flow cytometry; the expression level of each marker is compared in hCV-MSCs (blue) and in DS-hCV-MSCs (red). The results, presented as percentage of marker-positive cells, are reported as average of three independent experiments ± standard deviation. *= $p < 0.05$, **= $p < 0.01$

3.5 Mesenchymal Markers

The expression of the mesenchymal stem cell-associated markers was then evaluated in both the cell lines after 48h treatment with pro-inflammatory cytokines (i.e. *TNF-α* and *IFN-ɣ)* by qPCR. All the markers showed an increase in the relative mRNA levels in hCV-DS-MSCs compared to hCV-MSCs, as shown in Figure 7. Specifically, the expression levels resulted 1.73 ± 0.05-fold for CD105, 3.61 ± 0.32-fold for CD90, 5.07 ± 0.18-fold for CD73, 5.85 ± 0.37-fold for CD44 and 8.90 ± 0.18-fold for CD29, respectively.

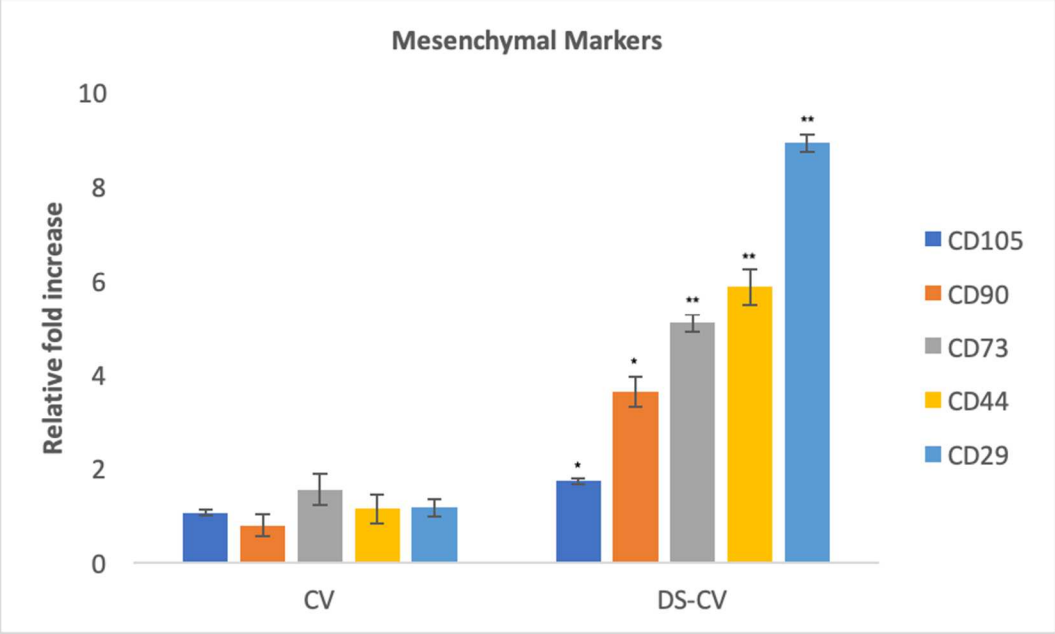

Figure 7. Determination of mesenchymal markers expression by qPCR; the expression level of each marker was determined by qPCR and compared in hCV-MSCs and in DS-hCV-MSCs exposed for 48h to TNF-α and IFN-ɣ. The results are reported as average of three independent experiments ± standard deviation. *= p< 0.05, **= p< 0.01.

3.6 Differentiation potential

The CV- and DS-CV at P2 were evaluated for their differentiative potential through specific stainings for osteogenic and for adipogenic tissues. Both the MSC lines from were able to produce mineralized extracellular matrix and to develop vacuoles containing lipid droplets under osteogenic- and adipogenic-inducing conditions, respectively. Osteogenic differentiation was then confirmed by Von Kossa staining in both cell lines (FIG 9), while the adipogenic differentiation was confirmed by Oil Red O staining as reported in the FIG 8. Interestingly, the hCV-MSCs appeared to be more reactive to differentiative stimuli respect to cells bearing the trisomy (DS-CV) (FIG 8).

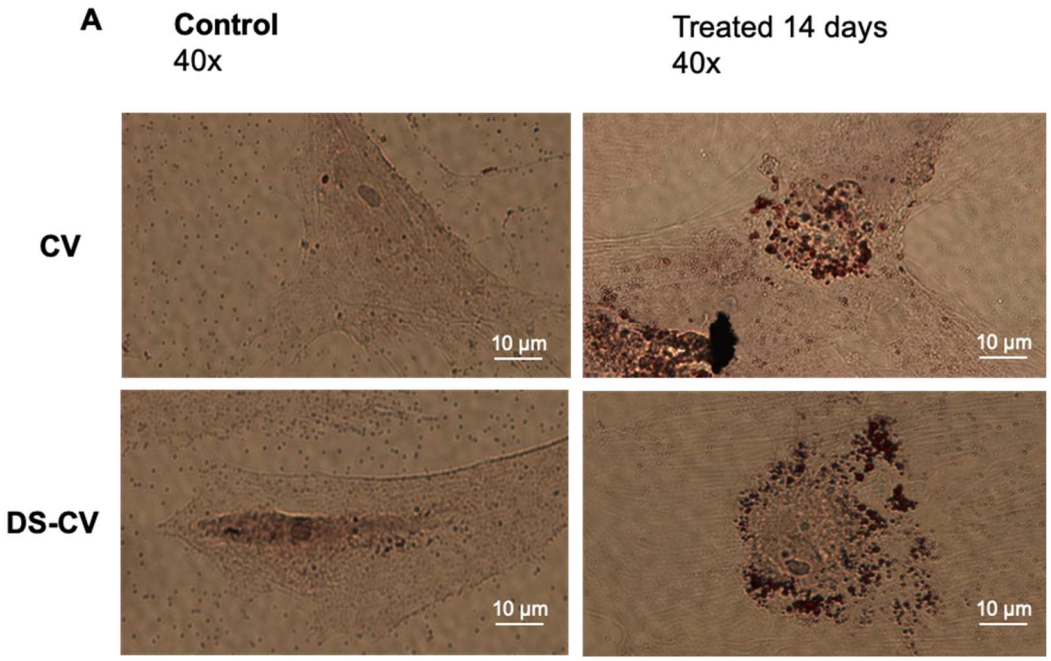

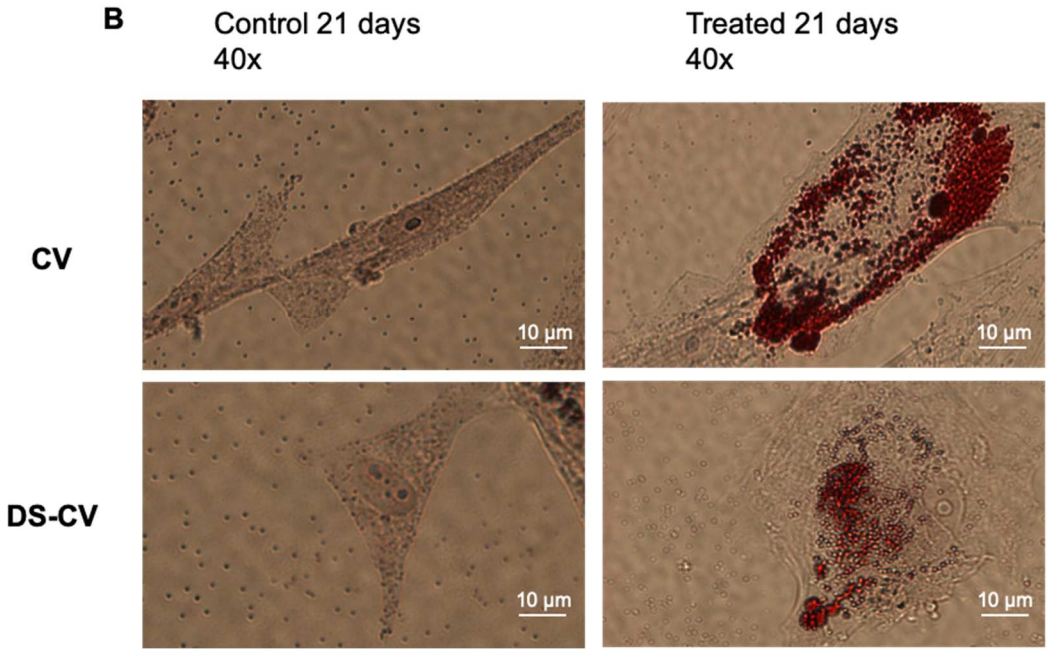

Figure 8. Staining of differentiated and undifferentiated (control) hCV- /DS-CV-MSCs. Cells were subjected to adipogenic differentiation for 21 days. All samples preparations, Oil red O-stained, were observed at a OLYMPUS BX51 microscope at 40x magnification after. (A) 14 days and (B) 21 days of adipogenic differentiation.

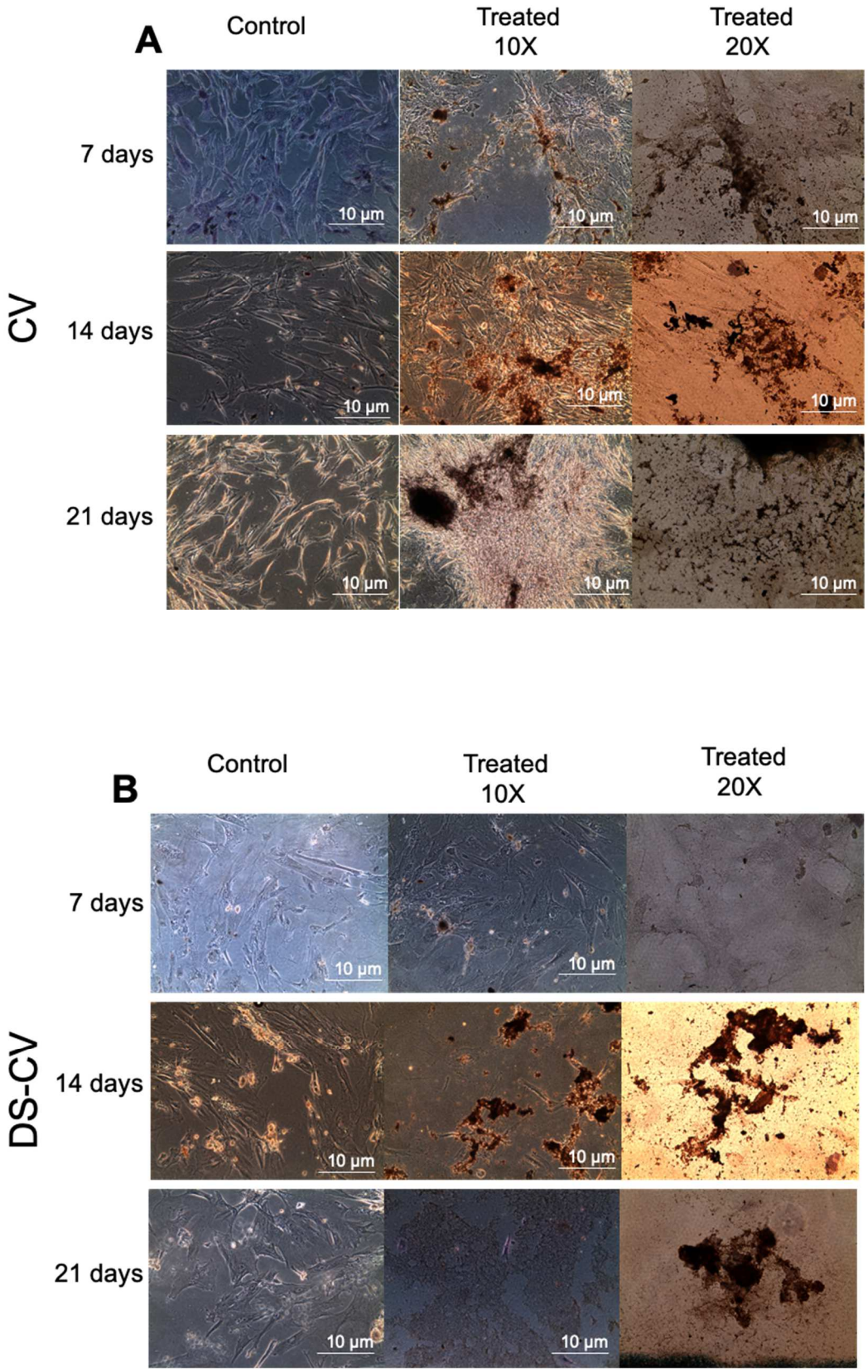

Figure 9. Staining of differentiated and undifferentiated (control) hCV- /DS-CV-MSCs. Cells were subjected to osteogenic differentiation for 21 days. Both hCV-MSCs (A) and DS-hCV-MSCs (B), specifically stained (Von Kossa staining), were observed at a BX51 (Olympus) microscope at 10 and 20X magnification every 7 days.

3.7 Reactive Oxygen Species (ROS) Detection

The basal levels of the normal metabolism of oxygen were observed in both in CV-s and DS-CV through the measurement of the ROS production by flow cytometry. As shown in Figure 10, the DS-CV released higher levels of ROS than hCV-MSCs, specifically around 670.4 ± 52.1 and 502.5± 49.3, respectively.

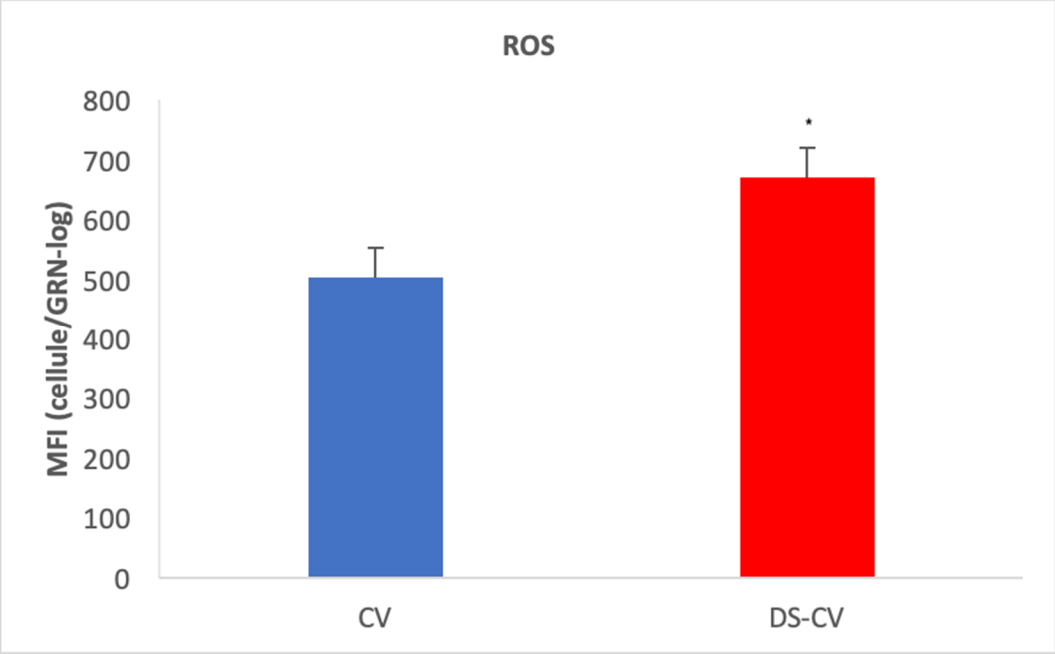

Figure 10. Evaluation of ROS production by CV (blue) and DS-CV (red) by Flow cytometry analysis. The data are reported as average of three biological replicates ± standard deviation.

3.8 RNA-sequencing – Differential Expression Analysis

All RNA samples showed an integrity number (RIN) >9. The obtained reads were about 30 millions for each sample. (table 4) The main differences between CV and DS-CV were evidenced by the analysis of their gene expression, showing a specific pattern of up-/down-regulated genes for each cell line (FIG 11). Consistently with the observed phenotypical features, DS-CV reported the down-regulation of genes involved in proliferative processes, in the DNA replication and in the Mitotic Cell cycle phase transition (FIG 13). Specifically, a negative regulation of G1/S phases transition during cell cycle, was observed (FIG 13). On the other hand, the up-regulated genes are mainly involved in the extracellular matrix organization, in the response to beta-amyloid and in astrocyte activation (FIG 15).

Sample Name	Experimental group	Raw Reads	Aligned Reads
hCV_1	Chorionic villus	32,119,080	31,712,178
hCV_2		29,440,066	29,059,187
hCV_3		33087547	32660877
DS.hCV_1	Chorionic villus from Down syndrome	34,198,925	33,768,003
DS.hCV_2		35,575,785	35,086,438
DS.hCV_3		37,819,995	37,312,349

Table 4. Gene reads obtained during the RNAseq for each experimental group of hCV. In the table, Raw and aligned reads indicate the reads before and after the bioinformatics processes respectively.

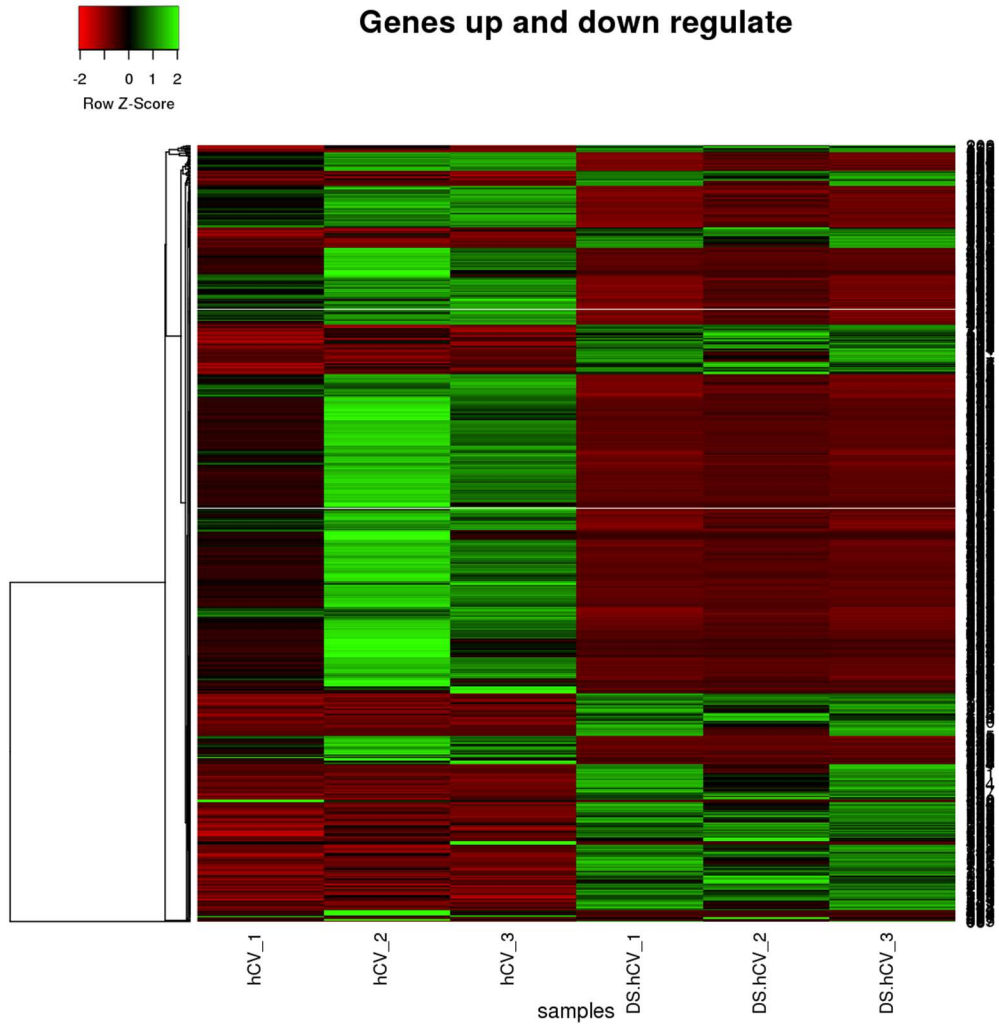

Figure 11: Heatmap of all expressed genes compared between hCV and DS-hCV. The expression levels of genes are displayed as color-coded: red = constitutive expression, green= over-expression (padj 0.01).

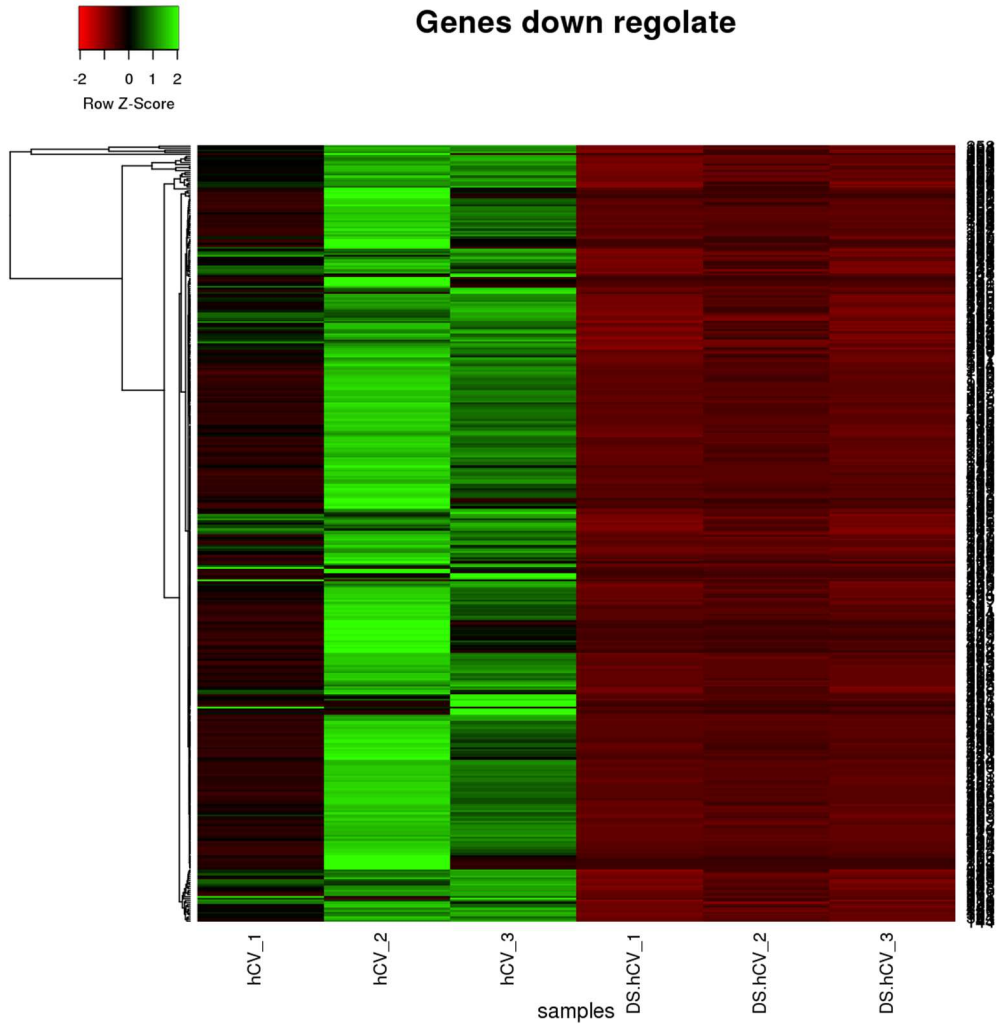

Figure 12: Heatmap of down-regulated genes, compared between hCV and DS-hCV. The expression levels of genes are displayed as color-coded: red = under- expression, green= over-expression (padj 0.01).

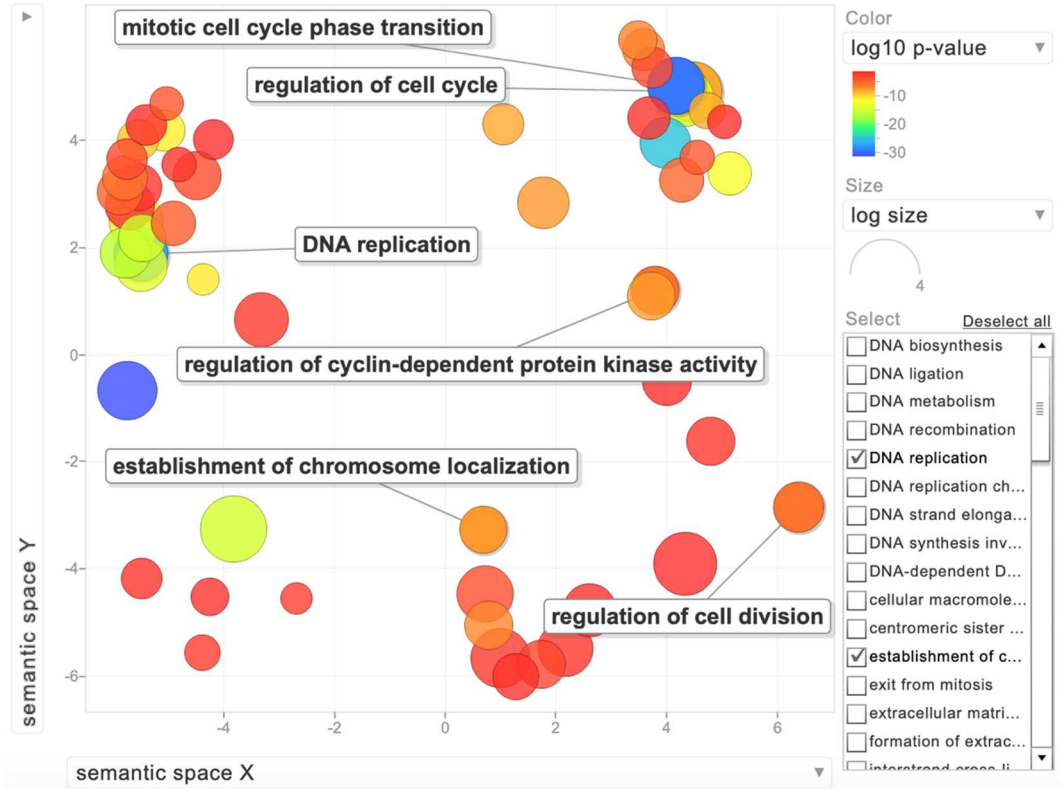

Figure 13: Biological process involving the down-regulated genes in DS-CV-MSCs. Biological processes are grouped as color-coded according to log10 p-value.

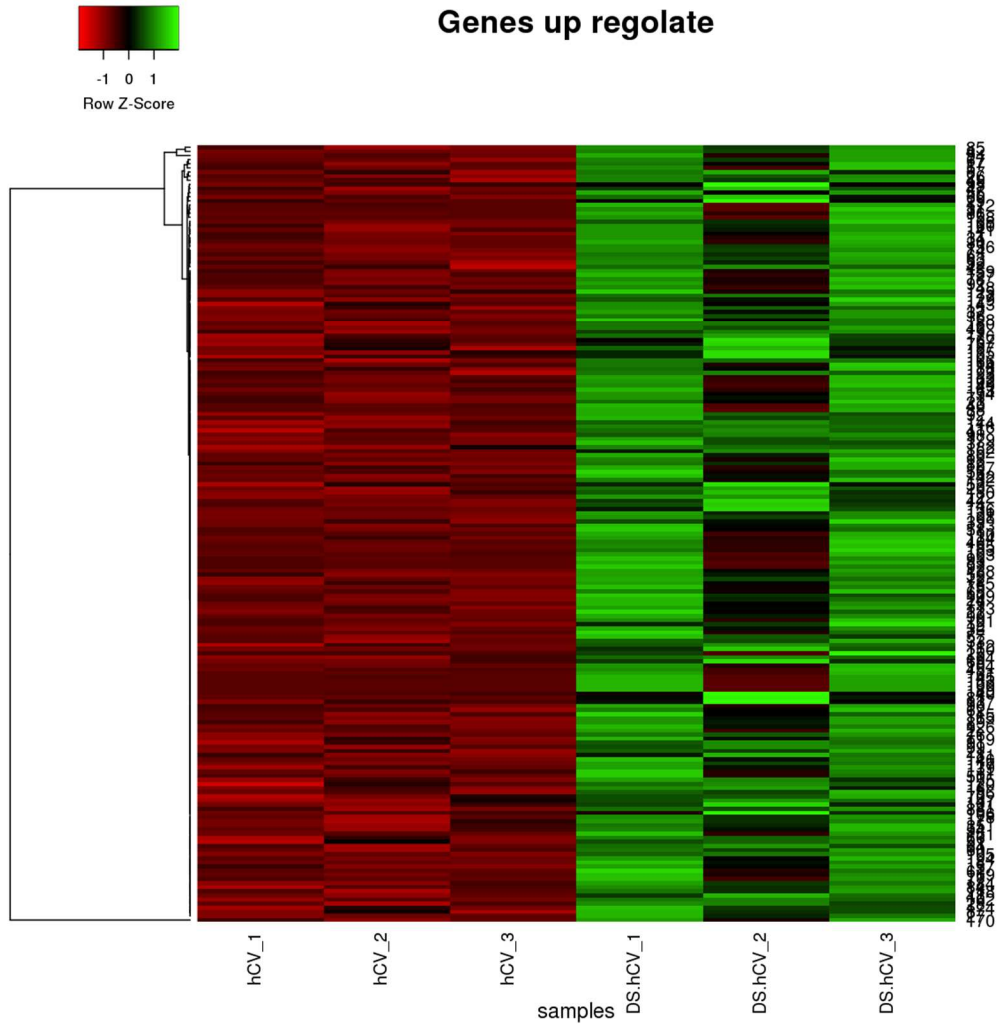

Figure 14: Heatmap of up-regulated genes, compared between hCV and DS-hCV. The expression levels of genes are displayed as color-coded: red = under- expression, green= over-expression (padj 0.01).

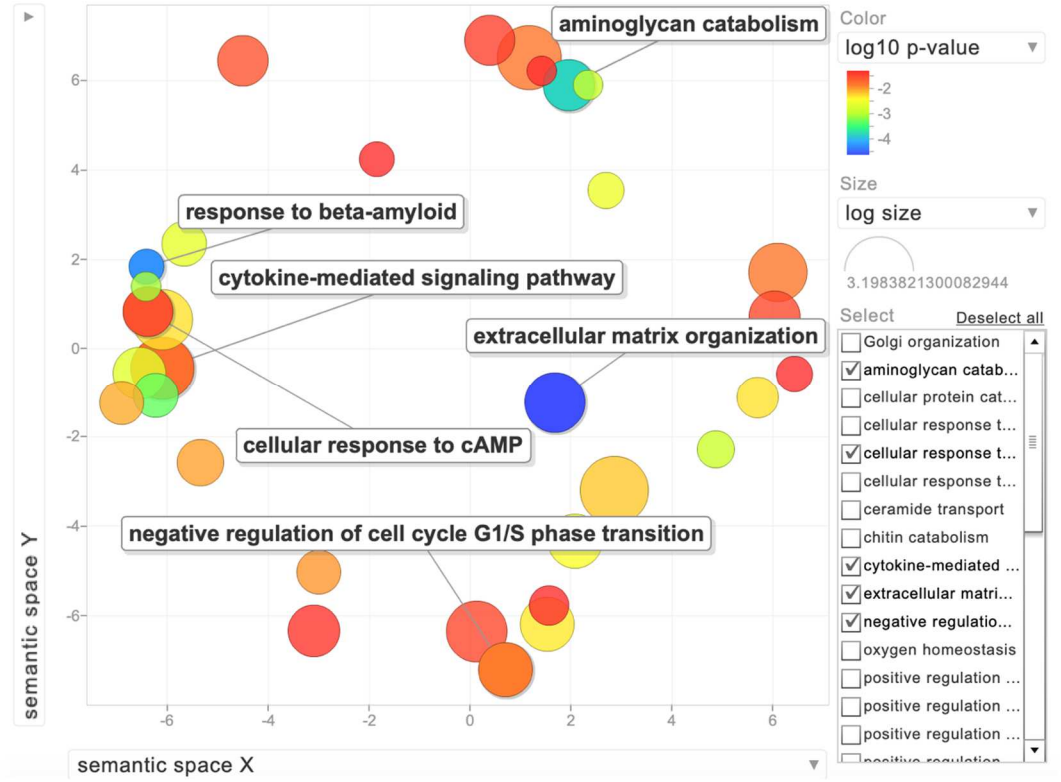

Figure 15: Biological process involving the up-regulated genes in DS-CV-MSCs. Biological processes are grouped as color-coded according to log10 p-value

3.9 Immunosuppressive potential

The production of cytokines by hCV-MSCs and DS-hCV-MSCs after the treatment with the pro-inflammatory cytokines *TNF-α* and *IFN-γ* has been evaluated through qPCR. A general increase of the levels of immunosuppressive genes was detected in DS-CV in comparison to CV. As shown in Figure 16 (A), already after 24 h of treatment, the expression of *PGE-2*, *TGF-β,* and *TNF-α* resulted 3.2± 0,6-fold, 2.9 ± 0.2–fold and 14 ± 0.5–fold higher, respectively in DS-CV-MSCs compared to hCV-MSCs. On the contrary, the expression levels of *Il-6* decreased of 0.8 ± 0.4 –fold in DS-CV-MSCs compared to hCV-MSCs. After 48h, as shown in figure 16 (B), the *TNF-α* expression levels resulted even higher (103 ± 0.2-fold) in DS-CV compared to hCV.

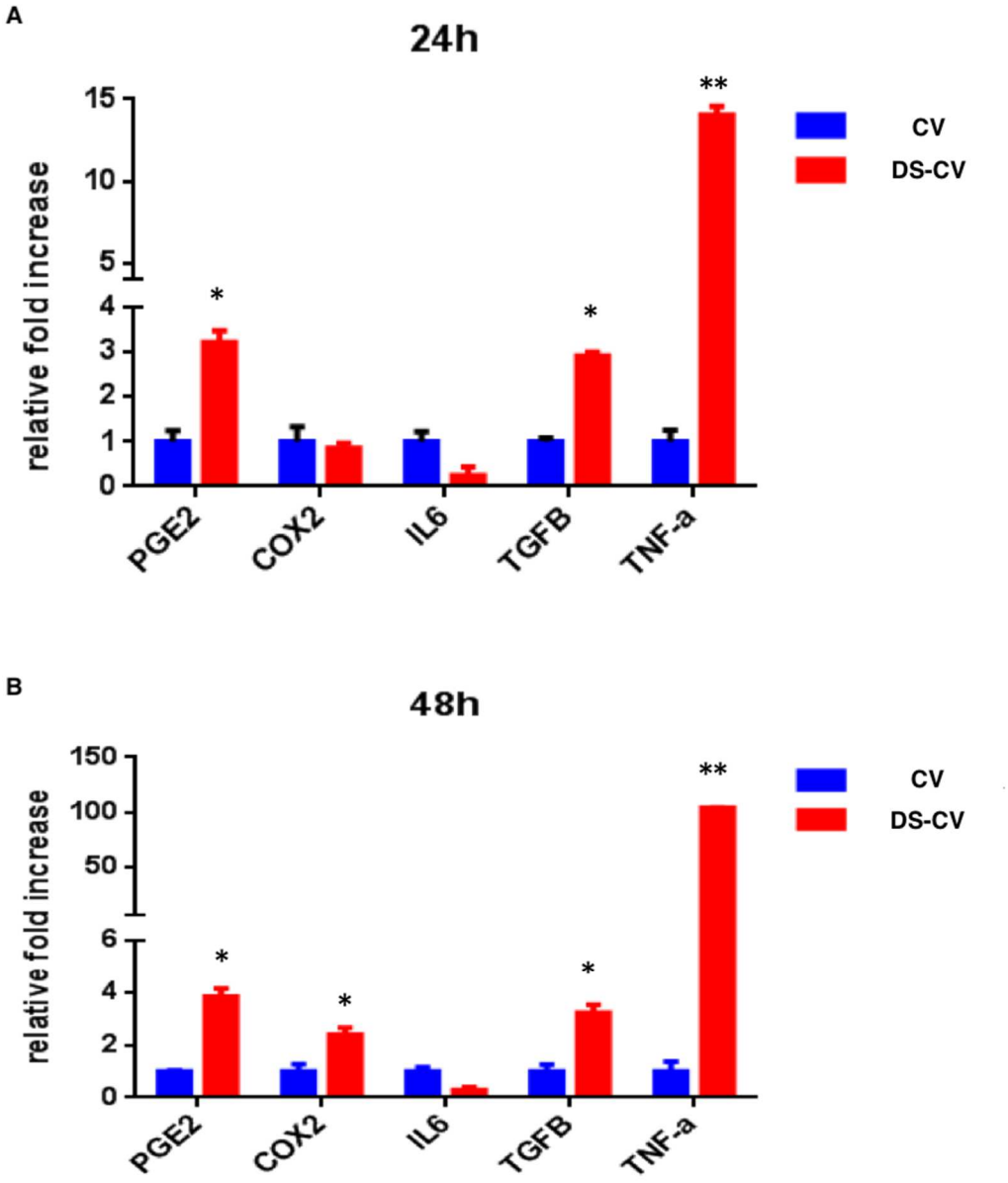

Figure 16 Quantitative PCR analysis of the expression of genes associated to MSC-immunosuppressive potential. The *PGE2, COX2, IL-6, TGF-β and TNF-α* gene expression was compared between CV (blue) and DS-CV (red) after 24 (A) and 48h (B) of exposure to *TNF-α* and *IFN-ɣ*. Data represent the mean and the standard deviations of at least three independent experiments. *= $p<0.05$, **= $p<0.01$

3.10 Immunomodulation

After the exposure to conditional medium derived from CV (CM-CV) and DS-CV (CM-DS-CV), monocyte cells have been tested for the expression of inflammatory-associated markers. As reported in Figure 17, after 24h of the treatment, the anti-inflammatory genes expression levels increased in THP-1 cells treated with CM DS-CV in comparison to the treatment with CM CV, specifically: *PGE-2:* 16 ± 0.3-fold, *TGF-β* 7.4 ± 0.1-fold and *COX2* 2.2 ± 0.3-fold higher than CM CV- treated cells, respectively. Differently, the pro-inflammatory gene *IL-6* expression was similar in both cell lines, whereas the *IL-1B* levels resulted still higher after stimulation with CM DS-CV. Interestingly, our data show a downregulation after 48h of the treatment in THP-1 treated with CM-DS-CV, with a 14. 5-; 1.2-; and fold 5-fold reduction for *PGE-2* (±0.3), *TGF-β* (±0.4) and *COX2 (*±0.3*)* respectively (FIG 19). On the other hand, as reported in Figure 20, the level of *IL-6* (pro-inflammatory genes) resulted 1.4-fold increased, while *IL1β* levels remained quite stable over time.

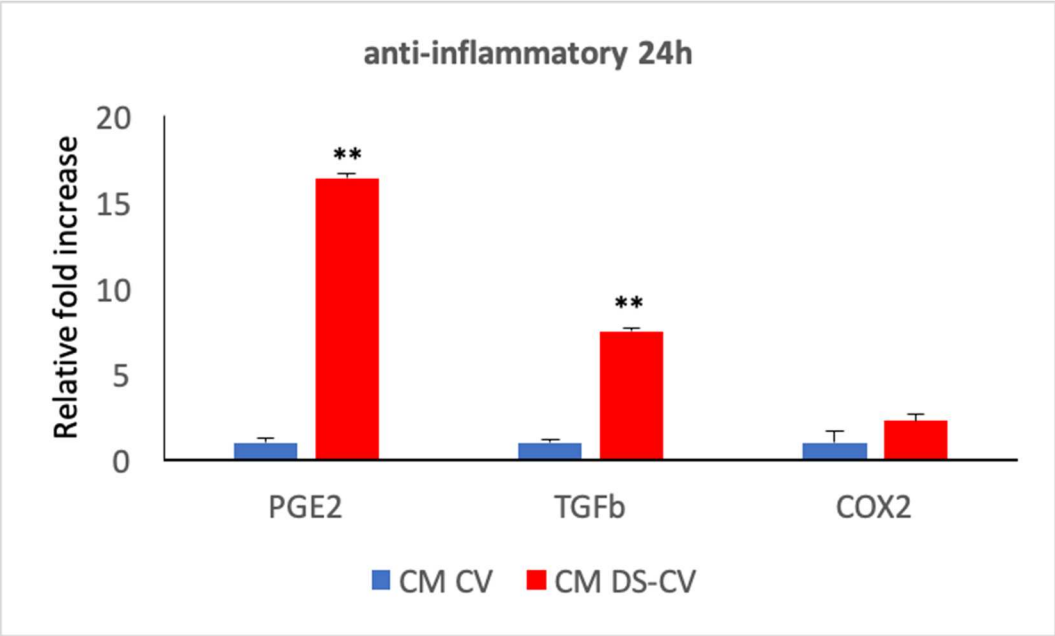

Figure 17. Anti-inflammatory genes expression quantified by qPCR analysis. The gene expression was compared between CM CV (blue)- and CM DS-CV- (red) treated THP-1 cells after 24h. The results are reported as average of at least three independent experiments ± standard deviation. *= p<0.05, **= p<0.01

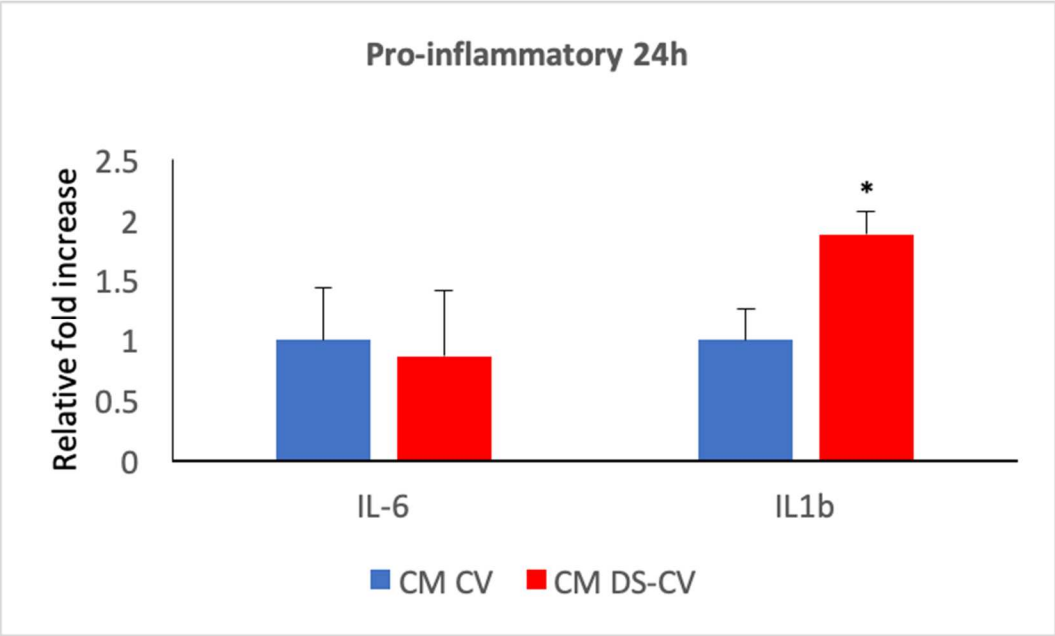

Figure 18. Pro-inflammatory genes expression quantified by qPCR analysis. The gene expression was compared between CM CV (blue)- and CM DS-CV- (red) treated THP-1 cells after 24h. The results are reported as average of at least three independent experiments ± standard deviation. *= p<0.05, **= p<0.01

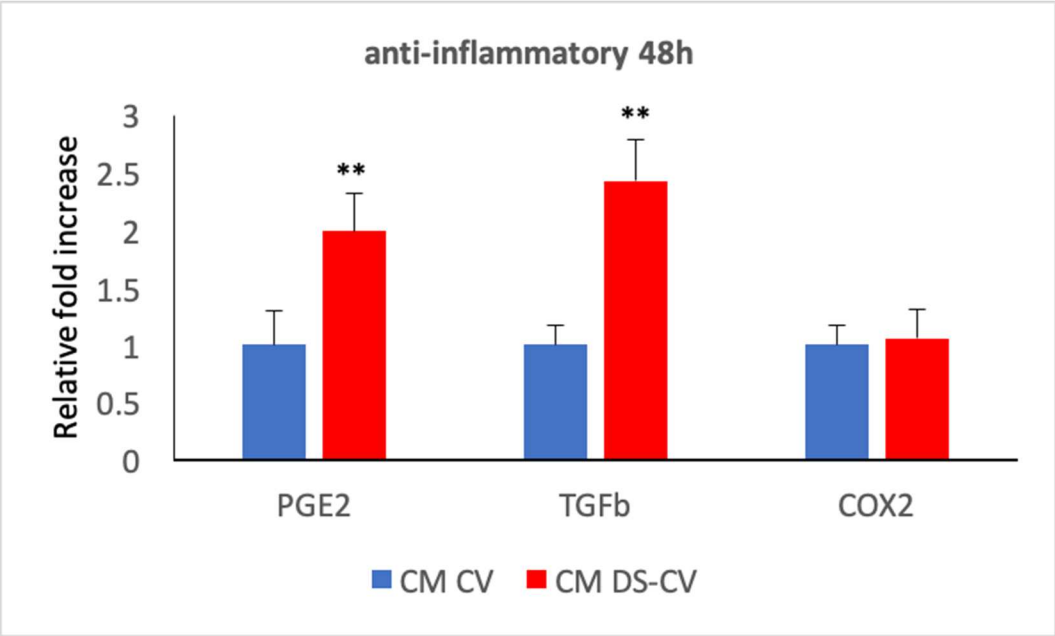

Figure 19 Anti-inflammatory genes expression quantified by qPCR analysis. The gene expression was compared between CM CV (blue)- and DS CM-CV- (red) treated THP-1 cells after 48h. The results are reported as average of at least three independent experiments ± standard deviation. *= p<0.05, **= p<0.01

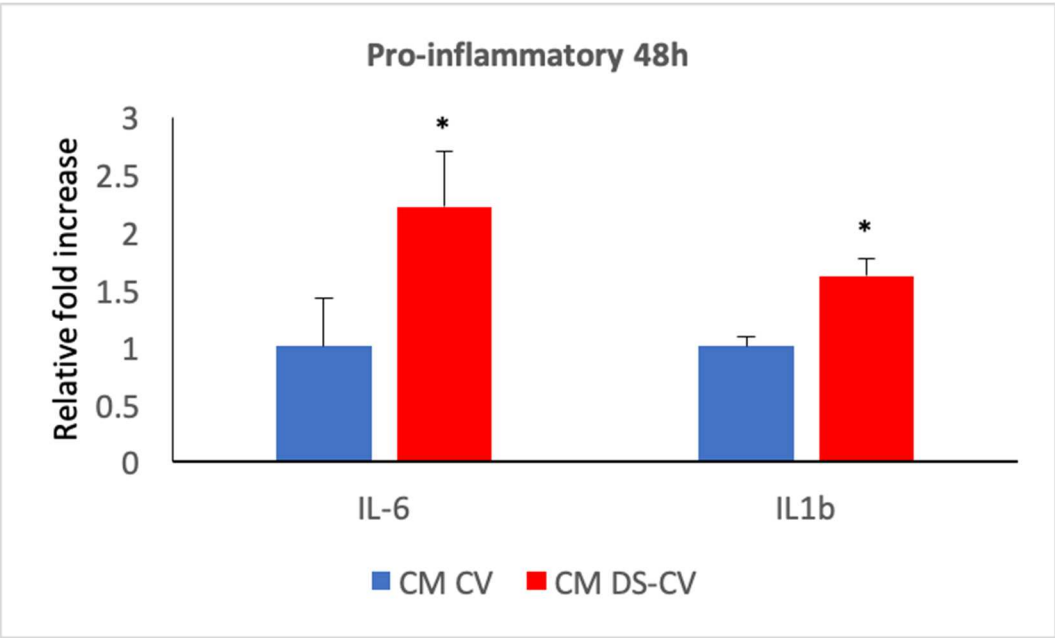

Figure 20 Pro-inflammatory genes expression quantified by qPCR analysis. The gene expression was compared between CM CV (blue)- and DS CM-CV- (red) treated THP-1 cells after 48h. The results are reported as average of at least three independent experiments ± standard deviation. *= p<0.05, **= p<0.01

4.Discussion and Conclusion

Extra-embryonic compartments have attracted great interest in recent years as a valuable source of stem cells for a possible application in regenerative medicine, due to the MSCs higher proliferation rates, broader differentiation and extensive proliferative potential in comparison with cells obtained from adult tissues (121-123).

In this study, we aimed to evaluate if Down Syndrome could interfere with the stemness properties in term of proliferative rate, MSC-associated markers, immune-suppressive and immune-modulatory properties.

At first, the minimal criteria to define if DS-CV were Mesenchymal Stem Cells were evaluated, confirming through DT, CFU, structure, differentiative potential and the detection of mesenchymal associate markers, that these cells exhibited the mesenchymal stem phenotype (101). However, the DS-CV showed a significant reduction in growth curve and also some differences in cell cycle in comparison to CV. These phenotypic data were also confirmed by RNAseq, which underlined the main differences between the two cell lines in the gene pathways involved in the proliferative capability. Remarkably, when examining the MSC-associated markers, the major discrepancy between DS-CV- and CV were detected in the expression of the CD73 marker, higher in the formers, as reported mainly by flow cytometry

analysis. It must be noted that the CD73 marker is a membrane protein involved in regenerative and inflammatory processes, thus we decided to investigate the immune-suppressive and immune-modulatory properties in DS-CV in comparison to CV. Consistently with the flow cytometry data, ROS production (immune-suppressive) resulted greater in the formers, suggesting their greater reactivity to external stimuli; this was further confirmed by RNAseq, which showed the up-regulation of genes involved in response to external stimuli. Based on these obtained results, we hypothesized the presence of different soluble factors released in the growth medium by CV-and DS-CV, acting as mediators of the immune-modulation. We thus tested their conditioned medium on THP-1 cells; indeed, after the exposure to both conditioned medium of both the cell lines, a significant increase of anti-inflammatory genes (*TGF-β, COX2 and PGE2*) levels was found, suggesting the induction of the M2 phenotype in THP-1 cells, as reported in literature (124). All these data obtained herein not only indicate that trisomy 21 didn't interfere with the cells stemness properties, but also highlight the immunomodulatory role of soluble factors released by DS-CV. Future studies will be required to elucidate the specific paracrine signals, which have a principal role in the cross-talk (112), involved in this mechanism. Particular emphasis will be given to the macrovesicles and exosomes role, which have been

demonstrated to be important in cell to cell communication (2). Moreover, our preliminary studies describe CV- and DS-CV as possible new source of soluble factors able to regulate the immune-system, with a potential use in regenerative medicine.

Chapter III Bioactive Immunomodulatory Compounds: A Novel Combinatorial Strategy for Integrated Medicine in Oncology? BAIC Exposure in Cancer Cells

1. Introduction

The first studies reporting the efficacy of natural compounds in integrative medicine date back to the past 2 decades. However, during recent years, the use of nutritional supplements to integrate standard medical treatments has considerably increased. A plethora of natural products are currently being screened for their potential as adjuvant therapeutics for the control of the side effects of particularly aggressive approaches, including but not limited to chemotherapy. To date, complementary therapies relying on the use of natural compounds have demonstrated efficacy in the treatment of serious diseases, such as cancers and inflammatory diseases, including rheumatoid arthritis, atherosclerosis, chronic hepatitis, pulmonary fibrosis, and inflammatory brain diseases (56, 125, 126).

Our journey in integrative medicine began with the enzyme-fermented extract of the mushrooms *Lentinula edodes*, the active hexose correlated compound (AHCC). AHCC is commercially available as a nutritional supplement, and its clinical efficacy has been demonstrated in both human and animal models. Its most active component, α-glucan,(65, 127) plays multiple roles in cancer (including breast, ovaries, and pancreas (128)), host protection during viral (129) or bacterial (130, 131), infections, chronic diseases (i.e., diabetes (132)),

and cardiovascular pathologies. In this context, it is worth mentioning the anticancer effect of α-glucans, which has been reported in patients with squamous cell lung carcinoma, as well as their role in reducing the adverse effects observed in patients with advanced cancer during chemotherapy (127, 128). Moreover, several groups around the world are currently exploiting the beneficial properties that α-glucan exerts on human health in combination with other bioactive molecules, respectively, with CpG oligodeoxynucleotide and tamoxifen showing they modulate oxidative stress and immune responses in cancer patients and anticancer hormonal agent (133, 134). Furthermore, the effectiveness of AHCC supplementation has been mainly ascribed to its role in interfacing with the immune system. Specifically, AHCC stimulates the immune system by modulating the response against pathogens(135) and is capable of enhancing it via multiple mechanisms, including through the augmentation of macrophage and natural killer cell proliferation (135). In particular, AHCC is known to induce a high production of various cytokines by macrophages and T lymphocytes, such as interferon-γ (IFN-γ), interleukin (IL)-8, IL-1β, and tumor necrosis factor (TNF-α, IL-2, and IL-12) (63). Whereas *Wasabia japonica* (reported here as Wasabi) is an aromatic component of the Japanese typical pungent spice used as a condiment in Asia to prepare traditional foods like sashimi and sushi. The active component of

Wasabi is methylsulfinyl hexyl isothiocyanate (6-MITC), which is also known for its apoptotic effects on cancer cells (136), anti-inflammatory potential (137), and detoxifying properties (138). In the inflammatory process, macrophages play a central role in the activation of the metabolic pathways responsible for the release of inflammatory enzymes, cytokines, chemokines, and other inflammatory factors. Overexpression of these inflammatory factors by macrophages has been attributed to the pathophysiology of many inflammatory diseases. It was observed that Wasabi retains the capability to suppress the expression of cyclooxygenases (*Cox-2*) and prostaglandins (*Pge2*) in human U937 monocytic cells (137) and macrophages (59, 139). Furthermore, 6-MITC has been shown to selectively suppress breast cancer and melanoma cell progression as reported by Nomura et al (140). According to Watanabe et al, the apoptotic properties and the consequent anticancer effect associated to Wasabi is mediated by the presence of another compound found in Wasabi, allyl isothiocyanate (6-HITC), which has been found to also induce detoxification through the activation of enzymes such as glutathione S-transferases 21. Based on this evidence, the aim of this study was to test for a combinatorial effect between AHCC and Wasabi (depicted in this study as bioactive immunomodulatory compound [BAIC]) in contrasting the growth of 2 human adenocarcinoma cell lines, the breast adenocarcinoma (MCF-7)

and pancreas adenocarcinoma (Panc02) cells. To this end, we first defined the minimal dose of AHCC and Wasabi able to reduce cell viability in MCF-7 compared with their use as single agents (AHCC or Wasabi). Subsequently, we verified if the observed effect was due to a cell cycle arrest or to the induction of apoptotic cascade within the cells following the treatment. In parallel, preliminary insights of the role the combination of AHCC and Wasabi plays in modulating the size and growth of mammo- spheres produced by MCF-7-derived cancer stem cells (CSC) were also obtained. Finally, we asked whether the combination of AHCC and Wasabi at the concentrations found to be effective in reducing cancer cell progression could concomitantly lead to side effects. To answer this question, the minimal concentration able to induce a detrimental role on MCF-7 and Panc02 cells was administered to monocytic cells (ThP-1 cell line) to evaluate viability and phenotype, as compared with the treatment with their single counterparts.

2. *Materials and Methods*

2.1 AHCC and Wasabia japonica

AHCC used in this study was provided by Amino Up Chemical Co, Ltd (Sapporo, Japan). A lyophilized extract titrated and standardized by the rhizome of *Wasabia japonica* was purchased from Pharmagen BG Sofia (Bulgaria), its official suppliers.

2.2 Cell Culture

Cells used in this study include human breast adenocarcinoma (MCF-7), human pancreas adenocarcinoma (Panc02), and human leukemia monocytic (ThP-1) cell lines (from ATCC). Cancer cells were cultured in high-glucose Dulbecco's Modified Eagle Medium (Corning) supplemented with 10% fetal bovine serum (Corning), 1% L-glutamine, and 2% antimitotic/antibiotic. ThP1 cells were cultured in RPMI-1640 media (Gibco) supplemented with 10% fetal bovine serum (Corning), 1% L-glutamine, and 2% antimitotic/antibiotic. Cells were maintained at 37°C in a humid atmosphere with 5% CO.

2.3 Experimental Design

For the treatments, a stock solution of the single components was prepared in Dulbecco's phosphate-buffered saline (Sigma), incubated for 72 hours, filtered using a 0.45-μm filter, and stored at 4°C. MCF-7 and Panc02 cells were treated with different concentrations of Wasabi and AHCC (ranging from 7.5 to 500 μg/mL) for 24 and 48 hours, in combination or as single components. At the end of each time point, a cell viability assay was used to determine the minimal concentration able to induce a significant reduction. Once defined through the MTT (3-(4,5-dimethylthiazol- 2-yl)-2,5-diphenyltetrazolium bromide) assay, the optimal combination was used to perform further analyses and assess the effect on cell cycle and apoptosis. The cytotoxic effect as well as the immunomodulatory potential of the Wasabi and AHCC combination have been also investigated on ThP-1 cells after 48-hour treatment as reported below.

2.4 Evaluation of Cancer Cells Viability

The effect on cell viability of Wasabi and AHCC, as single compounds or in combination (BAIC), was determined on MCF-7 and Panc02 following 24- and 48-hour treatment using MTT. The colorimetric

MTT assay allowed identifying the minimum doses of BAIC able to reduce cell viability. Briefly, cells were seeded at the density of 10 000 cells/ well into 96-well flat-bottomed plates to allow them to cover the whole surface of the dish. Cells were then treated with different concentrations of Wasabi and AHCC (range = 7.5-500 μg/mL) and analyzed following the manufacturer's indications (Vybrant MTT Cell Proliferation Assay Kit, Life Technologies). Absorbance was measured at 570 nm using a microplate reader (Biotech), and data were analyzed by using the software Gen05.

2.5 Cell Cycle Assessment

The effect of BAIC on cell cycle distribution was examined using flow cytometry. In brief, MCF-7 and Panc02 were seeded at a density of $1 \times 10^4/cm^2$ on 6-well plates and treated with the optimal combination of BAIC (7.5 μg/mL for Wasabi and 10 μg/mL for AHCC) or with Wasabi (7.5 μg/mL) and AHCC (10 μg/mL) for 48 hours. Following the treatment cells were collected, centrifuged at room temperature at 500 × *g* for 5 minutes, and incubated overnight with cold 70% ethanol. Cells were then resuspended in phosphate-buffered saline containing propidium iodide (40 μg/ mL) and RNase (100 μg/mL). Flow cytometry data were acquired using a Guava Millipore cytometer. At least 20 000

cells/sample were run. The percentage of cells in sub G0, G1, S, and G2/M was established using FlowJo software.

2.6 Evaluation of Apoptosis

To analyze the possible apoptotic effect induced on MCF-7 and Panc02 by BAIC, the Annexin V-FITC Apoptosis Detection Kit I (BioLegend) was used. Briefly, cells were treated with Wasabi and AHCC in combination (7.5 μg/mL for Wasabi and 10 μg/mL for AHCC) or as single agents (7.5 μg/mL and 10 μg/mL for Wasabi and AHCC, respectively) for 48 hours, collected, and washed in a binding buffer solution. Cells were then incubated in the staining solution containing propidium iodide and Annexin V-FITC for 15 minutes at room temperature and in the dark. Flow cytometry data were acquired using a Guava Millipore cytometer. The percentage of normal, early apoptotic, apoptotic, and necrotic cells was established using FlowJo software by comparing experimental cells to control groups (untreated cells).

2.7 Molecular Analysis

Quantitative reverse transcription polymerase chain reaction (qRT-PCR) analysis was performed to evaluate the expression of specific pro-apoptotic markers on cancer cells and markers associated to inflammation on monocytes as shown in Table 1. In all cases, total RNA was isolated using TRI-reagent (Invitrogen). DNAse (Sigma) treatment followed the reaction. RNA concentration and purity were measured using a NanoDrop ND1000 spectrophotometer (NanoDrop Technologies). The cDNA was synthesized from 500 ng of total RNA using the PrimeScript RT Master Mix (TAKARA), and quantitative PCR was run in the StepOnePlus Real-time PCR system (Applied Biosystems) using commercially available master mix (PowerUp SYBER Green Master Mix; Applied Biosystems).

Table 1. Transcripts and Sequence of Each Primer Used in qPCR to Investigate the Apoptosis and the Inflammation[a].

Gene	Sequences (5′ → 3′)	T_m (°C)	Product Size (bp)
Pro-apoptotic markers			
BCL-2 associated X protein (*BAX*)	S: TCCCCCCGAGAGGTCTTTT A: CGGCCCCAGTTGAAGTTG	57	68
Apoptotic peptidase activating factor-1 (*Apaf-1*)	S: TGGCTGCTCTGCCTTCT A: CCATGGGTAGCAGCTCCTTC	57	142
p53	S: CCCCTCCTGGCCCCTGTCATCTTC A: GCAGCGCCTCACAACCTCCGTCAT	62	265
Immunomodulatory markers			
Interleukin 1β (*Il-1β*)	S: TGCTCTGGGATTCTCTTCAGC A: CTGGAAGGAGCACTTCATCTG	56	164
Transforming growth factor-β (*Tgf-β*)	S: ATGGTGGAAACCCACAACG A: GGAATTGTTGCTGTATTTCTGG	56	171
Cyclooxygenase-2 (*Cox-2*)	S: TGAGTTATGTGTTGACATCCAG A: TCATTTGAATCAGGAAGCTGC	56	197
Glyceraldehyde-3-phosphatase dehydrogenase (*Gapdh*)	S: TCCACTGGCGTCTTCACC A: GGCAGAGATGATGACCCTTT	57	78

Abbreviations: qPCR, quantitative polymerase chain reaction; S, sense primer; A, antisense primer.
[a]For each gene, oligonucleotide sequence (5′ → 3′), melting temperature (T_m), and the length of the product are also reported.

Table 1. Transcripts and sequence of each primer used in qPCR to investigate the apoptosis and the inflammation. In the table, S indicates sense primer, A indicates antisense primer. For each gene, oligonucleotide sequence (5' → 3'), melting temperature (Tm) and the length of the product are also reported.

2.8 Monocytic Cells Viability and Differentiation

To evaluate the side effects of the doses of BAIC defined as the most efficient in inhibiting cancer cells proliferation, monocytic cells (ThP1) were seeded at the density of $2 \times 10^5/cm^2$ on 6-well plates and treated accordingly. After 48 hours of incubation, cells were harvested, and the percentage of viable cells was evaluated by trypan blue exclusion dye using a Burker chamber.

2.9 Nonadherent Mammosphere Formation Assay and Treatment

Cancer stem cells from MCF-7 cells (ProMab) were cultured at a density of 1×10^3 cells/mL and grown in a 6-well ultralow attachment plate with Premium Cancer Stem Cell Media (ProMab) to enable the cells to grow and form spheres. A further 1 mL of fresh medium was added to each well every other day. Incubation of the primary culture MCF-7-derived CSC with BAIC was conducted under mammosphere-forming conditions for 5 days when the size of the formed mammospheres was compared with those found in the control group (CTRL, untreated cells). A BX51 microscope (Nikon) was used to acquire images that have been captured by using the open source Spot Advanced software and analyzed by ImageJ.

2.10 Statistical Analysis

Statistical analysis was performed using GraphPad Instat 3.00 (GraphPad Software). Three replicates for each experiment (quantitative PCR, flow cytometry analyses, and cell counts) were performed, and the results are reported as mean ± standard deviation (SD). One-way analysis of variance for multiple comparisons by the

Student-Newman- Keuls multiple comparison test was used to assess differences between groups. Differences were considered statistically significant for *P* values <.05. For quantitative PCR data, nonparametric tests were used.

3. Results

3.1 BAIC Inhibits, at Defined Concentrations, Cancer Cell Growth

Before starting the experiments, we aimed at determining the minimal concentration of Wasabi and AHCC able to drastically reduce the percentage of viable cancer cells at 48 hours. To this the MCF-7 cell line was chosen and the MTT assay was applied to determine the effect of the combination of AHCC and Wasabi at different concentrations, as reported in Supplementary Figure 1A. The percentage of active cells after the treatment with different combinations are shown in Supplementary Figure 1B.

Results of this part of the study indicated no significant differences among the treatments although significant differences ($P < .01$) were found compared with the control cells (CTRL). Among the possible combinations, we identified in the concentrations 7.5 and 10 μg/mL for Wasabi and AHCC, respectively, the efficient cocktail to inhibit the growth of MCF-7 cells. Figure 1A shows a statistically significant ($P < .01$) effect of BAIC on MCF-7 cells compared with AHCC (10 μg/mL) and Wasabi (7.5 μg/mL) provided as single agents, with a marked inhibition in cell proliferation at 48 hours (values assessed 48%). The percentage of active Panc02 cells registered following the exposure to

Wasabi and AHCC demonstrated a slight increase com- pared with control at 24 hours. Values assessed around 109% and 110%, respectively. In contrast, a slight reduction was observed at 48 hours. At 48 hours, the reduction of proliferative cells was assessed around 45% for BAIC, 43% for Wasabi, and 64% for AHCC (Figure 1B).

A

		AHCC (µg/ml)			
		7.5	10	100	500
Wasabi (µg/ml)	7.5	1	2	3	4
	10	5	6	7	8
	100	9	10	11	12
	500	13	14	15	16

B

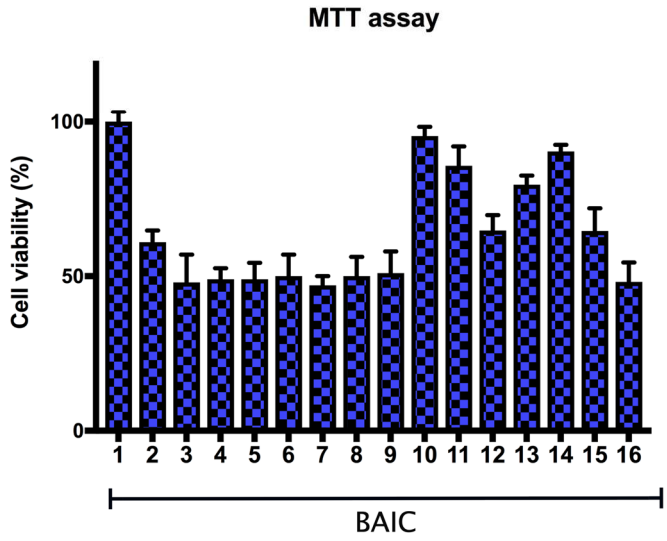

Supplementary Figure 1. Table showing the matrix used to combine different concentrations of Wasabi and AHCC in the range of 7.5-500 µg/ml **(A)**. The numbers associated to each combination of BAIC (from 1 to 16) have been reported in the graph showing the percentage of viable MCF-7 cells before (CTRL) and at 48 hrs of treatment **(B)**. Data are normalized to control cells and reported as mean±standard deviation (n=3). *: significant ($p<0.05$) and **: highly significant ($p<0.01$) compared to CTRL.

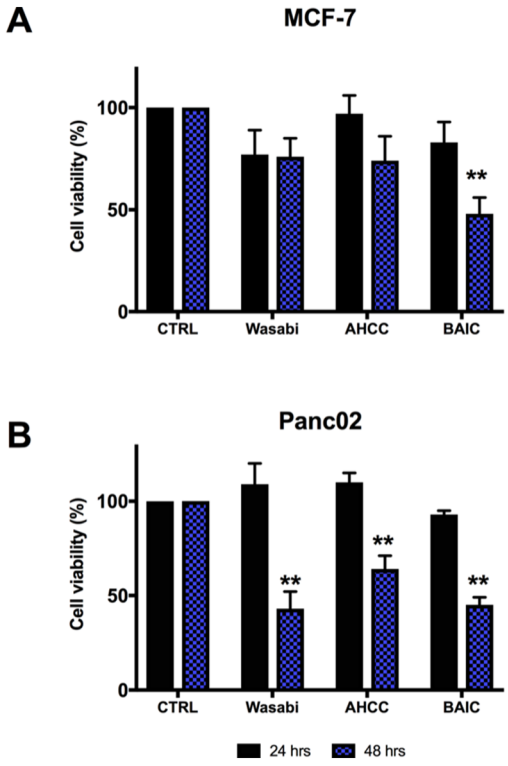

Figure 1. MTT assay demonstrating the effect of bioactive immunomodulatory compound (BAIC; 7.5 and 10 μg/mL, respectively) on the viability of MCF-7 (A) and Panc02 (B) after 24 and 48 hours of treatment. Data obtained exposing both cell lines to active hexose correlated compound (AHCC) and Wasabi used as single agents are also reported for comparison at 24 and 48 hrs. Data are normalized to control cells (CTRL) and reported as mean ± standard deviation (n = 3). **Highly significant ($P < .01$) and *significant ($P < .05$) compared with CTRL.

3.2 BAIC Determines an Arrest in Cell Cycle Progression

Cell cycle represents the most fundamental and important processes in eukaryotic cells. Cell cycle analysis was performed to determine the influence of BAIC on cell cycle phase distribution (G_0, G_1, S, G_2, and M) in MCF-7 and Panc02 cells at 48 hours. Our results indicated that the combination of Wasabi and AHCC halted the cell cycle progression in the G_0/G_1 phase ($P < .05$) in both cell types (Figure 2). They also suggest that such inhibition occurs in a crucial phase of the cycle, being the transition from G1 to S responsible for controlling cell proliferation (141).

Figure 2A shows greater G_0/G_1 phase arrest in MCF-7 cells, which accounts for 55.7% following the treatment with BAIC ($P < .05$). MCF-7 cells treated with single Wasabi and AHCC revealed similar G_0/G_1 phase distribution (40.8% and 42.3%), which was comparable to control cells (40%). An increase in the percentage of cells in the G_0/G_1 phase (51%) was also registered when Panc02 were treated with AHCC compared with control cells (43%; Figure 2B). Intermediate results for the percentage of cells in G_0/G_1 phase were found as the consequence of the single treatment with Wasabi, with values assessed around 48%. On the contrary, a marked reduction (30%) in the percentage of cells in

G_0/G_1 was found as the result of AHCC exposure, although the percent- age of resting cells (subG_0) was greater than the other experimental groups.

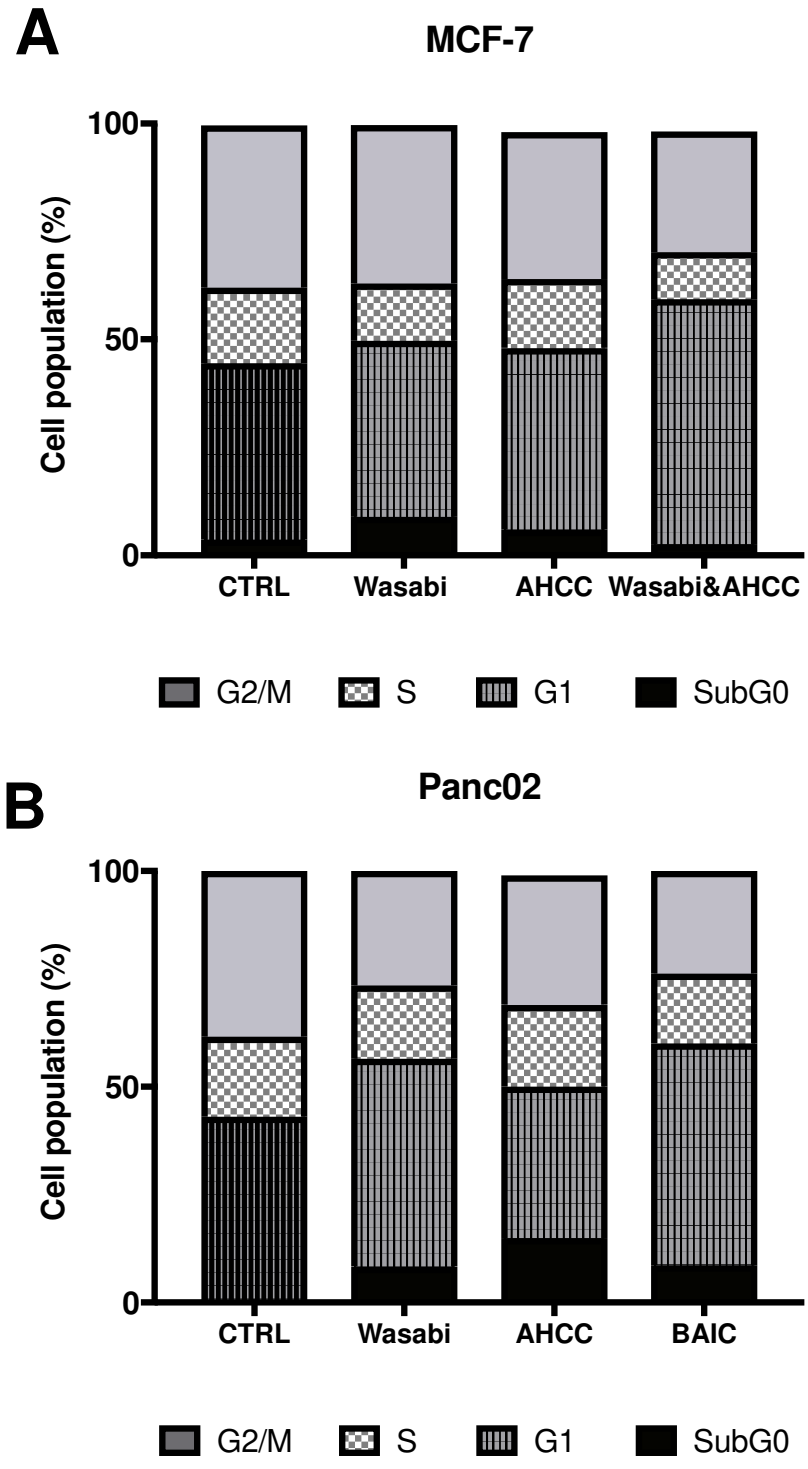

Figure2. CellcycleanalysisperformedonMCF-7(A)andPanc02 cells (B) following the treatment with bioactive immunomodulatory compound (BAIC) for 48 hours. Data obtained from untreated cells (CTRL) and cells treated with the single compounds (7.5 μg/mL Wasabi and 10 μg/mL active hexose correlated compound [AHCC]) are also reported for comparison. Data are reported as average of the percentage of cells distributed in the subG0, G1, S, and G2/M phase ± SD (n = 3). $^{**}P < .01$, highly significant differences compared with CTRL.

3.3 BAIC Induces Apoptosis in Cancer Cells

Annexin V assays and gene expression evaluation were performed to confirm data obtained from the cell cycle and proliferation assays. Although all treatment groups showed significant increases in apoptosis compared with control groups ($P < .05$), flow cytometry assays showed marked changes in MCF-7 and Panc02 cell profiles after treatment with BAIC at 48 hours, compared with Wasabi (7.5 μg/mL) and AHCC (10 μg/mL) used as single agents (Figure 3A and B). Apoptotic rates ranged around 17% for Wasabi- and AHCC-treated Panc02 cells and increased to 25% when cells were treated with BAIC, registering a 5-fold increase compared with untreated cells (5% apoptotic cells). These rates were found even greater in MCF-7 where 50% of apoptotic cells were detected, whereas the percent- age was decreased to 30% and 36% following the treatment with AHCC and Wasabi, respectively. The apoptotic cascades are tightly regulated by a variety of factors; among these factors, the Bcl-2 protein family plays central roles in apoptotic event (142). We further investigated the expression of effectors of the apoptotic mechanisms, such as *Bax-2* and *Apaf-1*, both at 24 and 48 hours (Figure 4). Following the treatment with BAIC, a statistically significant increase compared with control in the expression of *Bax-2* was found in MCF-7 (8.32 ± 0.41) but not in Panc02 cells (1.14 ± 0.34) at 48 hours. When MCF-7 cells treated with Wasabi and AHCC as

single agents a slight increase in the expression levels of *Bax-2* was found at the same time point (48 hours), with values assessed around 1.28 ± 0.04 for Wasabi and 1.5 ± 0.16 for AHCC. A 2-fold increase in *Apaf-1* expression was found at mRNA level in MCF-7 cells treated with BAIC (2.08 ± 0.25) compared with the control group and to the other experimental groups at 48 hours. On the contrary, significant differences compared with control cells were found in the expression of *Apaf-1* when Panc02 cells were exposed to the combination of Wasabi and AHCC (3.68 ± 0.04) at 48 hours. A 2-fold increase in the expression of *Apaf-1* was observed following the treatment with AHCC at 24 hours (1.98 ± 0.14). Furthermore, the expression of P53 included as a stress-responsive transcription factor and potent tumor suppressor was investigated (Figure 5). A slight increase in the expression of *p53* was observed when MCF-7 cells were treated with BAIC and AHCC (1.3 ± 0.7 and 1.6 ± 0.3-fold, respectively) compared with control cells, showing an advantage in the use of BAIC compared with Wasabi. In Panc02 cells, a greater upregulation was found following the treatment with values assessed around 2.3 ± 0.1-fold for BAIC, 2.1 ± 0.1-fold for AHCC, and 1.9 ± 0.1-fold for Wasabi, compared with control.

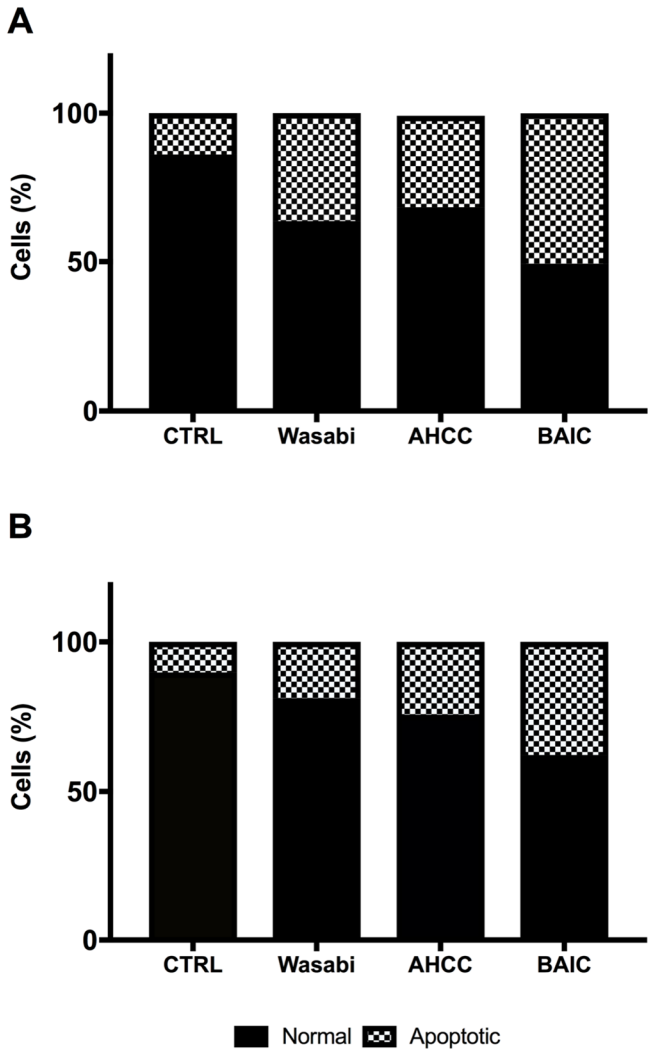

Figure 3. Representative flow cytometric analysis of MCF-7 (A) and Panc02 (B) showing normal and apoptotic cells after 48 hours treatment with Wasabi and active hexose correlated compound (AHCC) in combination (bioactive immunomodulatory compound [BAIC]), as single agents (Wasabi at 7.5 μg/mL and AHCC 10 μg/mL), or in standard conditions (CTRL). Data represent the means ± standard deviations (n = 3). *Significant and **highly significant differences compared with CTRL at $P < .05$ and $P < .01$, respectively. Solid bars depict normal cells, and patterned bars depict apoptotic cells.

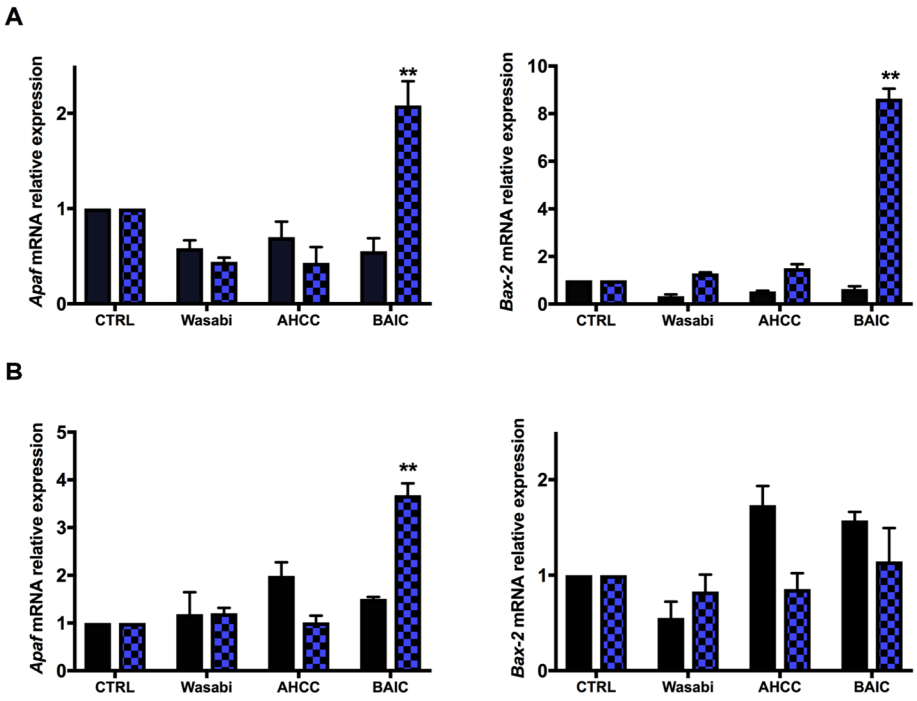

Figure 4. Quantitative polymerase chain reaction for the expression of pro-apoptotic genes (*Apaf-1* and *Bax-2*) on MCF-7 (A) and Panc02 (B) cell lines following the treatment with bioactive immunomodulatory compound (BAIC), 7.5 μg/mL Wasabi (Wasabi), and 10 μg/mL active hexose correlated compound (AHCC). Data are represented as fold-change compared with the expression levels found in untreated cells (CTRL, baseline). *Significant and **highly significant differences compared with CTRL at $P < .05$ and $P < .01$, respectively.

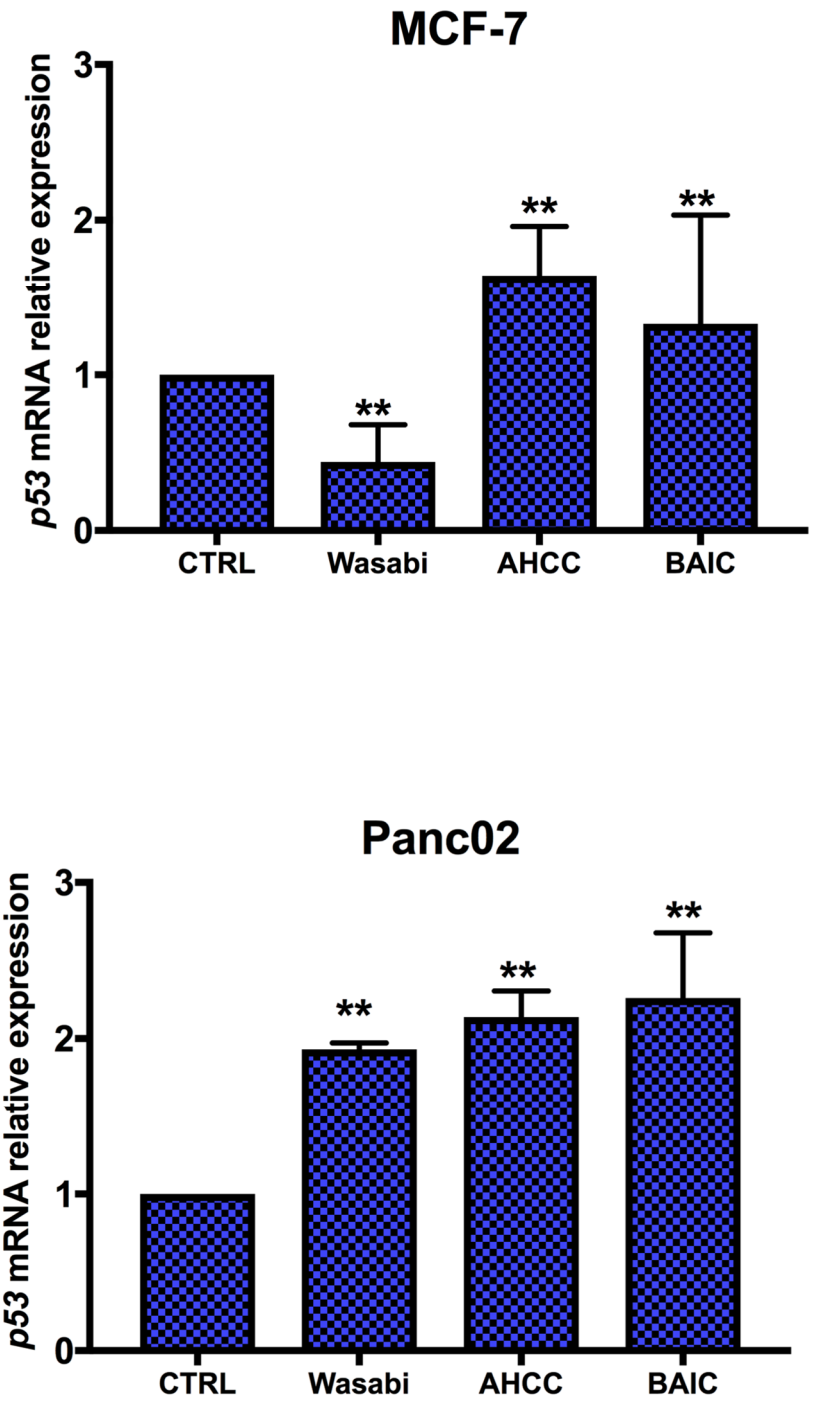

Figure 5. Quantitative polymerase chain reaction for the expression of the oncosuppressor p53 following the treatment of MCF- 7 and Panc02 cells with bioactive immunomodulatory compound (BAIC), 7.5 µg/mL Wasabi (Wasabi), and 10 µg/mL active hexose correlated compound (AHCC), at 48 hours. Data are represented as fold-change compared with the expression levels found in untreated monocytic cells (CTRL) (n = 3; $^{**}P < .01$).

3.4 Effect of BAIC on Monocytic Cells

To analyze the role BAIC has on the immune system, a proof of concept study was performed. Following the exposure to BAIC, monocytic cells have been tested for viability and the expression of inflammatory-associated markers. As reported in Figure 6, the combination of Wasabi and AHCC at low concentrations is capable of supporting the proliferation of monocytic cells. No cytotoxic effects were found in any of the experimental groups considered, where viability was comparable to control (Figure 6A). A 2-fold increase in the number of adherent cells was found on the surface of the dish where monocytes were grown in presence of BAIC compared with cells grown in standard conditions (CTRL; Figure 6B). Similar or reduced numbers were found when cells were exposed to Wasabi and AHCC at the same concentrations, respectively. Molecular analysis performed on ThP-1 treated with BAIC for the evaluation of inflammatory genes demonstrated the immunomodulatory potential of the mixture compared with the single components (Figure 7). In particular, the expression of all the tested genes was found dramatically increased as a consequence of the treatment with Wasabi at 24 hours, with values of around 682 (±59)-fold for *Tfg*-β, 8060 (±53)-fold for *Cox-2*, and 3167(±16.7)- fold for *Il-1*β compared with control cells, respectively. Monocytes treated with BAIC increased the expression levels of 4 ± 0.27-fold, 185 ± 27-fold,

and 90 ± 38-fold, respectively. An average of 2-fold increase with regard to control was observed in cells treated with AHCC at the same time point. An interesting downregulation was found at 48 hours, when the expression levels of *Il-1*β and *Cox-2* were significantly decreased following the treatment with BAIC, thus becoming more comparable to or even lower than untreated cells.

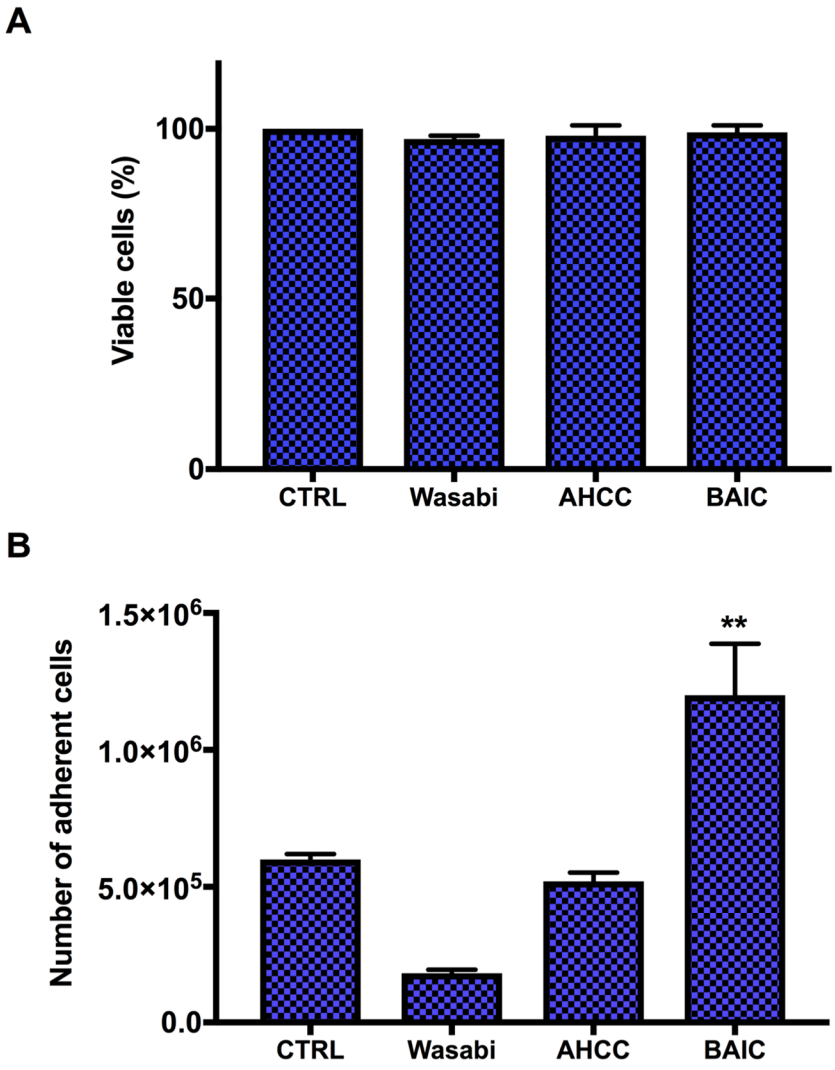

Figure 6. Graphs showing the effect of the combination BAIC on monocytic cells (ThP1 cell line). Cell viability following the treatment with bioactive immunomodulatory compound (BAIC) at 48 hours, compared with cells grown in standard conditions (CTRL), or treated with 7.5 μg/mL Wasabi (Wasabi) and 10 μg/mL active hexose correlated compound (AHCC) (A). The number of adherent cells is also reported following the treatment with BAIC (B).

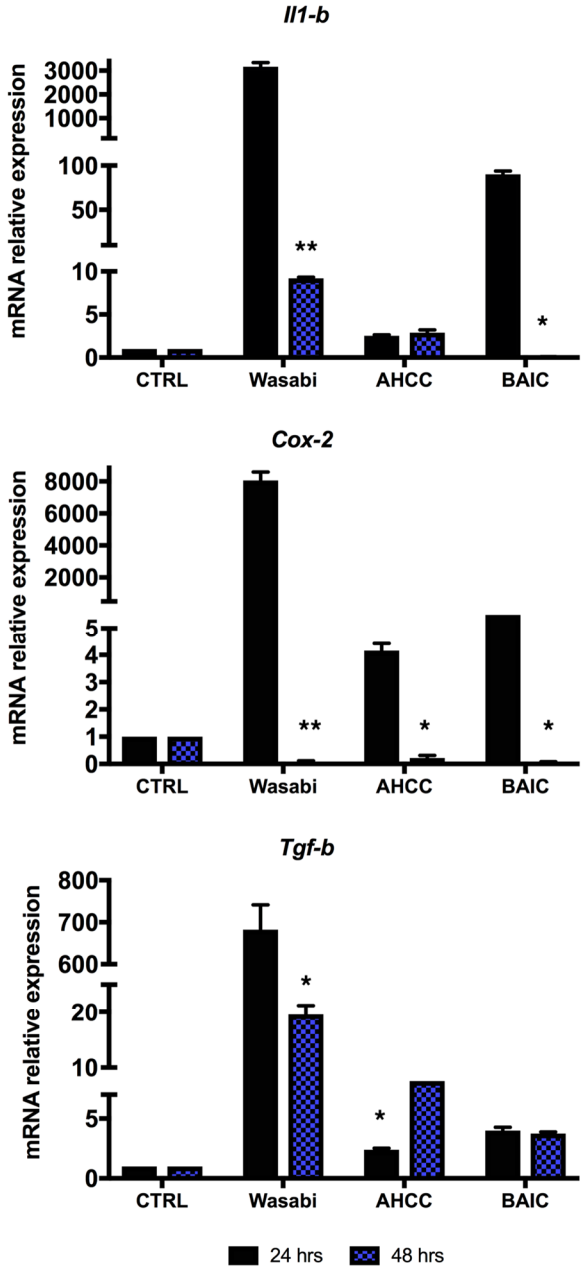

Figure 7. Quantitative polymerase chain reaction for the expression of immunomodulatory genes (*Tgf*-β, *Il-1*β, and *Cox-2*) following the treatment of ThP1 cells with bioactive immunomodulatory compound (BAIC), 7.5 μg/mL Wasabi (Wasabi), and 10 μg/mL active hexose correlated compound (AHCC), at 24 and 48 hours. Data are represented as fold-change compared with the expression levels found in untreated monocytic cells (CTRL) (n = 3; $^{**}P < .01$).

3.4 BAIC Inhibits Mammosphere Growth

The assessment of mammosphere growth following the treatment with a bioactive compound is crucial to define its potential role in inhibiting tumor initiative and progression. Formed mammospheres from MCF-7-derived CSC were visualized with a BX51 microscope (Nikon). Mammosphere size was determined following the exposure to BAIC (Figure 8A) and compared with those obtained treating cells with standard media (CTRL, Figure 8B). Results clearly demonstrated a 2-fold decrease in size, which was induced by the treatment with AHCC and Wasabi compared with CTRL. Values assessed around 40.61 ± 9.10 and 24.26 ± 5.1, respectively (Figure 8C).

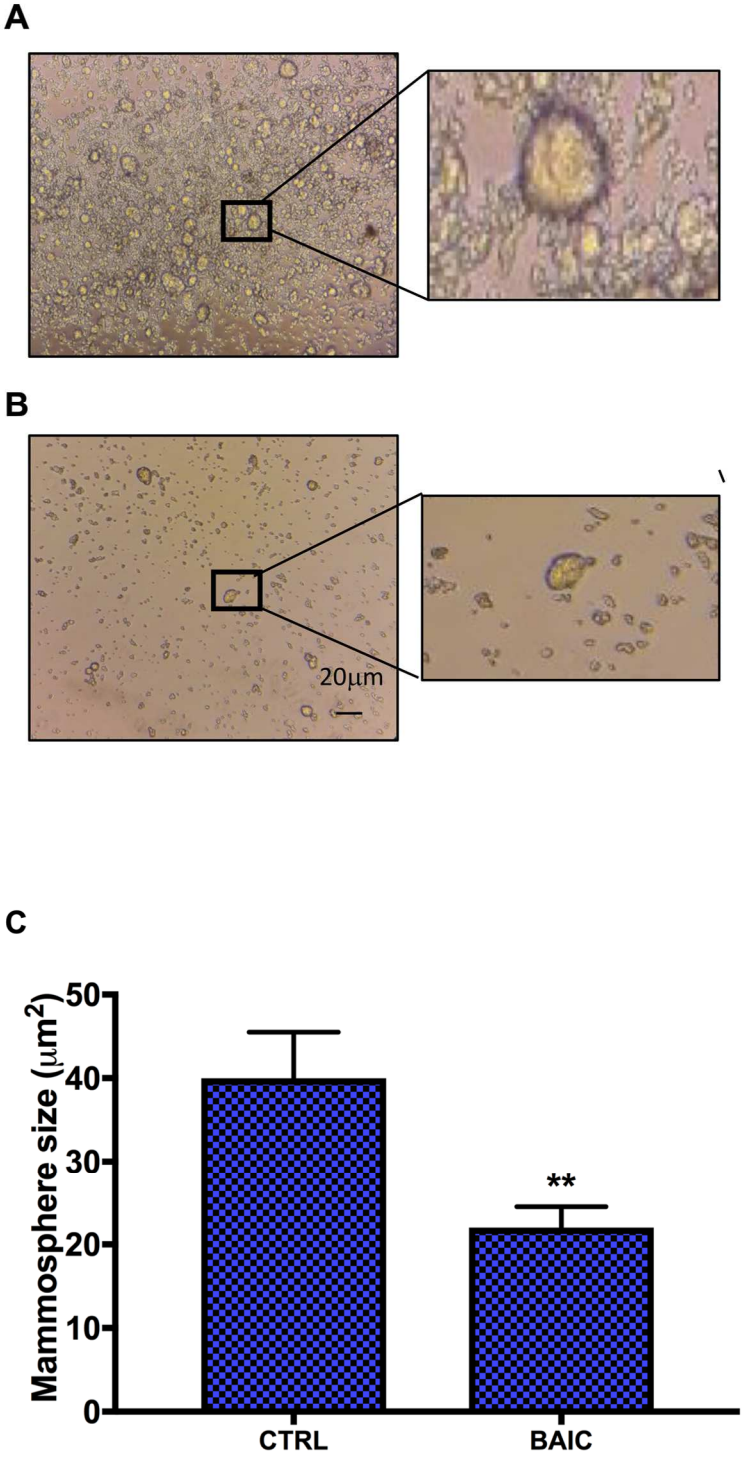

Figure 8. The potential inhibitory effect of bioactive immunomodulatory compound (BAIC) on mammospheres formation. Preliminary results show mammospheres containing MCF-7 cancer stem cells on day 5 after being cultured in the presence of BAIC (7.5 µg/mL Wasabi and 10 µg/ml active hexose correlated compound [AHCC]) (A) or in standard media (CTRL, B). Following the treatment, a statistically significant ($P < .01$) reduction in number and size of primary mammospheres is observed compared with control cells (CTRL) (C). Data are represented as means ± standard deviations (n = 3).

4. Discussion

In this study, we aimed at evaluating the combinatorial effect between 2 natural compounds, AHCC and Wasabi, for their possible use as a nutritional supplement for integrative medicine. We first tested different concentrations of AHCC and Wasabi (ranging from 7.5 to 500 μg/mL) and evaluated their effectiveness in reducing viability in 2 adenocarcinoma cell lines (MCF-7 and Panc02). Once the minimal concentration capable of inducing more than a 50% decrease in cell proliferation following 48 hours exposure was defined, we further tested whether the observed effect relied on the combination of AHCC and Wasabi, thus estimating whether by providing cells with the ingle compounds, it would be possible to achieve the same result. Interestingly, data obtained showed a marked reduction in viability when the compounds were combined even at very low concentrations (7.5 μg/mL for Wasabi and 10 μg/mL for AHCC) compared with their single counterparts. Results were assessed around 52% and 55% for MCF-7 and Panc02, respectively. Literature reports that a greater reduction (of about 64.9%) in MCF-7 proliferation can be achieved by the sole use of Wasabi only if a greater concentration (250 μg/mL) of the crude extract was applied (143) . Contrarily, we only observed a slight decrease (23%) in the percentage of proliferative MCF-7 cells following the treatment with Wasabi as single agent. However, by

combining Wasabi with AHCC, we demonstrated that only a 33.3-fold less Wasabi is required to obtain a marked reduction in MCF-7 proliferation. When the pancreatic Panc02 cell line was tested, we showed that also the single agents (Wasabi and AHCC) were able to induce a significant reduction in cell proliferation (57% and 36%, respectively), with Wasabi revealing a reduction that was found similar to BAIC (55%). Furthermore, according to the existing literature, no cytotoxic activity of AHCC used as single agent was observed at 24 hours on MCF-7 and Panc02 [134] (data not shown). By providing cells with 10 μg/mL AHCC, we found a 20% reduction at 48 hours in MCF7. It is worth mentioning that previous evidence coming from other research groups highlights no cytotoxic effect that could be ascribed to AHCC even at clinically relevant concentrations (134). The above findings demonstrated that BAIC has an antiproliferative impact on the adenocarcinoma cell lines tested (MCF-7 and Panc02) with differences that are probably associated to the nature of the cells used. In agreement with our study, Chen et al also reported a great reduction in human pancreatic cancer cells viability following the exposure to the natural Wasabi compound, the 6-MITC, and its chemical derivatives (144). Based on the evidence provided by other studies on the role of natural compounds on cancer cells (145, 146) the anti-proliferative, effects could be the result of the induction of apoptosis, and/or cell cycle

arrest. The cell cycle analysis we performed demonstrated an increase in the percentage of cells in G_0/G_1 phases when MCF-7 and Panc02 cells were treated with BAIC at 48 hours. Similar results were observed following the treatment with other natural compounds with anticancer effect (147, 148), including curcumin (148), casticin, arctigenin (149) and α-mangatostin (150). Although in the line with these previous experiments, our data are in conflict with those obtained by other groups on the role of Wasabi on cell cycle distribution, which demonstrated a dose-dependent marked arrest in the G_2/M phase by providing colon cancer cells with *Wasabia japonica* extracts (144, 151). We hypothesize that discrepancies between ours and previously reported data may be the result of the lower concentrations used in the study. However, according to our studies, groups focusing on the effect of the active component of Wasabi, the 6-MITC, on other human cell lines (ie, acute promyelocytic leukemia, HL-60) demonstrated an increased percentage in cells at the G_0/G_1 phase following the treatment with 0.8 μg/mL Wasabi (152). On the other hand, no significant differences have been noticed in cell cycle distribution following the treatment with AHCC, which is consistent with its role as coadjutant of antitumorigenic therapies than as single agent (134, 153). Since the mode of action of natural compounds inducing the cell cycle arrest has been closely related to the activation of the apoptotic cascade

(154),[SEP]We investigated whether the reduction of viable cells following the treatment with BAIC could also be ascribed to apoptosis in both cell lines. Following the treatment, a statistically significant increase in the percentage of apoptotic Panc02 and MCF-7 cells was demonstrated (up to 24% for apoptotic cells for Panc02 and 50% for MCF-7). A general increase was also observed following the treatment with Wasabi and AHCC as single agents compared with control cells. In both cases, the results are in line with those obtained from the MTT assay. To confirm our observations, we proceeded with analyzing the expression of 2 factors related to the apoptotic cascades, the pro-apoptotic member of the *Bcl-2* family Bax-2 (155) and the effector molecule responsible for the activation of apoptosis through the caspases pathway, *Apaf-1(156)*. Our data indicated that an increase in the mRNA levels of *Bax- 2* was induced in MCF-7 cells by the BAIC treatment and was found enhanced compared with the single counterparts (Wasabi and AHCC). A relative upregulation in the expression of *Apaf-1* was also observed although at lower levels with regard to those displayed by Panc02. In fact, we hypothesize that BAIC activates different apoptotic mechanisms in the 2 cell lines tested, with MCF-7 undergoing a marked trigger of the Bcl-2-dependent cascade (157) and Panc02 eliciting the family of cysteine proteases, the caspases 4. Whether this activation is p53 dependent is still under consideration

in our laboratory as data obtained show differences between the cell lines and support the existing literature on the discrepancy in the apoptotic pathways elicited by cancer cells following the exposure to Wasabi (158) (159) or AHCC (160). It has been widely established that a small population of tumorigenic cells (CSC) exists in several human cancers. CSC are able to self-renew and to perpetually proliferate to initiate and develop cancer(161). As such, their fundamental involvement in tumor progression has highlighted the urgency to develop therapeutic strategies capable of targeting CSC for cancer treatment or prevention (162, 163). With this in mind, we also wanted to test the combinatorial effectiveness of BAIC on the activity of MCF-7-derived CSC. The preliminary data obtained emphasize the potential role of the combination of AHCC and Wasabi in suppressing breast CSC progression and were consistent with previously published studies showing antitumorigenic agents with marked potential in inhibiting mammospheres development (157). Specifically, our study demonstrates a 2-fold decrease in mammosphere size and number when mammospheres produced by MCF-7-enriched CSC were treated with BAIC for 5 days. Fani et al suggested that the reduction in mammosphere size is correlated to the decrease in cancer progression (157). While no reports exit on the effect of Wasabi on CSC-derived mammospheres, a recently published article highlights the role of

AHCC extracts to inhibit mammosphere growth in 3 cell lines (164). Finally, when BAIC were provided to monocytes to understand whether such combination could concomitantly exert negative effects on immune cells, no cytotoxic effects were detected. Cell viability was found to be comparable to control groups in all experimental conditions. Interestingly, we also observed a hypothetical activation of the monocytic cells used following the treatment, as demonstrated by the adhesive properties they acquired (64). Based on these observations and on previously published evidence on the role ThP-1-derived macrophages play in modulating the apoptotic response to cancer cells (165), we moved forward and aimed at shedding light on the phenotype of such macrophages-like cells. We then evaluated the expression levels of inflammatory genes suggesting the immunomodulatory potential of the BAIC mixture compared with the single components. Our data demonstrated an upregulation of the cyclooxygenase-2 (*Cox-2*) soon after the treatment with a significant reduction compared with control cells at 48 hours. This gene has not been generally associated to normal cells or tissues, nor to resting cells, although its results are highly expressed following cell exposure to inflammatory cytokines, growth factors, and molecules able to induce carcinogenesis (166). We also analyzed the expression of *IL1*-β following the exposure to BAIC and found a statistically significant increase following the

exposure to Wasabi at 24 hours, which appeared to be reduced over time, with expression levels that were comparable to control. This result is particularly interesting as it has been reported that macrophage-derived *Il-1*β also stimulates the growth of cancer cells (167), and a decrease in its expression could lead to the inhibition of cancer progression. According to previous studies showing a marked increase in *Il-1*β in in vivo setting following the treatment with AHCC 48, we only observed an average of 2.5-fold upregulation in its expression at 24 and 48 hours. Furthermore, there was no increase in the expression levels of the third marker analyzed, transforming growth factor-β (*Tgf-*β), which has been suggested to determine an augmentation of the angiogenic properties of tumor and support its progression (168, 169). In our experiment, an average 4-fold increase was found at 24 and 48 hours in the BAIC group, which was reduced compared with the single use of AHCC and Wasabi. Taken together, data obtained herein not only indicate a combinatorial effect of BAIC but also highlight the immunomodulatory role of the combination as no cytotoxic effect to immune system was observed while beneficial effects were rather found. Further studies will be required to elucidate the mechanisms targeted by such combination of natural compounds. Particular emphasis will be given to the NF-κb, Wnt, and Notch self-renewal pathways, which have been demonstrated to be activated by other

bioactive natural products such as curcumin (170, 171) in tumor cells and CSC, as well as to the apoptotic cascades activated by the BAIC. Our preliminary studies on the immunomodulatory role of BAIC opens the possibility to further investigate paracrine signals between cancers cells and the immune system. Our study provides evidence on the combinatorial action that occurs when 2 natural compounds with demonstrated anti-inflammatory and anticancer effects are combined and suggests such combination as novel adjuvant therapy to support chemo- therapy while controlling side effects. Further investigations are required to highlight the role BAIC play in modulating the immune system in case of inflammation as compared with physiological conditions.

References:

1. Thurley K, Wu LF, Altschuler SJ. Modeling Cell-to-Cell Communication Networks Using Response-Time Distributions. Cell Syst. 2018;6(3):355-67 e5.
2. Raposo G, Stoorvogel W. Extracellular vesicles: exosomes, microvesicles, and friends. J Cell Biol. 2013;200(4):373-83.
3. Oeckinghaus A, Hayden MS, Ghosh S. Crosstalk in NF-kappaB signaling pathways. Nat Immunol. 2011;12(8):695-708.
4. Vert G, Chory J. Crosstalk in cellular signaling: background noise or the real thing? Dev Cell. 2011;21(6):985-91.
5. Guo X, Wang XF. Signaling cross-talk between TGF-beta/BMP and other pathways. Cell Res. 2009;19(1):71-88.
6. Mittelbrunn M, Sanchez-Madrid F. Intercellular communication: diverse structures for exchange of genetic information. Nat Rev Mol Cell Biol. 2012;13(5):328-35.
7. Lopez-Verrilli MA, Caviedes A, Cabrera A, Sandoval S, Wyneken U, Khoury M. Mesenchymal stem cell-derived exosomes from different sources selectively promote neuritic outgrowth. Neuroscience. 2016;320:129-39.
8. Hajimiri M, Shahverdi S, Kamalinia G, Dinarvand R. Growth factor conjugation: strategies and applications. J Biomed Mater Res A. 2015;103(2):819-38.
9. Turner N, Grose R. Fibroblast growth factor signalling: from development to cancer. Nat Rev Cancer. 2010;10(2):116-29.
10. Quezada C, Torres A, Niechi I, Uribe D, Contreras-Duarte S, Toledo F, et al. Role of extracellular vesicles in glioma progression. Mol Aspects Med. 2018;60:38-51.
11. Heijnen HF, Schiel AE, Fijnheer R, Geuze HJ, Sixma JJ. Activated platelets release two types of membrane vesicles: microvesicles by surface shedding and exosomes derived from exocytosis of multivesicular bodies and alpha-granules. Blood. 1999;94(11):3791-9.
12. Cocucci E, Racchetti G, Meldolesi J. Shedding microvesicles: artefacts no more. Trends Cell Biol. 2009;19(2):43-51.
13. Ratajczak J, Wysoczynski M, Hayek F, Janowska-Wieczorek A, Ratajczak MZ. Membrane-derived microvesicles: important and underappreciated mediators of cell-to-cell communication. Leukemia. 2006;20(9):1487-95.
14. Trams EG, Lauter CJ, Salem N, Jr., Heine U. Exfoliation of membrane ecto-enzymes in the form of micro-vesicles. Biochim Biophys Acta. 1981;645(1):63-70.
15. Simons M, Raposo G. Exosomes--vesicular carriers for intercellular communication. Curr Opin Cell Biol. 2009;21(4):575-81.
16. Thery C, Zitvogel L, Amigorena S. Exosomes: composition, biogenesis and function. Nat Rev Immunol. 2002;2(8):569-79.
17. Hsu C, Morohashi Y, Yoshimura S, Manrique-Hoyos N, Jung S, Lauterbach MA, et al. Regulation of exosome secretion by Rab35 and its GTPase-activating proteins TBC1D10A-C. J Cell Biol. 2010;189(2):223-32.
18. Ekstrom EJ, Bergenfelz C, von Bulow V, Serifler F, Carlemalm E, Jonsson G, et al. WNT5A induces release of exosomes containing pro-angiogenic and immunosuppressive factors from malignant melanoma cells. Mol Cancer. 2014;13:88.

19. Thery C, Boussac M, Veron P, Ricciardi-Castagnoli P, Raposo G, Garin J, et al. Proteomic analysis of dendritic cell-derived exosomes: a secreted subcellular compartment distinct from apoptotic vesicles. J Immunol. 2001;166(12):7309-18.
20. Wilusz JE, Sunwoo H, Spector DL. Long noncoding RNAs: functional surprises from the RNA world. Genes Dev. 2009;23(13):1494-504.
21. Schorey JS, Bhatnagar S. Exosome function: from tumor immunology to pathogen biology. Traffic. 2008;9(6):871-81.
22. Melo SA, Luecke LB, Kahlert C, Fernandez AF, Gammon ST, Kaye J, et al. Glypican-1 identifies cancer exosomes and detects early pancreatic cancer. Nature. 2015;523(7559):177-82.
23. Zijlstra C, Stoorvogel W. Prostasomes as a source of diagnostic biomarkers for prostate cancer. J Clin Invest. 2016;126(4):1144-51.
24. Boulikas T. Clinical overview on Lipoplatin: a successful liposomal formulation of cisplatin. Expert Opin Investig Drugs. 2009;18(8):1197-218.
25. Van Deun J, Mestdagh P, Sormunen R, Cocquyt V, Vermaelen K, Vandesompele J, et al. The impact of disparate isolation methods for extracellular vesicles on downstream RNA profiling. J Extracell Vesicles. 2014;3.
26. Delves PJ, Roitt IM. The immune system. First of two parts. N Engl J Med. 2000;343(1):37-49.
27. Abeles RD, McPhail MJ, Sowter D, Antoniades CG, Vergis N, Vijay GK, et al. CD14, CD16 and HLA-DR reliably identifies human monocytes and their subsets in the context of pathologically reduced HLA-DR expression by CD14(hi) /CD16(neg) monocytes: Expansion of CD14(hi) /CD16(pos) and contraction of CD14(lo) /CD16(pos) monocytes in acute liver failure. Cytometry A. 2012;81(10):823-34.
28. Zhang L, Wang CC. Inflammatory response of macrophages in infection. Hepatobiliary Pancreat Dis Int. 2014;13(2):138-52.
29. Murray PJ. Macrophage Polarization. Annu Rev Physiol. 2017;79:541-66.
30. Mantovani A, Sica A, Sozzani S, Allavena P, Vecchi A, Locati M. The chemokine system in diverse forms of macrophage activation and polarization. Trends Immunol. 2004;25(12):677-86.
31. Mackaness GB. The monocyte in cellular immunity. Semin Hematol. 1970;7(2):172-84.
32. Martinez FO, Sica A, Mantovani A, Locati M. Macrophage activation and polarization. Front Biosci. 2008;13:453-61.
33. Gordon S. Alternative activation of macrophages. Nat Rev Immunol. 2003;3(1):23-35.
34. Grivennikov SI, Greten FR, Karin M. Immunity, inflammation, and cancer. Cell. 2010;140(6):883-99.
35. Ruffell B, Coussens LM. Macrophages and therapeutic resistance in cancer. Cancer Cell. 2015;27(4):462-72.
36. Ishida Y, Gao JL, Murphy PM. Chemokine receptor CX3CR1 mediates skin wound healing by promoting macrophage and fibroblast accumulation and function. J Immunol. 2008;180(1):569-79.
37. Soroosh P, Doherty TA, Duan W, Mehta AK, Choi H, Adams YF, et al. Lung-resident tissue macrophages generate Foxp3+ regulatory T cells and promote airway tolerance. J Exp Med. 2013;210(4):775-88.
38. Mauer J, Chaurasia B, Goldau J, Vogt MC, Ruud J, Nguyen KD, et al. Signaling by IL-6 promotes alternative activation of macrophages to limit endotoxemia and obesity-associated resistance to insulin. Nat Immunol. 2014;15(5):423-30.

39. Koc ON, Lazarus HM. Mesenchymal stem cells: heading into the clinic. Bone Marrow Transplant. 2001;27(3):235-9.
40. Gebler A, Zabel O, Seliger B. The immunomodulatory capacity of mesenchymal stem cells. Trends Mol Med. 2012;18(2):128-34.
41. Trubiani O, Di Primio R, Traini T, Pizzicannella J, Scarano A, Piattelli A, et al. Morphological and cytofluorimetric analysis of adult mesenchymal stem cells expanded ex vivo from periodontal ligament. Int J Immunopathol Pharmacol. 2005;18(2):213-21.
42. In 't Anker PS, Scherjon SA, Kleijburg-van der Keur C, de Groot-Swings GM, Claas FH, Fibbe WE, et al. Isolation of mesenchymal stem cells of fetal or maternal origin from human placenta. Stem Cells. 2004;22(7):1338-45.
43. Erices A, Conget P, Minguell JJ. Mesenchymal progenitor cells in human umbilical cord blood. Br J Haematol. 2000;109(1):235-42.
44. in 't Anker PS, Noort WA, Scherjon SA, Kleijburg-van der Keur C, Kruisselbrink AB, van Bezooijen RL, et al. Mesenchymal stem cells in human second-trimester bone marrow, liver, lung, and spleen exhibit a similar immunophenotype but a heterogeneous multilineage differentiation potential. Haematologica. 2003;88(8):845-52.
45. Kaplan JM, Youd ME, Lodie TA. Immunomodulatory activity of mesenchymal stem cells. Curr Stem Cell Res Ther. 2011;6(4):297-316.
46. Chamberlain G, Wright K, Rot A, Ashton B, Middleton J. Murine mesenchymal stem cells exhibit a restricted repertoire of functional chemokine receptors: comparison with human. PLoS One. 2008;3(8):e2934.
47. Meirelles Lda S, Fontes AM, Covas DT, Caplan AI. Mechanisms involved in the therapeutic properties of mesenchymal stem cells. Cytokine Growth Factor Rev. 2009;20(5-6):419-27.
48. Devine SM, Cobbs C, Jennings M, Bartholomew A, Hoffman R. Mesenchymal stem cells distribute to a wide range of tissues following systemic infusion into nonhuman primates. Blood. 2003;101(8):2999-3001.
49. Baell JB. Feeling Nature's PAINS: Natural Products, Natural Product Drugs, and Pan Assay Interference Compounds (PAINS). J Nat Prod. 2016;79(3):616-28.
50. Rochlani Y, Pothineni NV, Kovelamudi S, Mehta JL. Metabolic syndrome: pathophysiology, management, and modulation by natural compounds. Ther Adv Cardiovasc Dis. 2017;11(8):215-25.
51. Sadeghalvad M, Mohammadi-Motlagh HR, Karaji AG, Mostafaie A. In vivo anti-inflammatory efficacy of the combined Bowman-Birk trypsin inhibitor and genistein isoflavone, two biological compounds from soybean. J Biochem Mol Toxicol. 2019:e22406.
52. Clarke JO, Mullin GE. A review of complementary and alternative approaches to immunomodulation. Nutr Clin Pract. 2008;23(1):49-62.
53. Nomura M, Ma W, Chen N, Bode AM, Dong Z. Inhibition of 12-O-tetradecanoylphorbol-13-acetate-induced NF-kappaB activation by tea polyphenols, (-)-epigallocatechin gallate and theaflavins. Carcinogenesis. 2000;21(10):1885-90.
54. Xia N, Daiber A, Forstermann U, Li H. Antioxidant effects of resveratrol in the cardiovascular system. Br J Pharmacol. 2017;174(12):1633-46.
55. Lin Q, Ma L, Liu Z, Yang Z, Wang J, Liu J, et al. Targeting microRNAs: a new action mechanism of natural compounds. Oncotarget. 2017;8(9):15961-70.

56. Subedi L, Venkatesan R, Kim SY. Neuroprotective and Anti-Inflammatory Activities of Allyl Isothiocyanate through Attenuation of JNK/NF-kappaB/TNF-alpha Signaling. Int J Mol Sci. 2017;18(7).
57. Xiang J, Alesi GN, Zhou N, Keep RF. Protective effects of isothiocyanates on blood-CSF barrier disruption induced by oxidative stress. Am J Physiol Regul Integr Comp Physiol. 2012;303(1):R1-7.
58. Uto T, Hou DX, Morinaga O, Shoyama Y. Molecular Mechanisms Underlying Anti-Inflammatory Actions of 6-(Methylsulfinyl)hexyl Isothiocyanate Derived from Wasabi (Wasabia japonica). Adv Pharmacol Sci. 2012;2012:614046.
59. Uto T, Fujii M, Hou DX. 6-(Methylsulfinyl)hexyl isothiocyanate suppresses inducible nitric oxide synthase expression through the inhibition of Janus kinase 2-mediated JNK pathway in lipopolysaccharide-activated murine macrophages. Biochem Pharmacol. 2005;70(8):1211-21.
60. Suenaga S, Kuramitsu Y, Kaino S, Maehara S, Maehara Y, Sakaida I, et al. Active hexose-correlated compound down-regulates HSP27 of pancreatic cancer cells, and helps the cytotoxic effect of gemcitabine. Anticancer Res. 2014;34(1):141-6.
61. Fatehchand K, Santhanam R, Shen B, Erickson EL, Gautam S, Elavazhagan S, et al. Active hexose-correlated compound enhances extrinsic-pathway-mediated apoptosis of Acute Myeloid Leukemic cells. PLoS One. 2017;12(7):e0181729.
62. Ritz BW. Supplementation with active hexose correlated compound increases survival following infectious challenge in mice. Nutr Rev. 2008;66(9):526-31.
63. Yin Z, Fujii H, Walshe T. Effects of active hexose correlated compound on frequency of CD4+ and CD8+ T cells producing interferon-gamma and/or tumor necrosis factor-alpha in healthy adults. Hum Immunol. 2010;71(12):1187-90.
64. Lee WW, Lee N, Fujii H, Kang I. Active Hexose Correlated Compound promotes T helper (Th) 17 and 1 cell responses via inducing IL-1beta production from monocytes in humans. Cell Immunol. 2012;275(1-2):19-23.
65. Choi JY, Lee S, Yun SM, Suh DH, Kim K, No JH, et al. Active Hexose Correlated Compound (AHCC) Inhibits the Proliferation of Ovarian Cancer Cells by Suppressing Signal Transducer and Activator of Transcription 3 (STAT3) Activation. Nutr Cancer. 2018;70(1):109-15.
66. Dvorak HF. Tumors: wounds that do not heal-redux. Cancer Immunol Res. 2015;3(1):1-11.
67. Sullivan R, Maresh G, Zhang X, Salomon C, Hooper J, Margolin D, et al. The Emerging Roles of Extracellular Vesicles As Communication Vehicles within the Tumor Microenvironment and Beyond. Front Endocrinol (Lausanne). 2017;8:194.
68. Maacha S, Bhat AA, Jimenez L, Raza A, Haris M, Uddin S, et al. Extracellular vesicles-mediated intercellular communication: roles in the tumor microenvironment and anti-cancer drug resistance. Mol Cancer. 2019;18(1):55.
69. Ame-Thomas P, Maby-El Hajjami H, Monvoisin C, Jean R, Monnier D, Caulet-Maugendre S, et al. Human mesenchymal stem cells isolated from bone marrow and lymphoid organs support tumor B-cell growth: role of stromal cells in follicular lymphoma pathogenesis. Blood. 2007;109(2):693-702.
70. Kansy BA, Dissmann PA, Hemeda H, Bruderek K, Westerkamp AM, Jagalski V, et al. The bidirectional tumor--mesenchymal stromal cell interaction promotes the progression of head and neck cancer. Stem Cell Res Ther. 2014;5(4):95.

71. Hossain A, Gumin J, Gao F, Figueroa J, Shinojima N, Takezaki T, et al. Mesenchymal Stem Cells Isolated From Human Gliomas Increase Proliferation and Maintain Stemness of Glioma Stem Cells Through the IL-6/gp130/STAT3 Pathway. Stem Cells. 2015;33(8):2400-15.
72. Karnoub AE, Dash AB, Vo AP, Sullivan A, Brooks MW, Bell GW, et al. Mesenchymal stem cells within tumour stroma promote breast cancer metastasis. Nature. 2007;449(7162):557-63.
73. Li W, Zhou Y, Yang J, Zhang X, Zhang H, Zhang T, et al. Gastric cancer-derived mesenchymal stem cells prompt gastric cancer progression through secretion of interleukin-8. J Exp Clin Cancer Res. 2015;34:52.
74. Zhu W, Xu W, Jiang R, Qian H, Chen M, Hu J, et al. Mesenchymal stem cells derived from bone marrow favor tumor cell growth in vivo. Exp Mol Pathol. 2006;80(3):267-74.
75. Prantl L, Muehlberg F, Navone NM, Song YH, Vykoukal J, Logothetis CJ, et al. Adipose tissue-derived stem cells promote prostate tumor growth. Prostate. 2010;70(15):1709-15.
76. Sun B, Roh KH, Park JR, Lee SR, Park SB, Jung JW, et al. Therapeutic potential of mesenchymal stromal cells in a mouse breast cancer metastasis model. Cytotherapy. 2009;11(3):289-98, 1 p following 98.
77. Khakoo AY, Pati S, Anderson SA, Reid W, Elshal MF, Rovira, II, et al. Human mesenchymal stem cells exert potent antitumorigenic effects in a model of Kaposi's sarcoma. J Exp Med. 2006;203(5):1235-47.
78. Qiao L, Xu Z, Zhao T, Zhao Z, Shi M, Zhao RC, et al. Suppression of tumorigenesis by human mesenchymal stem cells in a hepatoma model. Cell Res. 2008;18(4):500-7.
79. Otsu K, Das S, Houser SD, Quadri SK, Bhattacharya S, Bhattacharya J. Concentration-dependent inhibition of angiogenesis by mesenchymal stem cells. Blood. 2009;113(18):4197-205.
80. Yaghoubi Y, Movassaghpour A, Zamani M, Talebi M, Mehdizadeh A, Yousefi M. Human umbilical cord mesenchymal stem cells derived-exosomes in diseases treatment. Life Sci. 2019;233:116733.
81. Ding Y, Cao F, Sun H, Wang Y, Liu S, Wu Y, et al. Exosomes derived from human umbilical cord mesenchymal stromal cells deliver exogenous miR-145-5p to inhibit pancreatic ductal adenocarcinoma progression. Cancer Lett. 2019;442:351-61.
82. Eleuteri S, Fierabracci A. Insights into the Secretome of Mesenchymal Stem Cells and Its Potential Applications. Int J Mol Sci. 2019;20(18).
83. Bailon-Moscoso N, Romero-Benavides JC, Ostrosky-Wegman P. Development of anticancer drugs based on the hallmarks of tumor cells. Tumour Biol. 2014;35(5):3981-95.
84. Pratheeshkumar P, Sreekala C, Zhang Z, Budhraja A, Ding S, Son YO, et al. Cancer prevention with promising natural products: mechanisms of action and molecular targets. Anticancer Agents Med Chem. 2012;12(10):1159-84.
85. Huang MT, Newmark HL, Frenkel K. Inhibitory effects of curcumin on tumorigenesis in mice. J Cell Biochem Suppl. 1997;27:26-34.
86. Zang S, Liu T, Shi J, Qiao L. Curcumin: a promising agent targeting cancer stem cells. Anticancer Agents Med Chem. 2014;14(6):787-92.
87. Marquardt JU, Gomez-Quiroz L, Arreguin Camacho LO, Pinna F, Lee YH, Kitade M, et al. Curcumin effectively inhibits oncogenic NF-kappaB signaling and restrains stemness features in liver cancer. J Hepatol. 2015;63(3):661-9.

88. Mitani T, Harada N, Tanimori S, Nakano Y, Inui H, Yamaji R. Resveratrol inhibits hypoxia-inducible factor-1alpha-mediated androgen receptor signaling and represses tumor progression in castration-resistant prostate cancer. J Nutr Sci Vitaminol (Tokyo). 2014;60(4):276-82.
89. Tili E, Michaille JJ, Alder H, Volinia S, Delmas D, Latruffe N, et al. Resveratrol modulates the levels of microRNAs targeting genes encoding tumor-suppressors and effectors of TGFbeta signaling pathway in SW480 cells. Biochem Pharmacol. 2010;80(12):2057-65.
90. Reid BM, Permuth JB, Sellers TA. Epidemiology of ovarian cancer: a review. Cancer Biol Med. 2017;14(1):9-32.
91. Testa U, Petrucci E, Pasquini L, Castelli G, Pelosi E. Ovarian Cancers: Genetic Abnormalities, Tumor Heterogeneity and Progression, Clonal Evolution and Cancer Stem Cells. Medicines (Basel). 2018;5(1).
92. Al-Alem LF, Pandya UM, Baker AT, Bellio C, Zarrella BD, Clark J, et al. Ovarian cancer stem cells: What progress have we made? Int J Biochem Cell Biol. 2019;107:92-103.
93. Corradetti B, Pisano S, Conlan RS, Ferrari M. Nanotechnology and Immunotherapy in Ovarian Cancer: Tracing New Landscapes. J Pharmacol Exp Ther. 2019;370(3):636-46.
94. Luo GF, Chen CY, Wang J, Yue HY, Tian Y, Yang P, et al. FOXD3 may be a new cellular target biomarker as a hypermethylation gene in human ovarian cancer. Cancer Cell Int. 2019;19:44.
95. Christie EL, Bowtell DDL. Acquired chemotherapy resistance in ovarian cancer. Ann Oncol. 2017;28(suppl_8):viii13-viii5.
96. Giornelli GH. Management of relapsed ovarian cancer: a review. Springerplus. 2016;5(1):1197.
97. Varas-Godoy M, Rice G, Illanes SE. The Crosstalk between Ovarian Cancer Stem Cell Niche and the Tumor Microenvironment. Stem Cells Int. 2017;2017:5263974.
98. Valdes-Rives SA, Gonzalez-Arenas A. Autotaxin-Lysophosphatidic Acid: From Inflammation to Cancer Development. Mediators Inflamm. 2017;2017:9173090.
99. Gao T, Yu Y, Cong Q, Wang Y, Sun M, Yao L, et al. Human mesenchymal stem cells in the tumour microenvironment promote ovarian cancer progression: the role of platelet-activating factor. BMC Cancer. 2018;18(1):999.
100. Chien KR. Regenerative medicine and human models of human disease. Nature. 2008;453(7193):302-5.
101. Ghannam S, Bouffi C, Djouad F, Jorgensen C, Noel D. Immunosuppression by mesenchymal stem cells: mechanisms and clinical applications. Stem Cell Res Ther. 2010;1(1):2.
102. Bobis S, Jarocha D, Majka M. Mesenchymal stem cells: characteristics and clinical applications. Folia Histochem Cytobiol. 2006;44(4):215-30.
103. Poloni A, Maurizi G, Babini L, Serrani F, Berardinelli E, Mancini S, et al. Human mesenchymal stem cells from chorionic villi and amniotic fluid are not susceptible to transformation after extensive in vitro expansion. Cell Transplant. 2011;20(5):643-54.
104. Sessarego N, Parodi A, Podesta M, Benvenuto F, Mogni M, Raviolo V, et al. Multipotent mesenchymal stromal cells from amniotic fluid: solid perspectives for clinical application. Haematologica. 2008;93(3):339-46.

105. Zhao JY, Zhao X, Yang Y, Zhang Y, Zhao S. [Effect of umbilical cord mesenchymal stem cells on biological characteristics of esophageal cancer EC1 cells]. Zhonghua Zhong Liu Za Zhi. 2019;41(2):97-101.
106. Bruno S, Collino F, Deregibus MC, Grange C, Tetta C, Camussi G. Microvesicles derived from human bone marrow mesenchymal stem cells inhibit tumor growth. Stem Cells Dev. 2013;22(5):758-71.
107. L PK, Kandoi S, Misra R, S V, K R, Verma RS. The mesenchymal stem cell secretome: A new paradigm towards cell-free therapeutic mode in regenerative medicine. Cytokine Growth Factor Rev. 2019;46:1-9.
108. Reza A, Choi YJ, Yasuda H, Kim JH. Human adipose mesenchymal stem cell-derived exosomal-miRNAs are critical factors for inducing anti-proliferation signalling to A2780 and SKOV-3 ovarian cancer cells. Sci Rep. 2016;6:38498.
109. Hui L, Chen Y. Tumor microenvironment: Sanctuary of the devil. Cancer Lett. 2015;368(1):7-13.
110. Riffle S, Pandey RN, Albert M, Hegde RS. Linking hypoxia, DNA damage and proliferation in multicellular tumor spheroids. BMC Cancer. 2017;17(1):338.
111. Ishiguro T, Ohata H, Sato A, Yamawaki K, Enomoto T, Okamoto K. Tumor-derived spheroids: Relevance to cancer stem cells and clinical applications. Cancer Sci. 2017;108(3):283-9.
112. Kusuma GD, Carthew J, Lim R, Frith JE. Effect of the Microenvironment on Mesenchymal Stem Cell Paracrine Signaling: Opportunities to Engineer the Therapeutic Effect. Stem Cells Dev. 2017;26(9):617-31.
113. Thoma CR, Zimmermann M, Agarkova I, Kelm JM, Krek W. 3D cell culture systems modeling tumor growth determinants in cancer target discovery. Adv Drug Deliv Rev. 2014;69-70:29-41.
114. Aziz M, Agarwal K, Dasari S, Mitra AAK. Productive Cross-Talk with the Microenvironment: A Critical Step in Ovarian Cancer Metastasis. Cancers (Basel). 2019;11(10).
115. Polak DJ. Regenerative medicine. Opportunities and challenges: a brief overview. J R Soc Interface. 2010;7 Suppl 6:S777-81.
116. Dominici M, Le Blanc K, Mueller I, Slaper-Cortenbach I, Marini F, Krause D, et al. Minimal criteria for defining multipotent mesenchymal stromal cells. The International Society for Cellular Therapy position statement. Cytotherapy. 2006;8(4):315-7.
117. Alberman E. The National Down Syndrome Cytogenetic Register (NDSCR). J Med Screen. 2002;9(3):97-8.
118. Antonarakis SE, Lyle R, Dermitzakis ET, Reymond A, Deutsch S. Chromosome 21 and down syndrome: from genomics to pathophysiology. Nat Rev Genet. 2004;5(10):725-38.
119. Antonarakis SE. 10 years of Genomics, chromosome 21, and Down syndrome. Genomics. 1998;51(1):1-16.
120. Ross JA, Spector LG, Robison LL, Olshan AF. Epidemiology of leukemia in children with Down syndrome. Pediatr Blood Cancer. 2005;44(1):8-12.
121. Igura K, Zhang X, Takahashi K, Mitsuru A, Yamaguchi S, Takashi TA. Isolation and characterization of mesenchymal progenitor cells from chorionic villi of human placenta. Cytotherapy. 2004;6(6):543-53.
122. Parolini O, Alviano F, Bagnara GP, Bilic G, Buhring HJ, Evangelista M, et al. Concise review: isolation and characterization of cells from human term placenta: outcome of the first international Workshop on Placenta Derived Stem Cells. Stem Cells. 2008;26(2):300-11.

123. Lim R. Concise Review: Fetal Membranes in Regenerative Medicine: New Tricks from an Old Dog? Stem Cells Transl Med. 2017;6(9):1767-76.
124. Martinez FO, Gordon S. The M1 and M2 paradigm of macrophage activation: time for reassessment. F1000Prime Rep. 2014;6:13.
125. Schneider Y, Vincent F, Duranton B, Badolo L, Gosse F, Bergmann C, et al. Anti-proliferative effect of resveratrol, a natural component of grapes and wine, on human colonic cancer cells. Cancer Lett. 2000;158(1):85-91.
126. Teiten MH, Eifes S, Dicato M, Diederich M. Curcumin-the paradigm of a multi-target natural compound with applications in cancer prevention and treatment. Toxins (Basel). 2010;2(1):128-62.
127. Ito T, Urushima H, Sakaue M, Yukawa S, Honda H, Hirai K, et al. Reduction of adverse effects by a mushroom product, active hexose correlated compound (AHCC) in patients with advanced cancer during chemotherapy--the significance of the levels of HHV-6 DNA in saliva as a surrogate biomarker during chemotherapy. Nutr Cancer. 2014;66(3):377-82.
128. Yanagimoto H, Satoi S, Yamamoto T, Hirooka S, Yamaki S, Kotsuka M, et al. Alleviating Effect of Active Hexose Correlated Compound (AHCC) on Chemotherapy-Related Adverse Events in Patients with Unresectable Pancreatic Ductal Adenocarcinoma. Nutr Cancer. 2016;68(2):234-40.
129. Roman BE, Beli E, Duriancik DM, Gardner EM. Short-term supplementation with active hexose correlated compound improves the antibody response to influenza B vaccine. Nutr Res. 2013;33(1):12-7.
130. Aviles H, Belay T, Fountain K, Vance M, Sun B, Sonnenfeld G. Active hexose correlated compound enhances resistance to Klebsiella pneumoniae infection in mice in the hindlimb-unloading model of spaceflight conditions. J Appl Physiol (1985). 2003;95(2):491-6.
131. Aviles H, O'Donnell P, Orshal J, Fujii H, Sun B, Sonnenfeld G. Active hexose correlated compound activates immune function to decrease bacterial load in a murine model of intramuscular infection. Am J Surg. 2008;195(4):537-45.
132. Ye SF, Ichimura K, Wakame K, Ohe M. Suppressive effects of Active Hexose Correlated Compound on the increased activity of hepatic and renal ornithine decarboxylase induced by oxidative stress. Life Sci. 2003;74(5):593-602.
133. Ignacio RM, Kim CS, Kim YD, Lee HM, Qi XF, Kim SK. Therapeutic effect of Active Hexose-Correlated Compound (AHCC) combined with CpG-ODN (oligodeoxynucleotide) in B16 melanoma murine model. Cytokine. 2015;76(2):131-7.
134. Mathew L, Gaikwad A, Gonzalez A, Nugent EK, Smith JA. Evaluation of Active Hexose Correlated Compound (AHCC) in Combination With Anticancer Hormones in Orthotopic Breast Cancer Models. Integr Cancer Ther. 2017;16(3):300-7.
135. Daddaoua A, Martinez-Plata E, Ortega-Gonzalez M, Ocon B, Aranda CJ, Zarzuelo A, et al. The nutritional supplement Active Hexose Correlated Compound (AHCC) has direct immunomodulatory actions on intestinal epithelial cells and macrophages involving TLR/MyD88 and NF-kappaB/MAPK activation. Food Chem. 2013;136(3-4):1288-95.
136. Morimitsu Y, Hayashi K, Nakagawa Y, Horio F, Uchida K, Osawa T. Antiplatelet and anticancer isothiocyanates in Japanese domestic horseradish, wasabi. Biofactors. 2000;13(1-4):271-6.
137. Uto T, Fujii M, Hou DX. Inhibition of lipopolysaccharide-induced cyclooxygenase-2 transcription by 6-(methylsulfinyl) hexyl isothiocyanate, a

chemopreventive compound from Wasabia japonica (Miq.) Matsumura, in mouse macrophages. Biochem Pharmacol. 2005;70(12):1772-84.
138. Uto T, Fujii M, Hou DX. Effects of 6-(methylsulfinyl)hexyl isothiocyanate on cyclooxygenase-2 expression induced by lipopolysaccharide, interferon-gamma and 12-O-tetradecanoylphorbol-13-acetate. Oncol Rep. 2007;17(1):233-8.
139. Chen J, Uto T, Tanigawa S, Yamada-Kato T, Fujii M, Hou DX. Microarray-based determination of anti-inflammatory genes targeted by 6-(methylsulfinyl)hexyl isothiocyanate in macrophages. Exp Ther Med. 2010;1(1):33-40.
140. Nomura T, Shinoda S, Yamori T, Sawaki S, Nagata I, Ryoyama K, et al. Selective sensitivity to wasabi-derived 6-(methylsulfinyl)hexyl isothiocyanate of human breast cancer and melanoma cell lines studied in vitro. Cancer Detect Prev. 2005;29(2):155-60.
141. Bertoli C, Skotheim JM, de Bruin RA. Control of cell cycle transcription during G1 and S phases. Nat Rev Mol Cell Biol. 2013;14(8):518-28.
142. Song XL, Zhang YJ, Wang XF, Zhang WJ, Wang Z, Zhang F, et al. Casticin induces apoptosis and G0/G1 cell cycle arrest in gallbladder cancer cells. Cancer Cell Int. 2017;17:9.
143. Weil MJ, Zhang Y, Nair MG. Tumor cell proliferation and cyclooxygenase inhibitory constituents in horseradish (Armoracia rusticana) and Wasabi (Wasabia japonica). J Agric Food Chem. 2005;53(5):1440-4.
144. Chen YJ, Huang YC, Tsai TH, Liao HF. Effect of Wasabi Component 6-(Methylsulfinyl)hexyl Isothiocyanate and Derivatives on Human Pancreatic Cancer Cells. Evid Based Complement Alternat Med. 2014;2014:494739.
145. Rajesh E, Sankari LS, Malathi L, Krupaa JR. Naturally occurring products in cancer therapy. J Pharm Bioallied Sci. 2015;7(Suppl 1):S181-3.
146. Nobili S, Lippi D, Witort E, Donnini M, Bausi L, Mini E, et al. Natural compounds for cancer treatment and prevention. Pharmacol Res. 2009;59(6):365-78.
147. Bailon-Moscoso N, Cevallos-Solorzano G, Romero-Benavides JC, Orellana MI. Natural Compounds as Modulators of Cell Cycle Arrest: Application for Anticancer Chemotherapies. Curr Genomics. 2017;18(2):106-31.
148. Sha J, Li J, Wang W, Pan L, Cheng J, Li L, et al. Curcumin induces G0/G1 arrest and apoptosis in hormone independent prostate cancer DU-145 cells by down regulating Notch signaling. Biomed Pharmacother. 2016;84:177-84.
149. Maimaitili A, Shu Z, Cheng X, Kaheerman K, Sikandeer A, Li W. Arctigenin, a natural lignan compound, induces G0/G1 cell cycle arrest and apoptosis in human glioma cells. Oncol Lett. 2017;13(2):1007-13.
150. Ibrahim MY, Hashim NM, Mohan S, Abdulla MA, Kamalidehghan B, Ghaderian M, et al. alpha-Mangostin from Cratoxylum arborescens demonstrates apoptogenesis in MCF-7 with regulation of NF-kappaB and Hsp70 protein modulation in vitro, and tumor reduction in vivo. Drug Des Devel Ther. 2014;8:1629-47.
151. Hsuan SW, Chyau CC, Hung HY, Chen JH, Chou FP. The induction of apoptosis and autophagy by Wasabia japonica extract in colon cancer. Eur J Nutr. 2016;55(2):491-503.
152. Lenzi M, Cocchi V, Malaguti M, Barbalace MC, Marchionni S, Hrelia S, et al. 6-(Methylsulfonyl) hexyl isothiocyanate as potential chemopreventive agent: molecular and cellular profile in leukaemia cell lines. Oncotarget. 2017;8(67):111697-714.

153. Cao Z, Chen X, Lan L, Zhang Z, Du J, Liao L. Active hexose correlated compound potentiates the antitumor effects of low-dose 5-fluorouracil through modulation of immune function in hepatoma 22 tumor-bearing mice. Nutr Res Pract. 2015;9(2):129-36.
154. Elkady AI, Abuzinadah OA, Baeshen NA, Rahmy TR. Differential control of growth, apoptotic activity, and gene expression in human breast cancer cells by extracts derived from medicinal herbs Zingiber officinale. J Biomed Biotechnol. 2012;2012:614356.
155. Burlacu A. Regulation of apoptosis by Bcl-2 family proteins. J Cell Mol Med. 2003;7(3):249-57.
156. Srinivasula SM, Ahmad M, Fernandes-Alnemri T, Alnemri ES. Autoactivation of procaspase-9 by Apaf-1-mediated oligomerization. Mol Cell. 1998;1(7):949-57.
157. Fani S, Kamalidehghan B, Lo KM, Nigjeh SE, Keong YS, Dehghan F, et al. Anticancer activity of a monobenzyltin complex C1 against MDA-MB-231 cells through induction of Apoptosis and inhibition of breast cancer stem cells. Sci Rep. 2016;6:38992.
158. Yano S, Wu S, Sakao K, Hou DX. Wasabi 6-(methylsulfinyl)hexyl isothiocyanate induces apoptosis in human colorectal cancer cells through p53-independent mitochondrial dysfunction pathway. Biofactors. 2018.
159. Porter AG, Janicke RU. Emerging roles of caspase-3 in apoptosis. Cell Death Differ. 1999;6(2):99-104.
160. Tokunaga M, Baron B, Kitagawa T, Tokuda K, Kuramitsu Y. Active Hexose-correlated Compound Down-regulates Heat Shock Factor 1, a Transcription Factor for HSP27, in Gemcitabine-resistant Human Pancreatic Cancer Cells. Anticancer Res. 2015;35(11):6063-7.
161. Hun Lee J, Shu L, Fuentes F, Su ZY, Tony Kong AN. Cancer chemoprevention by traditional chinese herbal medicine and dietary phytochemicals: targeting nrf2-mediated oxidative stress/anti-inflammatory responses, epigenetics, and cancer stem cells. J Tradit Complement Med. 2013;3(1):69-79.
162. Qin W, Huang G, Chen Z, Zhang Y. Nanomaterials in Targeting Cancer Stem Cells for Cancer Therapy. Front Pharmacol. 2017;8:1.
163. Dragu DL, Necula LG, Bleotu C, Diaconu CC, Chivu-Economescu M. Therapies targeting cancer stem cells: Current trends and future challenges. World J Stem Cells. 2015;7(9):1185-201.
164. Graham EA, Mallet JF, Jambi M, Nishioka H, Homma K, Matar C. MicroRNA signature in the chemoprevention of functionally-enriched stem and progenitor pools (FESPP) by Active Hexose Correlated Compound (AHCC). Cancer Biol Ther. 2017;18(10):765-74.
165. Genin M, Clement F, Fattaccioli A, Raes M, Michiels C. M1 and M2 macrophages derived from THP-1 cells differentially modulate the response of cancer cells to etoposide. BMC Cancer. 2015;15:577.
166. Hempel SL, Monick MM, Hunninghake GW. Lipopolysaccharide induces prostaglandin H synthase-2 protein and mRNA in human alveolar macrophages and blood monocytes. J Clin Invest. 1994;93(1):391-6.
167. Kaler P, Augenlicht L, Klampfer L. Macrophage-derived IL-1beta stimulates Wnt signaling and growth of colon cancer cells: a crosstalk interrupted by vitamin D3. Oncogene. 2009;28(44):3892-902.

168. Wrzesinski SH, Wan YY, Flavell RA. Transforming growth factor-beta and the immune response: implications for anticancer therapy. Clin Cancer Res. 2007;13(18 Pt 1):5262-70.
169. Massague J. TGFbeta in Cancer. Cell. 2008;134(2):215-30.
170. Takebe N, Harris PJ, Warren RQ, Ivy SP. Targeting cancer stem cells by inhibiting Wnt, Notch, and Hedgehog pathways. Nat Rev Clin Oncol. 2011;8(2):97-106.
171. Wang Z, Zhang Y, Banerjee S, Li Y, Sarkar FH. Notch-1 down-regulation by curcumin is associated with the inhibition of cell growth and the induction of apoptosis in pancreatic cancer cells. Cancer. 2006;106(11):2503-13.